Centralized Rate Allocation and Control in 802.11-based Wireless Mesh Networks

by

Kamran Jamshaid

A thesis
presented to the University of Waterloo
in fulfillment of the
thesis requirement for the degree of
Doctor of Philosophy
in
Electrical and Computer Engineering

Waterloo, Ontario, Canada, 2010

I hereby declare that I am the sole author of this thesis. This is a true copy of the thesis, including any required final revisions, as accepted by my examiners.

I understand that my thesis may be made electronically available to the public.

Abstract

Wireless Mesh Networks (WMNs) built with commodity 802.11 radios are a cost-effective means of providing last mile broadband Internet access. Their multihop architecture allows for rapid deployment and organic growth of these networks.

802.11 radios are an important building block in WMNs. These low cost radios are readily available, and can be used globally in license-exempt frequency bands. However, the 802.11 Distributed Coordination Function (DCF) medium access mechanism does not scale well in large multihop networks. This produces suboptimal behavior in many transport protocols, including TCP, the dominant transport protocol in the Internet. In particular, cross-layer interaction between DCF and TCP results in flow level unfairness, including starvation, with backlogged traffic sources. Solutions found in the literature propose distributed source rate control algorithms to alleviate this problem. However, this requires MAC-layer or transport-layer changes on all mesh routers. This is often infeasible in practical deployments.

In wireline networks, router-assisted rate control techniques have been proposed for use alongside end-to-end mechanisms. We evaluate the feasibility of establishing similar centralized control via gateway mesh routers in WMNs. We find that commonly used router-assisted flow control schemes designed for wired networks fail in WMNs. This is because they assume that: (1) links can be scheduled independently, and (2) router queue buildups are sufficient for detecting congestion. These abstractions do not hold in a wireless network, rendering wired scheduling algorithms such as Fair Queueing (and its variants) and Active Queue Management (AQM) techniques ineffective as a gateway-enforceable solution in a WMN. We show that only non-work-conserving rate-based scheduling can effectively enforce rate allocation via a single centralized traffic-aggregation point.

In this context we propose, design, and evaluate a framework of centralized, measurement-based, feedback-driven mechanisms that can enforce a rate allocation policy objective for adaptive traffic streams in a WMN. In this dissertation we focus on fair rate allocation requirements. Our approach does not require any changes to individual mesh routers. Further, it uses existing data traffic as capacity probes, thus incurring a zero control traffic overhead. We propose two mechanisms based on this approach: aggregate rate control (ARC) and per-flow rate control (PFRC). ARC limits the aggregate capacity of a network to the sum of fair rates for a given set of flows. We show that the resulting rate allocation achieved by DCF is approximately max-min fair. PFRC allows us to exercise finer-grained control over the

rate allocation process. We show how it can be used to achieve weighted flow rate fairness. We evaluate the performance of these mechanisms using simulations as well as implementation on a multihop wireless testbed. Our comparative analysis show that our mechanisms improve fairness indices by a factor of 2 to 3 when compared with networks without any rate limiting, and are approximately equivalent to results achieved with distributed source rate limiting mechanisms that require software modifications on all mesh routers.

Acknowledgements

In the name of Allah, the most Beneficent, the most Merciful

I wish to thank my adviser Prof. Paul Ward for taking me under his tutelage and for providing me this opportunity to work with him. I have benefited from his advice on many aspects of this research, whether it was helping me think through a problem, or his painstakingly-detailed feedback on various drafts of my writing. I am grateful to him for demanding high standards of scientific rigor in our research, and for his patience, understanding, and help in working with me at times when I would fall short of those exacting requirements.

I thank Prof. Sagar Naik, Prof. Guang Gong, Prof. Martin Karsten, and Prof. Thomas Kunz for serving on my committee. Their comments and feedback at different milestone requirements during the completion of this dissertation have helped with its correctness and clarity. Martin, in particular, went beyond the call of duty and his feedback was instrumental in helping me shape this work.

I also want to thank other faculty members associated with the Networks and Distributed Systems (NDS) group at Waterloo, including Prof. David Taylor, Prof. Jay Black, Prof. S. Keshav, Prof. Tim Brecht, and Prof. Raouf Boutaba. Our weekly NDS seminars provided me with ample opportunities to actively solicit their feedback at various stages of this work.

I was supported during my graduate studies, in part, by generous doctoral scholarship awards from NSERC Canada and University of Waterloo. Thank you.

I will forever be grateful to my former adviser at Wayne State University, Prof. Loren Schwiebert. I am fortunate to have him as a teacher, a guide, a mentor, and a friend. Though I graduated from Wayne State some 7 years ago, yet I continue to bank on him for advice and support. He has written countless letters to support my various admissions, visas, scholarships, and job applications. I am yet to meet someone who is as dedicated to their student's success as Loren. He is a role model that I wish to emulate in both my professional and personal life.

I consider myself fortunate in making friends with some wonderful people that I met at Waterloo. With them I shared some of the most memorable moments of my time spent here. Sajjad and Nabeel put up with me through the years when we shared an apartment. Along with other members of the 'gang', we would indulge in late-night dinners with spirited discussions on any irrelevant issue, movies, camping trips, and even a skydiving jump. Thank you all for the memories that I will always

cherish. In particular, I will fondly remember the kind generosity and the warm friendship of Omar and Farheen. These two were my extended family away from home.

I am indebted to my parents for helping me be whatever I am today. Their unconditional love and support emboldens me to take on new adventures, knowing that they will be there for me if and when I fall. They are my source of strength and inspiration. This thesis is dedicated to them.

The final word is for my Rabb, the Almighty. I bow with gratitude for all the opportunities in this life.

Dedication

To Ami & Aboo

Contents

List of Tables

List of Figures

Chapter 1

Introduction and Preview

Broadband access to the public Internet has emerged as a fundamental requirement in our new Information Age. These broadband access networks empower our lives in many ways: they are a conduit to linking people with essential services such as health-care, education, and employment opportunities; they enable communications and e-commerce; and they foster social participation and connectedness. These networks are recognized as an accelerator of economic and social well-being of a community [31]. Indeed, the American Recovery and Reinvestment Act of 2009 includes more than $7 billion to expand access to broadband services in United States as a means of spurring economic development [102].

One of the main challenges in ubiquitous availability of broadband networks is the last mile[1] access problem. A majority of Internet users today use some form of a wired last mile access network. From a service provider's perspective, developing this wired infrastructure is both costly and time-consuming, requiring conformance with a myriad of local municipal regulations related to trenching of cables and acquiring right-of-way across public property. This infrastructure development is particularly challenging in rural areas with low population densities where trenching cable may be prohibitively expensive.

Broadband wireless communication systems have emerged as a cost-effective alternative for providing last mile network access. These wireless systems can be set up relatively quickly at a fraction of the costs for an equivalent wired infrastructure. These systems have been particularly successful in developing regions of the world, including rural communities in Africa and India, where Wireless Local Loop (WLL)

[1]Last mile is the subscriber access network, also called the local loop, that connects the subscriber with the service provider's network. This is sometimes also referred to as the first mile.

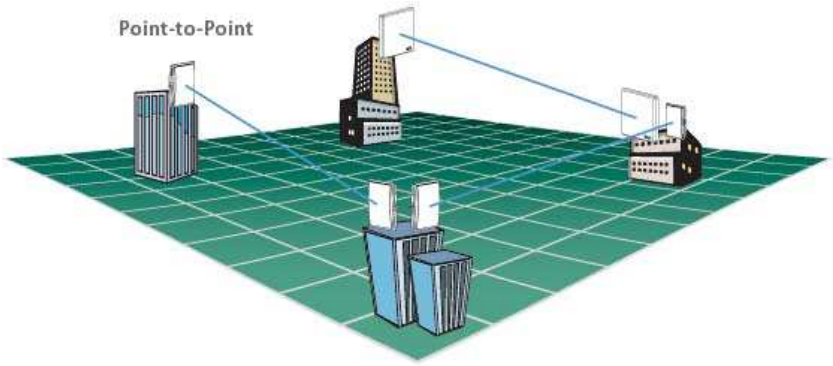

(a) Point-to-point wireless links

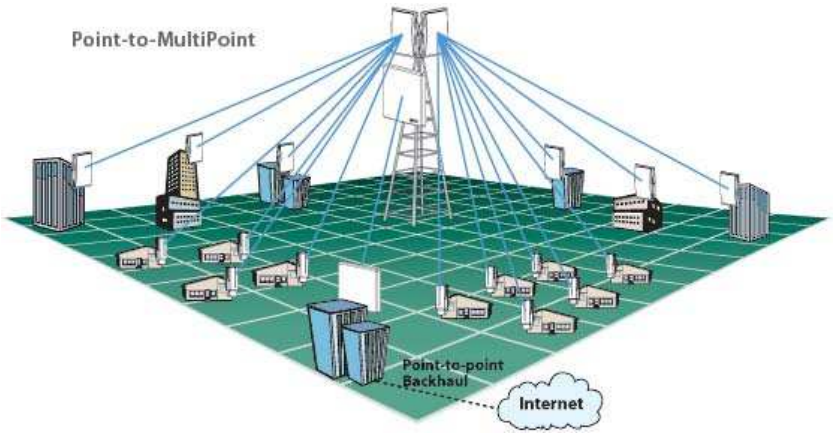

(b) Point-to-multipoint wireless links

Figure 1.1: In point-to-point wireless links, a single radio with a dedicated antenna is used at each end of the link. Point-to-Multipoint wireless links have a 'hub-and-spoke' topology, in which a centralized radio controller can directly communicate with multiple radio nodes over a single hop. Source: Trango Wireless

and cellular technologies are helping improve the quality of life of the local people in unique and significant ways [91].

Traditional Point-to-Point (PtP) (Figure 1.1a) and Point-to-Multipoint (PMP) (Figure 1.1b) wireless systems enable end-to-end communication between two wireless nodes. These networks require detailed site surveys, extensive planning, and deployment expertise for trouble-free operation. Multihop wireless networks (Figure 1.2) support a more flexible communication architecture, where intermediate nodes relay traffic between nodes that may not be able to communicate directly. This establishes end-to-end communication across larger distances and around obstructions, as well as in environments with otherwise high loss rates. Multihop communication architecture also facilitates the reuse of scarce spectral resources

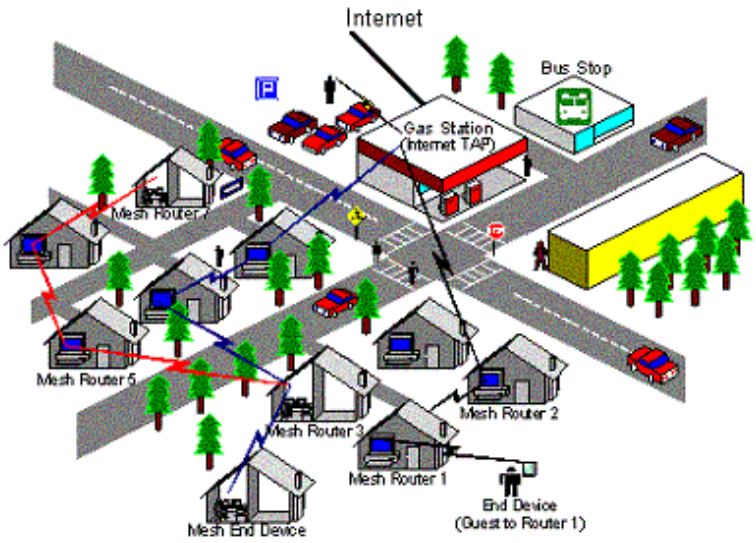

Figure 1.2: A community wireless mesh network. Mesh routers help relay traffic for nodes further away from the gateway. Source: Microsoft Research.

in both spatial and temporal domain [36] (provided the nodes are reasonably well-distributed in space).

1.1 Wireless Mesh Networks

Wireless Mesh Networks (WMNs) are a type of multihop wireless network in which the mesh nodes act both as a host as well as a traffic relay for other nodes in the network. WMNs have two types of nodes: regular *mesh nodes* that can act both as data sources as well as routers, and *gateway* nodes that bridge traffic between the mesh network and a wired network, typically the Internet. In IEEE 802.11s standards terminology, these nodes are referred to as *Mesh Points* (MP) and *Mesh Point Portal* (MPP), respectively. Client devices connect to their preferred mesh node either via wire or over a (possibly orthogonal) wireless channel, and use the multihop wireless relay to communicate with the gateway.

WMNs used for providing last mile backhaul Internet connectivity are also known as community or neighborhood wireless networks [13]. The following characteristics distinguish them from other multihop networks:

- Fixed location: The mesh nodes in a community wireless network are usually affixed to rooftops, utility poles, or some other fixed structures. The topology

of this network is mostly static; infrequent changes occur only with the addition of new nodes, failure/removal of existing nodes, or reconfiguration of links in the network. We anticipate that these topological changes would be rare relative to changes in the network traffic. The fixed location of nodes also implies that they can be powered by the electricity grid, thus not imposing any stringent power-constraints on the network architecture.

- Traffic pattern: The dominant traffic pattern in a WMN is between mesh routers and their designated gateway. Thus, there is many-to-one communication from mesh nodes to the gateway, and one-to-one communication from the gateway to the mesh nodes.

802.11-based WMNs In this dissertation we consider WMNs that use the IEEE 802.11 [26] radios for their multihop wireless backhaul. 802.11 radios are a commodity hardware, operate in license-exempt frequency bands, and can be used in any part of the world in conformance with the regional regulatory requirements. In addition, there is a thriving ecosystem of open source software for these mass-produced radios. A mesh node can be fitted with either a single radio interface or multiple radio interfaces, operating on non-interfering channels, without significantly altering the cost benefits of the system.

The IEEE 802.11 standard specifications were originally conceived for single-hop communication in a Wireless Local Area Network (WLAN). Studies have indicated that these radios exhibit suboptimal performance in multihop networks [126]. The benefits of commodity 802.11 radios, however, seem to far outweigh these performance challenges. A large number of commercial WMN vendors (*e.g.*, BelAir Networks, FireTide, Motorola, and Tropos, amongst others) as well as research testbeds (*e.g.*, TFA at Rice University [16] and MAP at Purdue University [69], amongst others) use 802.11 radios, preferring to address any performance challenges through modifications in other layers of the network stack.

Service model of a community wireless network With the last mile access provided through WMNs, we believe that wireless Internet Service Providers (ISPs) can build a business case for serving rural communities. ISPs only need to provide an Internet point-of-presence (PoP) by installing a gateway mesh router with always-on broadband Internet connectivity. In remote communities, this gateway connection to the Internet may also be a wireless link through satellite or

WiMax networks. Community residents interested in subscribing to the ISP's Internet service can simply configure their commodity 802.11-based mesh routers to communicate with this gateway, either directly or through multihop wireless links.

1.2 Problem Description and Research Goals

Our focus in this dissertation is on understanding and addressing the performance challenges associated with enforcing a policy-driven resource management in 802.11-based WMNs. Our goal is to develop a set of mechanisms that enable an ISP to efficiently manage their network resources while conforming to their desired resource allocation criterion.

Resource allocation has been extensively studied in wired networks. It is often modeled as a constrained optimization problem. The set of constraints in a wireless network are fundamentally different from that of a wired network, and this necessitates a fresh perspective into the problem. The wireless channel is a broadcast medium with its spectral resource shared between all contending nodes. In a localized neighborhood, only a single node can transmit at a time, as concurrent transmissions will results in collisions and subsequent packet loss. These networks also face other sources of packet loss and interference, including scattering and multi-path fading from obstructions in the area [101].

The study of resource management enforcement mechanisms in WMNs is important because it is essential in operating a scalable, functional network. The shared wireless medium limits the capacity of a multihop wireless network, theoretically providing at best $\frac{1}{4}$ to $\frac{1}{3}$ of the raw link bandwidth to the application layer [131]. Studies have indicated that 802.11-based multihop networks achieve only $\frac{1}{7}$ of the raw bandwidth using popular transport protocols [76]. In addition, these network also exhibits extreme unfairness, including starvation, for flows originating multiple hops away from the gateway [38]. This starvation is observed even with Transmission Control Protocol (TCP) which provides fair sharing of bottleneck links in wired networks. Overcoming these fundamental performance challenges is a key requirement for WMNs to become a viable competitor to other access technologies.

Our research objectives can be summarized as follows:

1. We wish to understand the requirement for managing the allocation of network resources in a WMN. In particular, we are interested in exploring the behavior of 802.11 MAC in multihop networks, the response of transport-layer

protocols, and the resulting interaction across these layers under varying traffic loads and network conditions.

2. Devise a framework of mechanisms that can enforce an efficient and a policy-driven allocation of available network capacity. The spectral resource of a wireless network is susceptible to temporal variance in capacity due to unpredictable losses from collisions, interference or other physical-layer phenomenon specific to the radio channel. We are interested in developing solutions that can adapt to these vagaries of the wireless channel.

3. We wish to limit the scope of any proposed resource management framework to a set of mechanisms that can be supported on the commodity 802.11 hardware. Further, the mechanisms need to be incrementally deployable for them to be of any practical utility to a network service provider.

Most of the prior literature for enforcing a rate allocation in WMNs propose some variant of distributed rate limiting protocols. These protocols require periodic flooding of time-varying state information to enable this distributed computation. Interpreting and reacting to this information requires software changes on all mesh routers. This is a significant overhead and challenge in practical deployments where the commodity mesh routers are customer-premises equipment (CPE) owned by the subscribers, and the ISP has little control over them.

In this dissertation we propose a framework of mechanisms based on centralized rate control algorithms to enforce a *fair* allocation of network capacity. (We formally describe various notions of fairness in Chapter 2, though for now it may be interpreted as equity in allocation.) Our approach is motivated by router-assisted flow control mechanisms that have been proposed for use alongside end-host based congestion control protocols in wired networks [35, 84]. We are interested in establishing similar centralized controls in a WMN. With the traffic flows predominantly directed to and from the gateways, the gateway router develops a unified view of the network state, making it a natural choice for policy enforcement or other traffic shaping responsibilities.

Centralized rate control mechanisms offer many advantages over distributed rate control schemes proposed in prior literature. First, since the gateway bridges all traffic between WMN and the wired Internet, it can formulate a unified, up-to-date view of traffic state without any additional signaling overhead. Second, the gateway rate control mechanism requires no software or firmware changes at individual mesh routers. This is advantageous when the mesh routers are commodity CPE, owned

and managed by subscribers with the ISP having little control over them. Third, centralized rate control is effective even when the nodes in the network cannot be trusted to correctly enforce the desired rate control mechanisms. Finally, the notion of centralized rate control also lends itself naturally to providing an auditing and a billing framework that can be essential in supporting the operations of an ISP.

In this dissertation we explore the range of centralized rate control mechanism designs for WMNs. We constrain our design criterion such that *no changes* are required on individual mesh routers, *i.e.*, we limit ourselves to using the standard 802.11 MAC on all mesh nodes and do not require modifications to the networking stack on the end-hosts. These constraints necessarily limit the efficacy of centralized control mechanisms to TCP-like adaptive traffic flows. We find this to be an acceptable trade-off, considering that (*i*) TCP is by far the dominant transport protocol on the Internet [121], and (*ii*), it is the backlogged TCP streams that exhibit the extreme unfairness and starvation in WMNs [38]. In this context we propose, design, and evaluate a set of mechanisms that can centrally manage the rate allocation process for these adaptive traffic streams using only the information locally available at the gateway. Through extensive experimental analysis, we establish that our proposed mechanisms can effectively limit these traffic flows to their allocated share of the network capacity.

1.3 Contributions

Our core contributions in this dissertation are as follows:

1. We demonstrate that commonly used router-assisted flow control mechanisms, including work-conserving packet scheduling and probabilistic packet drop techniques are ineffective as centralized rate allocation techniques in WMNs. We show that this is due to fundamental differences in the abstraction of wired and wireless networks, including link scheduling and packet loss characteristics. Our results show that non-work-conserving rate-based scheduling enforced via traffic aggregation points (*e.g.*, gateway node) can provide an effective control over resource allocation for adaptive traffic streams.

2. We show that when we regulate the *net* amount of traffic bridged by the gateway to an aggregate representing the sum of fair rates, the underlying 802.11 MAC apportions the allocated capacity fairly between all nodes. Based on these characteristics, we propose, design, and evaluate heuristics that allow

the gateway node to determine this aggregate value using only local information, thus incurring a *zero control traffic overhead*.

3. For finer-grained control over the rate allocation, we propose and evaluate per-node rate control at the gateway. This allows us to extend the rate allocation mechanism to support weighted fairness, amongst other criterion. We extend our zero-overhead heuristics to support per-flow rate control via gateway routers in a WMN.

4. We evaluate the performance of our proposed heuristics using simulations as well as experiments on a multihop wireless testbed. Further, we reproduce the testbed topology in our simulation framework to validate the results across the two environments. To the best of our knowledge, this is the first work to demonstrate centralized rate allocation mechanisms for multihop networks on an actual testbed.

In addition to these listed contributions, additional minor contributions have also been made. First, we dispel an implicit assumption often made in the literature (*e.g.*, [28]) that spectrum around the gateway is the main bottleneck that limits the performance of a WMN. We show that depending on the network topology and wireless link rates, distributed bottlenecks can exist even in a WMN where the traffic flows are predominantly directed towards the gateway. Second, we show how aggregate network capacity bounds can be computed at the gateway using only the local information. We demonstrate how these capacity bounds may be used with binary search heuristics to provide faster convergence towards the desired rate allocation.

1.4 Thesis Outline

This dissertation is organized into two parts. Part I provides background information and a literature survey of related work. In Chapter 2 we first review the fundamental concepts used in this dissertation: the notion of fairness in resource allocation, wireless communications and MAC protocols, and TCP. We then analyze the behavior of 802.11 radios in multihop networks and the resulting suboptimal performance of TCP in Chapter 3. A number of models have been proposed for estimating the capacity of a multihop wireless network and using that to compute the 'fair' rate allocation for a given set of flows. We describe two of these models,

the clique-graph model and the collision-domain model, in Chapter 4. Finally, in Chapter 5 we provide a literature review of different techniques for addressing the fairness and rate allocation performance challenges in wireless networks.

Part II of this dissertation details our proposed centralized rate controllers. In Chapter 6, we evaluate a number of commonly used router-assisted flow control mechanisms and establish that non-work-conserving rate-based centralized scheduling can enforce fairness in a WMN. Using both simulations and testbed analysis, we evaluate such centralized rate limiters and show that our results are comparable with techniques that require modifications on all mesh routers. In Chapter 7 we propose, design, and evaluate rate allocation heuristics that achieve max-min fairness across adaptive flows. We extend this work further in Chapter 8 to achieve weighted max-min rate allocation for given set of flows. We wrap up this dissertation by summarizing our conclusions and future work in Chapter 9.

Part I

Background and Related Work

Chapter 2

Review: Fairness, Wireless MAC Protocols, and TCP

In this chapter we introduce the various building blocks that shape the model of our system. We start by describing the fundamental notion of fairness in resource allocation as used in packet-switched data networks. We provide a taxonomy of commonly used fairness criterion and provide performance indices for quantifying the degree of fairness in an allocation. We then change gears into wireless networks. The wireless channel places fundamental limitations on the performance of radio communication systems. We first describe the radio propagation and communication models that we use to capture some of the intricacies of the wireless channel. We then describe the carrier sensing (CS) MAC protocols that provide distributed access to the shared wireless channel. In particular, we focus on the IEEE 802.11 DCF MAC. Finally we summarize the congestion control characteristics of TCP that determine its transmission rate in a given network.

2.1 Fairness

Fairness is a hard term to define as the notion of fairness varies widely depending upon policies and system objectives. For our purposes, fairness may be described as equality with respect to the proposed resource allocation [51]. In packet-switched data networks, resource could be network bandwidth, delay, or power (defined as the ratio of a flow's throughput to its round-trip delay [93]). Fairness is an important consideration in today's heterogeneous networks where there is no global deployment of admission control or minimum QoS-guarantee mechanisms. In this

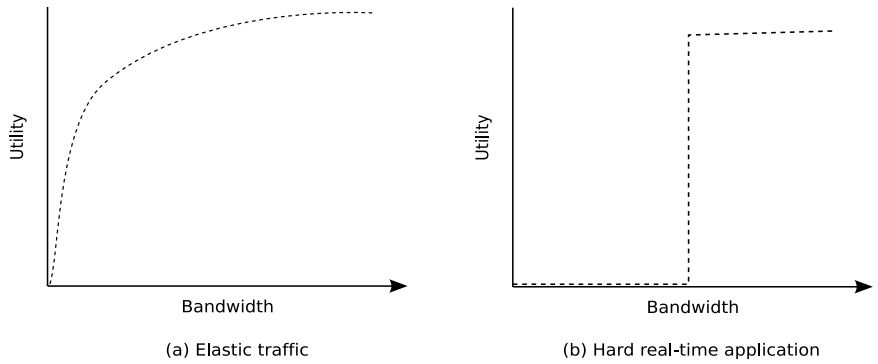

Figure 2.1: Utility function for an elastic application (Figure 2.1a) and for a hard-real-time application (Figure 2.1b).

best-effort network, fairness is usually studied in the context of scheduling algorithms that govern the provisioning of link bandwidth and buffer space between different flows across a router.

2.1.1 Taxonomy of Fair and Efficient Resource Allocation Mechanisms

The concept of fairness has been extensively studied in fields like political sciences or political economics. The notion of "utility theory" borrowed from economics is often used to study resource allocation in computer networks. Utility may be described as a measure of relative satisfaction based on a given allocation of a resource bundle, such that if the user prefers a resource bundle A over B, then the user's utility of A is greater than that of B. The user's preference for a resource can then be modeled using a utility function $U()$. If r is the allocated resource then $U(r)$ is a user's utility for that resource.

The utility function captures user's preference based on their resource-usage pattern. Elastic traffic (like HTTP, FTP using TCP, *etc.*) is modeled using a monotonically increasing, strictly concave, and continuously differentiable utility function (Figure 2.1a). In contrast, hard-real-time traffic with a strict predefined QoS requirements may have a simple on-off step utility function (Figure 2.1b).

Let $\mathbf{R} = \{r_1, r_2, ..., r_N\}$ be the vector of rates allocated to N users. Let C be the total capacity of the link that these users share. Then the corresponding utility vector $\mathbf{U} = \{U_1(r_1), U_2(r_2), ..., U_N(r_N)\}$. In this context, a fair allocation may be considered in different ways (Figure 2.2):

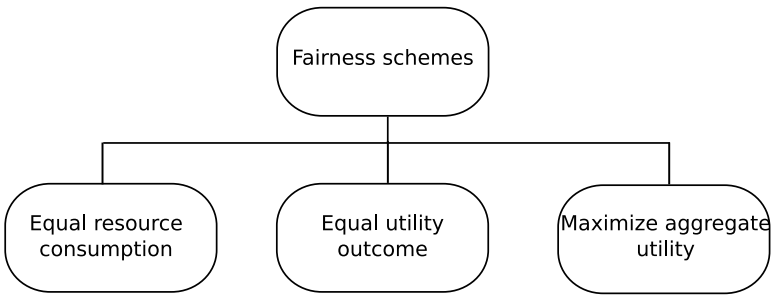

Figure 2.2: A Utility-theory based taxonomy of fairness criterion.

- One possibility is *equal resource consumption*, such that $r_i = r_j,\ \forall\ i, j \in N$. This allows resources to be distributed equally between the users.

- While equal resource consumption distributes resources equally, the utility of different users may be different for the same allocated resource. Another possible allocation is to provide *equal utility outcome*. This allocates the resource vector $\mathbf{R}$ such that all elements of the utility vector $\mathbf{U}$ are equal, *i.e.*, $U_i(r_i) = U_j(r_j),\ \forall\ i, j \in N$.

- Whenever resources are limited in comparison to demand, there is always a conflict between optimal vs. fair resource allocation. Equal utility outcome may be highly inefficient; the same resource may be valued much differently by the users, and a different allocation could have vastly improved the aggregate utility of the system. Thus, another allocation may be to to maximize *system aggregate utility*. If the utilities are additive, then the aggregate system utility is defined by the sum of individual user's utility.

$$\begin{aligned} \text{Maximize} \quad & \textstyle\sum_{i=1}^{N} U_i(r_i) \\ \text{subject to} \quad & \textstyle\sum_{i=1}^{N} r_i \ \leq C \\ & r_i \geq 0, \forall i \in N \end{aligned}$$

The constraints on this objective function are the *feasibility constraints* described by Kelly *et al.* [65]; a set of flow rates is feasible if rates are non-negative and the aggregate rate of all flows traversing a link is not greater than that link's capacity. These constraints ensure that a transmission schedule can achieve the prescribed rate vector.

2.1.2 Fairness Criterion

We now describe the allocation of flow rates $\mathbf{R} = \{r_1, r_2, ..., r_N\}$ based on three fairness criterion commonly used in the research literature.

Absolute Fairness

It is based on the premise that a user is entitled to as much of network resource as any other user, and no more. Thus under this fairness criterion, the rates are equally distributed between all the users, *i.e.*, $r_i = r_j, \ \forall \ i, j \in N$. This fairness criterion is used when all flows in the network have equal demand.

Max-Min Fairness

Typically, flows in a network exhibit varying resource demand. In such circumstances, max-min fairness can be defined as follows [66]:

1. Resources are allocated in order of increasing demand.
2. No source gets a resource share greater than its demand.
3. Sources with unsatisfied demands get an equal share of the resource.

This definition of max-min assumes a single bottleneck, and thus provides all sources with unsatisfied demand an equal share of the bottleneck link. In networks with multiple bottlenecks, it is possible that a flow might not be able to use all of its share in a given bottleneck because its rate is limited by a bottleneck in another part of the network. In such circumstances, the excess capacity may be shared fairly amongst the other nodes.

An allocation is max-min fair if no component in this rate vector can be increased without simultaneously decreasing another component that is already small. More formally, it is defined as follows [11]:

Max-min fairness Mathematically, a vector of rates $\mathbf{R} = (r_i, i \in N)$ is *max-min fair* if for each $i \in N$, r_i cannot be increased while maintaining feasibility without decreasing some r_{i^*}, for some i^* for which $r_{i^*} \leq r_i$.

Max-min fairness is based on the premise that a user is entitled to as much of network resource as any other user. Often this resource is the user's share of the network capacity. Max-min fairness attempts to allocate bandwidth equally

amongst all the sources with unsatisfied demand at a bottleneck link. It thus follows the notion of equal resource consumption described in Section 2.1.1 as it assumes the utility or benefit to each source is the same for the given throughput.

Proportional Fairness

An allocation $\mathbf{R} = (r_i, i \in N)$ is defined as *proportionally fair* if for any other feasible allocation $\mathbf{R}^* = (r_i^*, i \in N)$, the aggregate of the proportional change is 0 or negative [64].

$$\sum_{i \in N} \frac{(r_i^* - r_i)}{r_i} \leq 0$$

Proportional fairness follows the notion of maximizing aggregate utility described in Section 2.1.1. Using logarithmic utility functions to represent elastic traffic, Kelly [64] showed that the rate allocation that satisfies the utility maximization requirement must be such that any change in the distribution of rates would make the sum of proportional change less than or equal to zero. In a network with a single bottleneck, proportional fairness is the same as max-min fairness. However, in a network with multiple bottlenecks, proportional fairness allows excess capacity left from a flow that cannot use all its share to be instead given to flow(s) that would benefit from a proportionately larger increase in flow rate(s).

We illustrate these different notions of fairness using the network in Figure 2.3. The three nodes are connected via wired, tandem links of capacity R. Both absolute and max-min fairness criterion yield a rate vector of $(f_1, f_2, f_3) = (\frac{R}{2}, \frac{R}{2}, \frac{R}{2})$, where R is the link capacity of links 1 and 2. Proportional fairness gives a rate allocation vector of $(f_1, f_2, f_3) = (\frac{2R}{3}, \frac{2R}{3}, \frac{R}{3})$. Since flow 3 uses both links, it consumes more system resources. Proportional fairness results in greater system gain at the cost of sacrificing the throughput of f_3.

2.1.3 Fairness and Capacity Trade-off

There is a trade-off between the objectives of maximizing system capacity and providing fairness, *e.g.*, in Figure 2.3, flow f_3 consumes twice as much resource (as it traverses two links) as either flows f_1 or f_2. Thus total network capacity is maximized when f_1 and f_2 are allocated the entire capacity of links 1 and 2 respectively, while starving f_3.

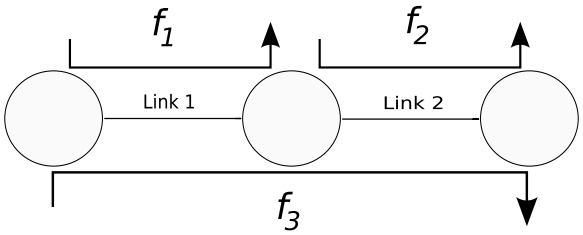

Figure 2.3: A simple topology with three nodes connected via wired, tandem links each of capacity R. The arrows denote three flows in this network. Both absolute and max-min fairness yield a rate vector of $(f_1, f_2, f_3) = (\frac{R}{2}, \frac{R}{2}, \frac{R}{2})$. Proportional fairness results in a rate vector of $(f_1, f_2, f_3) = (\frac{2R}{3}, \frac{2R}{3}, \frac{R}{3})$.

2.1.4 Pareto Efficiency

An allocation of resources is *Pareto efficient* (also called *Pareto optimal*) if there does not exist another allocation in which one component is better off and no component is worse off [70]. Both max-min fairness and proportional fairness are also Pareto optimal, though the converse is not necessarily true, *e.g.*, in Figure 2.3, an allocation of $(f_1, f_2, f_3) = (R, R, 0)$ is Pareto optimal as increasing the rate of f_3 requires decreasing the rate of f_1 and f_2.

2.1.5 Quantitative Measurement of Fairness and Efficiency

We now describe some metrics for quantitatively qualifying the degree of fairness in a given rate allocation. We note that both variance and standard deviation are frequently used as statistical measures of spread in a given distribution. However, these values are tightly coupled with the observed measurement and their unbounded nature does not lead to an intuitive interpretation across different environments.

Jain's Fairness Index

Jain's Fairness Index (JFI) [51] is commonly used for quantitatively measuring the degree of fairness achieved by a resource allocation mechanism. Let $\mathbf{R} = \{r_1, r_2, ..., r_N\}$ be the measured rate vector for N flows. JFI for this vector is defined as follows:

$$JFI = \frac{(\sum_{i=1}^{N} r_i)^2}{N \sum_{i=1}^{N} r_i^2}$$

This index measures the deviation from an ideal rate vector where *all components are equal*. For flows with max-min rate allocation, we adapt this index as follows: let $\mathbf{O} = \{o_1, o_2, ..., o_N\}$ be the fair rate allocation vector based on max-min optimality. The fairness index is then computed over normalized flow throughput $x_i = \frac{r_i}{o_i}$, $\forall i \in N$:

$$JFI = \frac{(\sum_{i=1}^{N} x_i)^2}{N \sum_{i=1}^{N} x_i^2}$$

It can be shown that JFI is a decreasing function of the Coefficient of Variation (CoV $= \frac{s}{\mu}$, *i.e.*, the standard deviation s of a distribution scaled by its mean, μ) as follows:

$$JFI = \frac{1}{1 + CoV^2}$$

The fairness index is always bounded between $\frac{1}{N}$ and 1. A perfectly fair system will have a JFI of 1, while a totally unfair system, in which all resources are allocated to a single user, will have a JFI of $\frac{1}{N}$.

Normalized Flow Throughput

While JFI is a popular measure of the fairness, it can produce seemingly high values given skewed rate distributions. Consider a network with 10 flows in which 9 flows obtain equal throughput, while 1 flow starves. This allocation has a JFI value of 0.9. The same JFI value is also obtained if 5 flows receive 100% of their fair share, while the other half only get 50%. Thus additional metrics are necessary to isolate starving users that cannot be identified by JFI. In this dissertation we list $\frac{min.\,flow\,rate}{fair\,rate}$ and $\frac{max.\,flow\,rate}{fair\,rate}$ to illustrate the imbalance between the minimum and the maximum throughput flows in a given experiment.

Effective Network Utilization

Both fairness and capacity are important measures of a resource allocation criterion, *e.g.*, a network in which all flows starve is perfectly fair but practically useless.

We are thus also interested in quantifying the network capacity achieved by a given resource allocation. A simple sum of the elements of a given rate vector is insufficient as it does not factor in the bias that multihop flows consume more spectral resource than single hop flows. Instead, we define *effective network utilization* [132] $U = \sum_{i \in N} r_i \times l_i$, where r_i is the measured throughput for flow f_i, and l_i is a measure of the distance covered by that flow. We substitute l_i with the number of hops between the source and destination on the routing path of flow f_i. For analysis, we list the value of $\frac{U}{U_{opt}}$, where U_{opt} is the effective network utilization determined by some 'optimal' rate allocation algorithm.

2.1.6 Comparison: Congestion Control vs. Fairness

Congestion refers to a state of sustained network overload during which the demand for shared network resources equals or exceeds the provisioned capacity [42]. Typically, these resources are link bandwidth and router queue space.

Congestion control and fairness are both concerned with the utilization of network capacity resources. These two are thus conceptually related, though they have different objectives. When the resource is plentiful but the demand for it is limited, then the resource can be simply allocated according to demand, *i.e.*, there is no need to consider trade-offs in terms of fair allocation of resources. Fairness becomes an issue only when there are unsatisfied demands and users are required to compete for their share [42]. Thus, when the network is uncongested and demand is bounded, fairness is a non-issue. However, in periods of heavy network congestion, fairness must constitute an integral part of any feasible congestion control protocol.

In multihop wireless networks, congestion and fairness are independent network characteristics and one cannot necessarily be achieved through the other [20]. We illustrate this using the network topologies in Figures 2.4 and 2.5. We assume a *fair* wireless MAC protocol that allocates transmission opportunities equally between nodes. Figure 2.4 shows a topology in which the network is congested even when local fairness is enforced by the MAC. Figure 2.5 shows an uncongested yet unfair topology; per-flow fairness cannot be enforced simply by ensuring that sum of the input flows into node e does not exceed its output. Other network states when the network is uncongested and unfair or congested and unfair are also possible. They are respectively achieved when the network is underutilized or when the traffic-generation rate at the multihop wireless nodes exceeds the network carrying capacity.

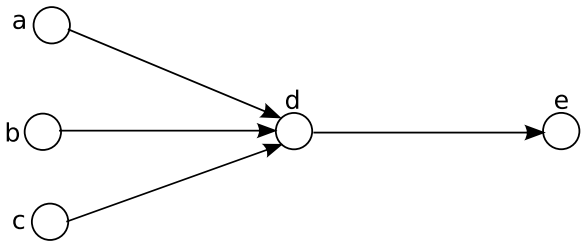

Figure 2.4: If a fair MAC allows each node to transmit only once in a sequence, congestion still builds up and results in queue overflow at node d which has to forward packets from nodes a, b, and c. Thus local fairness directly leads to buffer overflow at node d.

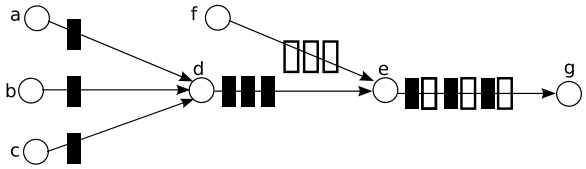

Figure 2.5: The congestion control algorithm at node e might allow e to transmit only 6 packets/s. When combined with local fairness, this provides node f three times the goodput of nodes a, b, or c. Thus resolving congestion does not guarantee fairness.

2.2 Wireless Communication Models

Radio propagation model Radio propagation in a wireless channel is characterized by pathloss through signal attenuation, as well as shadowing due to lack of a clear Line of Sight (LoS) between the transmitter and receiver. Radio propagation models are used to predict the average received signal strength at a given distance from the transmitter. The *free-space* path propagation model is used when the distance between the sender and the receiver is small, such that the unobstructed line-of-sight propagation is the dominant path [101]. Over larger distances ($>$ 100 m.), reflections from other objects also need to be accounted. For our simulations, we use the *two-ray ground reflection* model which considers the direct path as well the ground-reflected propagation path between the transmitter and receiver. According to this model, the mean received signal power follows an inverse distance power-loss law with an exponent α approximately equal to 4, *i.e.*, the received

power P_r at a distance d from a transmitter with transmit power P_t is given by:

$$P_r(d) \propto \frac{P_t}{d^4}$$

This model is known to be reasonably accurate in estimating signal strengths in outdoor environments [101].

Communication model Frame reception at a receiver can be modeled as a function of the received signal strength. In particular, if the received signal strength is above the receiver sensitivity threshold RX_{Thresh}, the frame is received correctly. RX_{Thresh} is a function of the modulation technique used for encoding the information. If the received power of the incoming frame is less than receive threshold RX_{Thresh} but greater than carrier sense threshold CS_{Thresh}, the frame is marked as error and then passed to the higher (MAC) layer. Finally, if the received power is less than CS_{Thresh}, the frame is discarded as noise. Per the radio propagation model described earlier, the signal strength drops as a function of the distance between the transmitter T and receiver R. RX_{Thresh} can then be used to define the maximum $T - R$ separation at which a frame can be successfully decoded if there are no concurrent transmissions from interfering nodes. Similarly, CS_{Thresh} can be used to define the minimum separation outside of which the transmissions cannot be detected. We use these distance separation requirements to define the following radio ranges [117] shown in Figure 2.6:

- Transmission range: The *transmission range* of a transmitter T is the distance space around T within which the received signal strength of T's transmissions remains high enough to allow a successful reception.
- Interference range: The *interference range* is the distance space around a receiver R within which a transmission from node T_1 will corrupt the message exchange between R and the transmitter T.
- Carrier sense range: The *carrier sense range* is the distance space around the transmitter T within which the radio strength of T's transmission is greater than the receiver's carrier sense threshold.

2.3 Wireless MAC protocols

The performance of a wireless network is largely dependent on the Medium Access Control (MAC) protocol that controls and coordinates access to the shared wireless

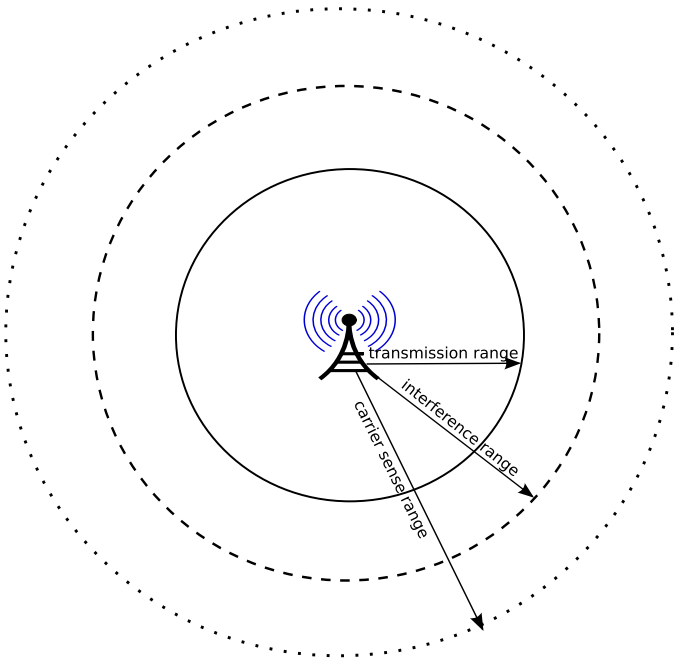

Figure 2.6: A simplified wireless communication model showing the transmission, interference, and carrier sense range associated with a radio

spectrum. Wireless MAC protocols can be broadly classified into contention-free and contention-based protocols [71]. Contention-free protocols such as Time Division Multiple Access (TDMA) typically require a centralized arbitrator to coordinate medium access. This increases the complexity of MAC protocols, *e.g.*, TDMA requires at least some course-level time synchronization between the network nodes. In contrast, contention-based protocols can be enforced via simple distributed mechanisms, but they introduce the risk of collisions. Multihop networks are often built using contention-based protocols.

The simplest contention-based MAC protocols are random access protocols such as ALOHA in which a node transmits whenever it has data to send. ALOHA scales poorly under increased traffic load, with collisions reducing the efficiency to 18% of the link capacity [113]. Carrier Sense Multiple Access (CSMA) protocols can alleviate some of these collisions by requiring a node to defer its transmission if it can carrier sense an ongoing transmission. Various methods such as p-persistent and nonpersistent algorithms can be used to determine how long a node waits before it attempts the next transmission. In p-persistent schemes, a node either transmits with a probability p or defers with a probability $1 - p$ if the channel is idle; if the channel is busy, it waits for a random time and then contends again. In

nonpersistent schemes, a node makes the transmission if the medium is idle; if the medium is busy, it waits for a random time before repeating this algorithm.

2.3.1 CSMA/CA protocols

Carrier sense protocols can alleviate collisions, though they cannot eliminate them. From an efficiency perspective, it makes sense for a node to immediately stop its transmission when it detects a collision. This is the basis of CSMA with Collision Detection (CSMA/CD) protocol used in wired Ethernet. Collision detection, however, is not possible in wireless environments due to two reasons: (1) Most radios are half-duplex and cannot transmit and detect collisions at the same time. Full-duplex radios are expensive to build as they require additional filters to carefully separate transmit and receive functions at different frequencies so to prevent the transmitter from overwhelming the receiver circuitry. (2) Even a full-duplex radio cannot detect all collisions, since the collisions occur at the receiver and not the transmitter (see the section on Hidden terminals below).

Many wireless networks use CSMA with Collision Avoidance (CSMA/CA) protocols that use carrier sensing along with a random backoff to avoid collisions. CSMA/CA as used in Apple Localtalk network [62] introduced Request To Send and Clear To Send (RTS/CTS) control frames that preceded a data transmission. The utility of RTS/CTS has evolved over the years (see below), but in Localtalk its primary use was to prepare the receiver for data reception by having it allocate an appropriate buffer space.

Hidden and Exposed Terminals

A CSMA/CA transmitter uses carrier sensing to schedule its transmissions in a way to avoid collisions with other ongoing transmissions. However, collisions can still occur at a receiver because of transmissions from another station that cannot be carrier sensed by the first transmitter [115]. Consider a transmission from node A to node B as shown in Figure 2.7. The solid circle represents the transmission range of A and the dotted circle represents the transmission range of B. Hidden terminals (*e.g.*, node H) are nodes in the transmission range of the receiver B but out of the carrier sense range of the transmitter A. When A transmits to B, H cannot carrier sense this communication and may attempt to schedule its own transmission. This produces a collision at B. Hidden terminals produce excess collisions, reducing the aggregate capacity of the network.

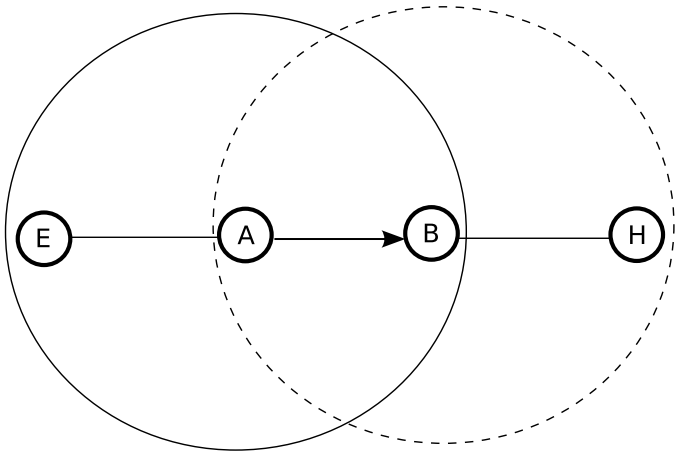

Figure 2.7: Hidden/Exposed terminals in a multihop network.

Exposed terminals refer to the inability of the transmitters to simultaneously use the wireless medium for transmissions, even when their transmissions will not collide at their respective receivers. Exposed terminals (*e.g.*, node E in Figure 2.7) occur when a node is in the carrier sense range of a transmitter (node A) but not in the interference range of a receiver (node B). When there is an ongoing transmission from A to B, E cannot initiate a transmission even though B is outside its transmission range. Exposed terminals result in wasting good transmission opportunities, reducing achievable network capacity.

RTS/CTS Control Packets

Karn [62] pointed out that carrier sensing by a transmitter is of little use since packet reception depends upon the interference around the receiver, and not the transmitter. He proposed MACA (Medium Access with Collision Avoidance) protocol that forgoes carrier sensing and instead uses RTS/CTS control frames used by Localtalk network to counter hidden and exposed terminals. When node A wishes to transmit to node B, it first sends an RTS frame containing information about the size of data it wishes to transmit. B responds with a CTS frame and echoes the data size information. Node A then transmits its data to B. When node E hears the RTS frame from A addressed to B, it only inhibits its transmission long enough for B to respond with a CTS. Similarly, when node H hears B's CTS, it inhibits its transmission long enough for B to receive the data frame from A.

2.3.2 IEEE 802.11 MAC

The IEEE 802.11 specifications [26] is a standard for medium access control (MAC) and physical layer (PHY) specifications for wireless connectivity within a local area. A number of extensions to the PHY specifications have been proposed over the years, resulting in standards such as IEEE 802.11a and IEEE 802.11g, which use the same MAC but different PHY layer specifications to support data rates up to 54 Mb/s for 802.11a/g and 11 Mb/s for 802.11b radios.

The IEEE 802.11 MAC specifies two coordination functions for medium access: the mandatory contention-based protocol called Distributed Coordination Function (DCF), and the optional contention-free access protocol called Point Coordination Function (PCF). DCF can operate in infrastructure mode called infrastructure Basic Service Set (BSS) or ad hoc mode called Independent Basic Service Set (IBSS). PCF requires the presence of a Point Coordinator (typically an Access Point) that performs polling, thus enabling the polled stations to transmit without contending for channel access. PCF is an optional part of the standard, and hence supported by only a limited number of vendors. Multihop networks operate in IBSS mode as there is no central controller to coordinate polling between all stations in the network.

DCF

DCF uses CSMA/CA with positive acknowledgments (ACKs) for unicast data frames. DCF uses a combination of mandatory physical carrier sensing and optional virtual carrier sensing to avoid collisions at the transmitter and receiver, respectively. Physical carrier sensing is provided by the radio circuitry which interprets the presence of carrier as a sign of ongoing transmissions. Virtual carrier sensing is provided by RTS/CTS frames. These frames announce the duration of a pending data exchange. Stations that hear either the RTS or CTS then set their Network Allocation Vector (NAV) equal to this duration; the standard requires these stations to wait out this NAV duration before contending for medium access [40].

Interframe spacing 802.11 uses five different interframe spaces (IFS). In effect, these create priority levels for different types of traffic: higher priority traffic waits a shorter IFS before transmission [40]. We briefly discuss the IFS relevant to our work below:

- Short IFS (SIFS) is for highest priority transmissions, including CTS and ACK following an RTS and Data frame, respectively. SIFS has the smallest duration of all IFS, thus allowing these high priority transmissions before other frames. Its exact value is dependent on the particular PHY in use; SIFS is 10 μs for Direct Sequence (DS) PHY used in 802.11b and 16 μs for OFDM PHY used in 802.11a/g.

  One practical implication of SIFS is that it limits the physical distance across which an 802.11 link can operate. Assuming that the speed of light through air is 3×10^8 m/s, 10 μs correspond to a round-trip distance of 3000 m. or 1500 m. one-way. Loose implementation of the standard specifications, however, allow 802.11 links spanning tens of kilometers [48].

- DCF IFS (DIFS) defines the minimum medium idle time for transmissions in the contention period. It is defined in terms of SIFS as follows:

$$DIFS = SIFS + 2 \times Slot\,Time$$

  The slot duration is PHY-dependent; a higher-speed PHY uses shorter slot times. The slot times for DS PHY and OFDM PHY are 20 μs and 9 μs, respectively. The corresponding DIFS intervals are 50 μs and 34 μs, respectively.

- PCF IFS (PIFS) is used in PCF mode. We refer the reader to the standard specifications [26] for related details.

- Extended IFS (EIFS) is used only when errors are detected in frame reception. If a node in carrier sense range detects a transmission it cannot decode, it cannot correctly set its NAV counter for the duration of that transaction. To prevent a collision with the ACK at the transmitter, such nodes wait for an EIFS duration which the standard declares as longer than the duration of an ACK transmission. EIFS is defined as follows:

$$EIFS = SIFS + DIFS + ACK\,transmission\,time$$

  where ACK transmission time is the time in μs required to transmit an ACK frame.

- Arbitration IFS (AIFS) was introduced by Task Group E as a part of amendments for supporting QoS in the 802.11 MAC. We describe AIFS in Section 2.3.2 below.

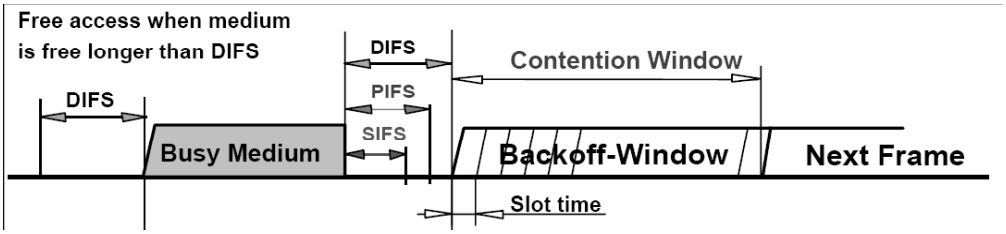

Figure 2.8: IFS relationships

DCF uses the CSMA/CA protocol as follows: A station wishing to transmit senses the medium. If the medium remains free for a DIFS duration, then the station is allowed to transmit. If however, the medium is busy, then the station waits until the channel becomes idle for a DIFS duration, and then computes a random backoff time in the range of [0, CW] time slots, where CW is the current contention window size [95]. The station then starts decrementing its backoff timer until either the medium becomes busy again, or the timer reaches zero. The station freezes the timer when the medium becomes busy, and restarts when the medium again becomes idle for a DIFS duration. When the timer finally decrements to zero, the station transmits the frame.

If the timer for two or more stations decrements to zero at the same time, a collision occurs. The two transmitters cannot detect a collision and timeout waiting for their respective ACKs. Each transmitter then doubles the value of its CW, chooses a new backoff, and the process is restarted. The CW is doubled after every timeout, increasing exponentially till it reaches CWmax set to 1023 in the standard. Depending on its size, a frame may be retransmitted up to a maximum of short retry count or long retry count, after which it is eventually discarded and CW reset to CWmin, equal to 31 for DS PHY and 15 for OFDM PHY. CW is also reset to CWmin after a successful transmission.

Hidden and Exposed Terminals in DCF

Virtual carrier sensing through RTS/CTS and the use of NAV can address the basic hidden terminal problem. Figure 2.9 shows a message transaction using RTS/CTS control frames in a DCF MAC. RTS/CTS, however, does not address scenarios in which a hidden node H lies in the interference range of a receiver B [124] (refer to Figure 2.7). H cannot decode B's CTS frames, but its transmissions can still disrupt packet reception at B. The standard attempts to limit such hidden terminals by

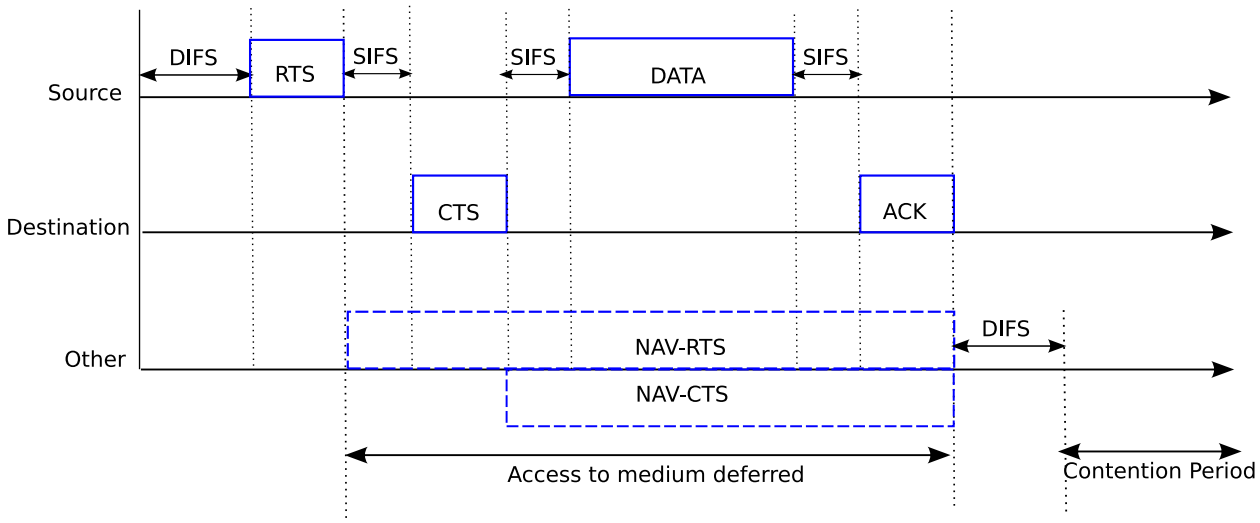

Figure 2.9: Use of RTS/CTS and NAV for virtual carrier sensing in DCF.

requiring that RTS/CTS control frames are exchanged at a base rate of 1 Mb/s or 2 Mb/s for 802.11b, and 6 Mb/s for 802.11a/g radios. The modulation schemes at these lower rates require reduced receiver sensitivity, and thus these messages can be interpreted by distant nodes. These lower data rates make RTS/CTS exchange a considerable overhead, specially for smaller data packets. The standard therefore allows defining a packet size threshold above which RTS/CTS handshake is used. Data frames shorter than this threshold are sent without the handshake.

We note that the combination of physical and virtual carrier sensing as used in DCF cannot resolve the exposed terminal problem. The two-way RTS-CTS-Data-ACK message exchange in DCF requires the MAC to clear the spectrum around both the transmitter and receiver for the duration of the message exchange, thus inhibiting transmissions from any exposed terminals. We revisit the hidden and exposed terminals in Section 5.1.1 where we describe other solutions to this problem.

802.11e Quality of Service

DCF does not include any service differentiation mechanism and can only provide a "best-effort" service irrespective of application requirements. To support MAC-level Quality of Service (QoS), Task Group E ratified a set of amendments that were eventually merged into the revised 802.11 standard [26]. A new coordination func-

tion called Hybrid Coordination Function (HCF) is introduced. It includes both a contention-based channel access called Enhanced Distribution Channel Access (EDCA) as well as contention-free access called HCF Controlled Channel Access (HCCA). The two mechanisms can operate concurrently like DCF and PCF. However similar to DCF, EDCA is expected to be the dominant of the two access mechanisms.

EDCA can support eight user priorities which map to four access categories (ACs). Each access category has its own transmission queue. Service differentiation is provided through a different set of channel access parameters for each AC: CWmin, CWmax, a new interframe space called Arbitration Interfame Space (AIFS), and transmission opportunity duration limit (TXOP limit). AIFS is defined as follows:

$$AIFS = SIFS + AIFSN \times aSlotTime$$

where $AIFSN$ is the AIFS number for the AC and $aSlotTime$ is the duration of a time slot corresponding to the modulation type. EDCA supports packet bursting to improve throughput performance and a station is allowed to send more than one frame without again contending for channel access. TXOP limit for an AC limits the size of the burst for an AC. High priority ACs are assigned smaller values for CWmin, CWmax, and AIFS, decreasing their channel access delay and thus increasing their access probability.

Fairness Characteristics of DCF

The DCF access mechanism is designed to provide each station in a BSS with an equal number of transmission opportunities (TXOPs) [26], irrespective of their wireless link rates. This mechanism translates to max-min throughput fairness as long as the stations use the same packet size and experience similar loss characteristics [112].

2.4 Transmission Control Protocol

The Transmission Control Protocol (TCP) is the de facto transport protocol for reliable delivery of data over the Internet. While the formal specifications of TCP were introduced in RFC 793 [94], a number of variants have been developed over

the years, including Tahoe, Reno, Vegas, SACK, and others [109]. In this section we describe the commonly used NewReno TCP specification [34]. We review the essential fundamentals of TCP that govern its transmission rate. We refer the reader to the relevant RFCs [8, 34, 94] for other details of the protocol.

TCP is a byte-stream-based connection-oriented protocol that uses sliding windows and acknowledgments (ACKs) to provide reliable, in-order delivery of data. A TCP *segment* is the basic unit of transmission. It is represented by a contiguous sequence of bytes identified by a 32-bit monotonically increasing *sequence number*. The size of a segment is bounded by the Maximum Segment Size (MSS) negotiated between the sender and receiver. The receiver acknowledges receipt of a segment by transmitting an ACK containing the sequence number of the next expected byte. TCP ACKs are cumulative, *i.e.*, an ACK with sequence number N acknowledges receipt of all bytes with sequence number up to $N - 1$.

2.4.1 Loss Discovery

TCP provides reliability through retransmission of lost segments. It uses two mechanisms to detect a loss: (1) timeout waiting for ACK, and (2) receipt of three duplicate ACKs. We discuss these below.

Timeouts The TCP sender assumes that a segment is lost if it does not receive an ACK covering that segment within a certain timeout interval called retransmission timeout (RTO). To set this timeout, the sender maintains an exponentially weighted moving average (EWMA) of the round-trip time (RTT) as follows:

$$SRTT = \alpha \times RTT + (1 - \alpha) \times SRTT$$

where α is a smoothing factor that determines how much weight is given to older values. The connection also maintains a mean linear deviation RTT_{dev} of all acknowledged segments. RTO is then set to

$$RTO = SRTT + 4 \times RTT_{dev}$$

If the retransmitted segment is also lost, the network is assumed to be in a state of severe congestion. RTO is then exponentially backed off after each unsuccessful retransmission. This slows down the rate of injecting retransmitted segments in the network. Additional details about timer management and RTT calculation can be found in the literature [49, 109].

Duplicate ACKs When the TCP receiver receives an out-of-sequence data segment, it is required to transmit a duplicate of the last ACK it sent out [8]. This serves the purpose of letting the sender know that a segment was received out-of-order, and which sequence number is expected. From the sender's perspective, duplicate ACKs can be caused by dropped segments, re-ordering of data segments, or replication of an ACK or data segment by the network. The sender considers the arrival of 3 duplicate ACKs packets in a row as an indication that a segment has been lost.

2.4.2 TCP Congestion Control Mechanisms

TCP uses a sliding window for flow control and congestion control. This window determines the number of bytes in flight. Its size is computed dynamically as follows:

$$min(rwnd, cwnd)$$

where *rwnd* is the most recently advertised receiver window used for flow control, and *cwnd* is a sender-maintained state-variable that tracks the congestion window used for congestion control [8]. In general, a TCP connection is bottlenecked by the network resources and not the receiver buffer *rwnd*, and therefore the transmission rate is governed by the congestion window size. Since the congestion window represents the number of bytes a sender can send without waiting for an ACK, the average rate of a TCP connection is approximately its window size divided by its RTT.

The congestion window adjustment algorithm has two phases: (i) slow start, and (ii) congestion avoidance.

Slow start To begin transmission into a network with unknown conditions, TCP probes the network to determine the available bandwidth. This is accomplished through the *slow-start* phase. In this phase, the *cwnd* is increased by one segment for every ACK that acknowledges new data. *i.e.*,

$$cwnd\,(segments) += 1$$

for every new ACK. Thus, there is an exponential increase in the size of the *cwnd*, with the window doubling every RTT. This growth continues until either the *cwnd* reaches the slow-start threshold called *ssthresh* or the network capacity is exceeded and segments are lost. The initial value of *ssthresh* is set high, sometimes equal to the *rwnd*, so as to allow the TCP sender to quickly probe the network capacity.

Congestion avoidance When $cwnd > ssthresh$, the sender switches to a slower rate of increases in *cwnd* of 1 segment for every window's worth of ACKs. *i.e.*,

$$cwnd\,(segments) += \frac{1}{cwnd\,(segments)}$$

for every new ACK. This is the TCP *congestion avoidance* phase. The resulting linear increase in *cwnd* aims to slowly continue probing the network for any additional network bandwidth. *cwnd* continues increasing linearly until either reaching the maximum TCP window size or when a segment loss is detected.

A packet loss is detected either by the expiration of the retransmission timer or receipt of three duplicate ACKs. TCP infers this loss as an indication of network congestion and reacts as follows:

1. If a timeout occurs, the *cwnd* is set to 1 and the connection enters the slow start phase again. Additionally, *ssthresh* is set as shown in Equation 2.1, where *flightsize* is the amount of data in transit and is min(rwnd, cwnd), while *SMSS* is the Sender Maximum Segment Size.

$$ssthresh = max(\frac{flightsize}{2}, 2 \times SMSS) \tag{2.1}$$

2. The sender considers the arrival of 3 duplicate ACKs packets in a row as an indication that a segment has been lost. The sender then invokes the *Fast Retransmit* algorithm by retransmitting the missing segment immediately, without waiting for the retransmission timer to expire. *ssthresh* is set per Equation 2.1, *cwnd* is set to 1, and the connection enters slow start phase.

   Fast Recovery was introduced with a view to prevent the 'pipe' from being empty after a fast retransmit. Following the transmission of missing segments per fast retransmit, the Fast Recovery algorithm governs the transmission of new data. *ssthresh* is set to the value as shown in Equation 2.1, while *cwnd* is artificially "inflated" to *ssthresh* + $3 \times$ *SMSS* to reflect that 3 additional data segments are no longer in the network but in the receiver's buffer. With *cwnd* greater than *ssthresh*, the sender enters the congestion avoidance phase instead of the slow-start mode. On receiving each subsequent duplicate ACK, the TCP sender increments the *cwnd* by the segment size to reflect that another segment has left the network. Additional segments can be transmitted if allowed by this new value of *cwnd*. Finally, when the ACK acknowledging the receipt of new data is received, the *cwnd* is reset to *ssthresh*, and the TCP sender enters the congestion avoidance phase.

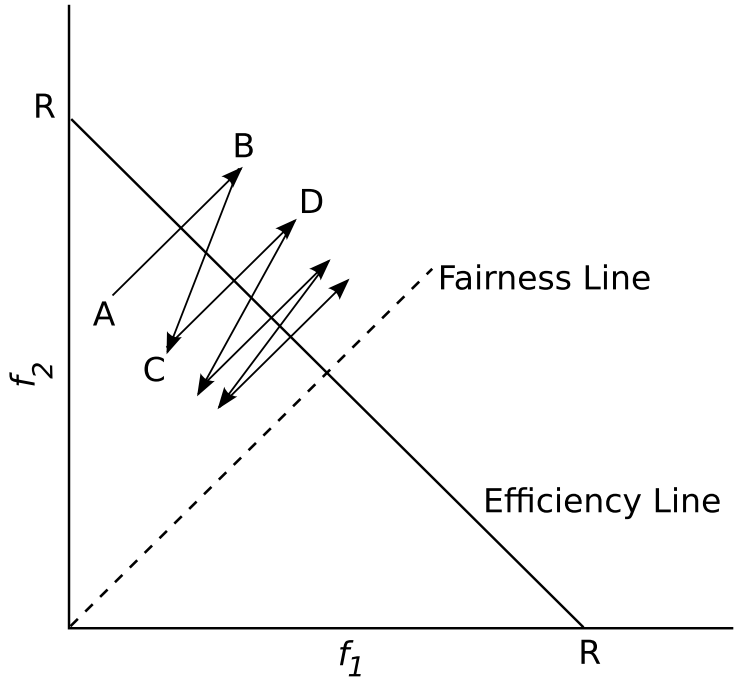

Figure 2.10: Additive Increase/Multiplicative Decrease mechanism of TCP allows it to converge to an optimally fair point at the intersection of fairness and efficiency lines.

2.4.3 AIMD Control and TCP Fairness

In congestion avoidance phase, the TCP congestion window increases by 1 segment per RTT when the network is not congested, and is reduced by half on detecting a loss through receipt of three duplicate ACKs. Chiu and Jain [23] show that this additive increase multiplicative decrease (AIMD) behavior of TCP converges to fair sharing of bottleneck bandwidth.

Consider a network of two TCP flows f_1 and f_2 that are sharing a bottleneck link of capacity R. The rate allocations of these flows can be represented in Figure 2.10 as a point in two-dimensional space. The optimally fair point is the intersection of the fairness and efficiency lines where the bottleneck link is fully utilized and fairly shared between the two flows. We assume that the two flows have the same RTT and SMSS. It can be shown that with the AIMD control behavior of congestion avoidance phase, any rate allocation in this two-dimensional space eventually converges around the optimal fair point. Intuitively, these rates converge because during the increase phase both flows gain throughput at the same rate, but with multiplicative decrease the flow with the higher rate loses more throughput.

Chapter 3

Performance Challenges in 802.11-based WMNs

The DCF access mechanism was originally designed for single-hop infrastructure WLANs. Studies have indicated that it does not scale well in multihop networks [126]. In this chapter we summarize these performance challenges for both UDP and TCP-based traffic. The performance of a WMN is a function of the offered load; as this load increases, even a single data stream experiences a drop in end-to-end throughput because of contention between different hops along the path to the destination [61]. TCP, the dominant transport protocol that also provides congestion control, results in similar suboptimal utilization of the wireless medium [76]. Further, in networks with multiple TCP streams, flows with unequal path lengths experience unfair sharing of wireless capacity, producing flow rate unfairness, including flow starvation [38, 108]. This response is an artifact of DCF behavior in a multihop network, TCP congestion control mechanisms, and cross layer interaction between the MAC and transport-layer protocols. We describe these performance challenges in detail below.

3.1 Terminology and Simulator Configuration

In this chapter we use simulation analysis, where necessary, to support our performance characterization of DCF-based multihop networks. Here we first summarize the terminology and simulation configuration that we employ in this analysis.

3.1.1 Terminology and Notation

1. A *stream* or a *flow* is defined as an exchange of data packets between a mesh node and the gateway router. An *active* stream or a flow is one for which data is currently being exchanged. We represent a stream with its source and destination node, using either the full notation source→destination, or the short-hand notation source>destination. Mesh nodes are identified by a positive integer index ID or an alphabet. We represent the gateway by an index ID of 0 or the string GW.

2. *Uplink* or *upstream* flows are sourced by a mesh router and destined to a gateway. *Downlink* or *downstream* flows traverse the opposite direction, *i.e.*, from the gateway node to a mesh router.

3. We use *transmitter* and *receiver* to identify the wireless nodes along the path of a stream, and *source* and *destination* for the end-hosts between which data is exchanged.

4. We use R to denote the data rate for a wireless link. We define *nominal MAC layer capacity* [61] as the maximum theoretical MAC layer throughput for this link. This nominal capacity is a function of the raw physical-layer data rate and MAC overhead. We denote the nominal capacity of a wireless link by W. We use r_i to denote the rate of a flow f_i.

3.1.2 Simulation Parameters and Configuration

We performed our simulations using the open source, discrete-event simulator, Network Simulator ns-2 [2]. Unless otherwise specified, the simulation parameters we used were as follows:

Transmission, interference, and carrier sense range The wireless physical layer in ns-2 is modeled after the 914 MHz Lucent WaveLAN DSS radio [116]. We use the ns-2 default configuration of this radio in our simulations: transmit power of 24.5 dBm, receiver sensitivity threshold of -64 dBm, and carrier sense threshold of -78 dBm. With two-ray ground reflection propagation model (Section 2.2), these parameters yield a transmission range of 250 m. and carrier sense/interference range of 550 m.

Wireless link rates We use a data rate of 1 Mb/s to simulate the radio link between two adjoining nodes. Using a uniform physical-layer specification allows us to focus on the performance characteristics of MAC and transport-layer protocols. We experiment with multi-rate links of 1 Mb/s and 2 Mb/s in Chapter 7.

RTS/CTS exchange RTS/CTS incurs a fixed overhead, yet cannot resolve all hidden terminals in a DCF-based multihop network (see Section 2.3.2). We disable RTS/CTS in our simulations.

Routing framework We use the static shortest-path routing framework developed by Li [77]. Using static routing allows us to remove any artifacts of cross-layer interaction between routing and transport layer protocols observed in the literature [87].

TCP traffic We use TCP NewReno [34] with an infinite file transfer to simulate an adaptive, backlogged traffic source. We use TCP segments of size 1460 bytes for an Ethernet-friendly Maximum Transmission Unit (MTU) of 1500 bytes.

Topology structures We experiment with a mix of topologies, including chains, grids, and random networks of various sizes. We describe the topology alongside each experiment. Chain topologies are the branch of a routing tree. We use equidistant node separation of 200 m. to keep these chains amenable to analysis. Thus given the communication ranges above, a node can directly communicate only with its 1-hop neighbor, and nodes 3-hops apart can transmit concurrently (see Figure 3.1). Grid-like deployments are often used to blanket wireless coverage in a given area [103]. We use grid topologies with equidistant node separation of 200 m. along both x and y-axes. Finally, we use random topologies to show that performance of chain and grid topologies are not a function of their regular structure, but applicable across a range of network topologies.

3.2 DCF and Multihop Flows

In general, a multihop flow in a wireless network is susceptible to both *intra-flow contention* and *inter-flow contention* for channel access [130]. Intra-flow contention is the contention between nodes while trying to forward packets for the same flow,

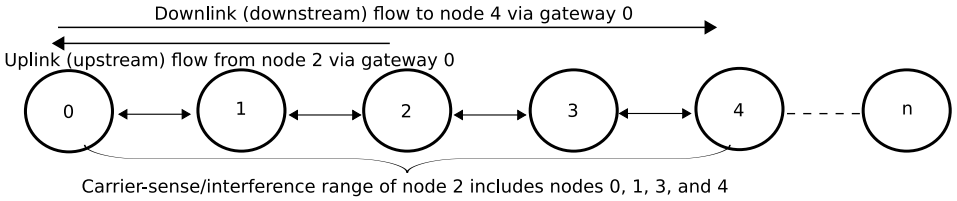

Figure 3.1: An n-hop chain with nodes indexed $0, 1, \ldots, n$. Node 0 is also the gateway to a wired network. Only the neighboring nodes may directly communicate, yet nodes within 2-hops are within carrier sense/interference range. Upstream flows are from mesh routers to a wired host *via* the gateway; downstream flows are in the other direction.

e.g., in a chain of wireless nodes in Figure 3.1, when node 1 transmits to node 2, node 0 cannot transmit to node 1, and node 2 cannot transmit to node 3. Inter-flow contention is the contention for channel access between neighboring nodes that are transmitting data for different flows.

A core function of any MAC protocol is to provide a *fair* and *efficient* contention resolution mechanism. In this section we describe the behavior of DCF in multihop networks when the contending nodes are (1) within, and (2) outside, mutual carrier sense range.

3.2.1 Nodes within Mutual Carrier Sense Range

On average, DCF provides equal transmission opportunities to all nodes within mutual carrier sense range [112]. This notion of per-station fairness has its roots in the BSS architecture of WLANs where all stations communicate directly with the AP. However, it does not translate to flow-level or end-to-end fairness in WMNs where nodes closer to the gateway relay an increasing amount of aggregate traffic [60]. Without a proportionate increase in the number of transmission opportunities, these nodes will experience higher queue drops. This results in capacity loss when the dropped packets originated from other nodes and had already consumed a portion of the shared spectrum. For example, in a 2-hop chain in Fig. 3.1 with two upstream flows from nodes 1 and 2 to a gateway node 0, the max-min fair share of nodes 1 and 2 is $\frac{R}{3}$ each, for an aggregate network capacity of $\frac{2R}{3}$. However with 802.11 MAC and continuously backlogged sources, the aggregate network capacity is reduced to $\frac{R}{2}$ with node 2 starving [61].

Note that this capacity loss from queue overflows affects upstream flows only [55].

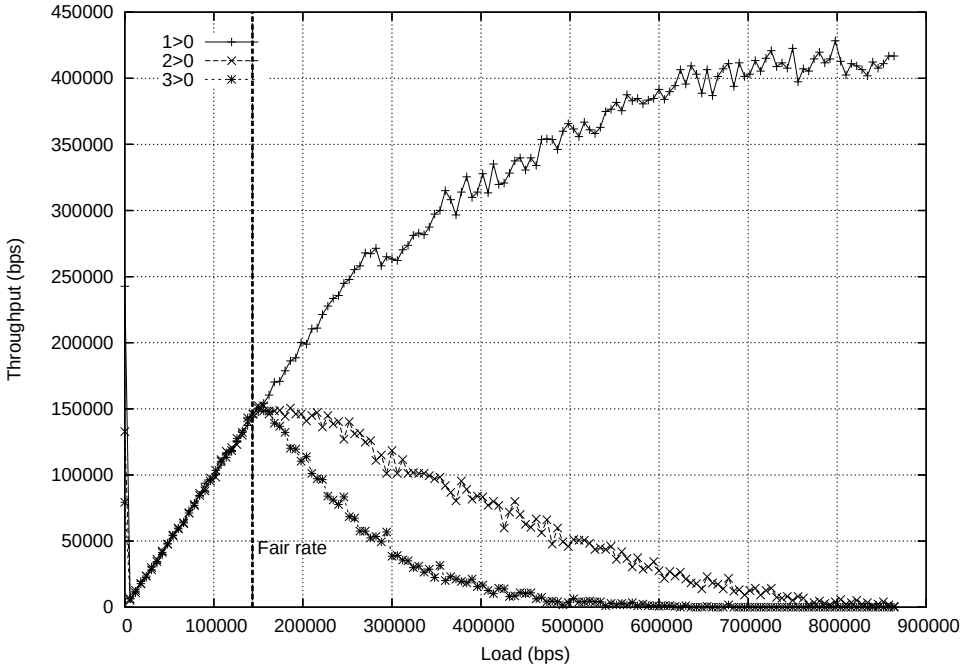

(a) Upload flows

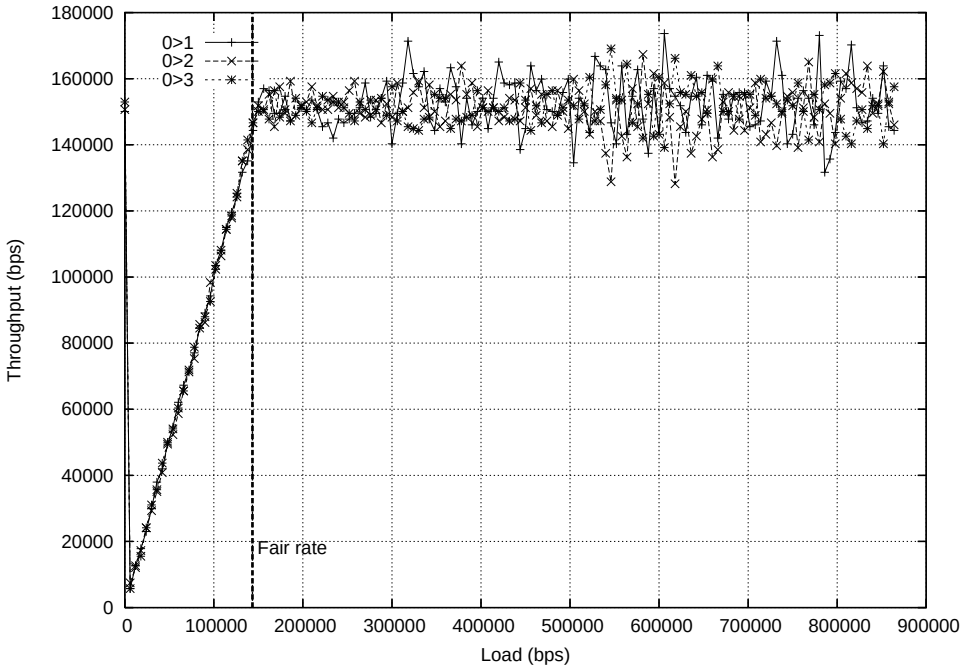

(b) Download flows

Figure 3.2: Offered load vs. throughput for (a) upstream and (b) downstream flows in a 3-hop chain.

For downstream flows, 802.11 MAC fairness limits the packets a gateway can inject in the wireless medium, while per-station fairness ensures that relay nodes always get sufficient transmission opportunities to deliver in-flight packets. Queue drops from excess traffic occur at the gateway router *before* entering the wireless medium, thus avoiding wireless capacity loss. We illustrate this for a 3-hop chain using simulations. Fig. 3.2 shows the throughput response for both upstream and downstream flows against the offered load. For 1 Mb/s wireless links, the max-min fair share per stream is about 150 Kb/s. All flows fairly share the medium till the offered load hits this fair-share point. Beyond this point, the upstream flows (Fig. 3.2a) exhibit increasing unfairness with rising load, first starving node 3 and then node 2 [61]. Node 1's throughput saturates around 400 Kb/s with other nodes starving; this capacity loss is due to queue overflows at intermediate routers. The downstream flows in Fig. 3.2b do not exhibit this unfairness and capacity loss.

3.2.2 Nodes outside Mutual Carrier Sense Range

When two transmitters are outside mutual carrier sense range, DCF's distributed scheduling driven by local carrier sensing may produce misaligned transmissions [39]. We use two illustrative topologies to show its impact on flow rate fairness: information asymmetry topology in Fig. 3.3a where S_1 experiences excessive packet loss because of collisions at R_1, and flow-in-the-middle topology in Fig. 3.3b where S_2 starves due to lack of transmission opportunities. In both cases, nodes disadvantaged due to their physical location develop very different views of the state of the wireless channel that they share with other contending nodes in their vicinity.

Starvation from Collisions

Consider the topology in Fig. 3.3a where both senders S_1 and S_2 have backlogged traffic for their respective receivers R_1 and R_2. The two senders are outside mutual carrier sense range, but are within communication range of R_1. Assume that both transmitters are in the first backoff stage, *i.e.*, they choose a random backoff between 0–31 time slots. A collision at R_1 is inevitable as the two transmissions can be at most 32 time slots (640 μs for 802.11b) apart, while it takes upwards of 1500 μs to transmit a 1500-byte Ethernet-friendly MTU and its subsequent link-level ACK using 802.11b physical layer parameters [107]. This collision only impacts S_1's packet to R_1. S_1 now doubles its MAC contention window, choosing a backoff between 0–63 time slots, while S_2 remains in the first backoff stage. S_2 is now twice

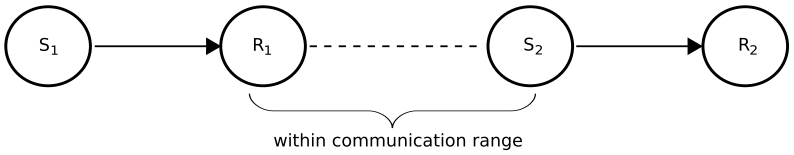

(a) Information asymmetry topology. R_1 is susceptible to collisions from S_2's transmissions. With backlogged traffic, S_1 starves while S_2's throughput equals the link capacity.

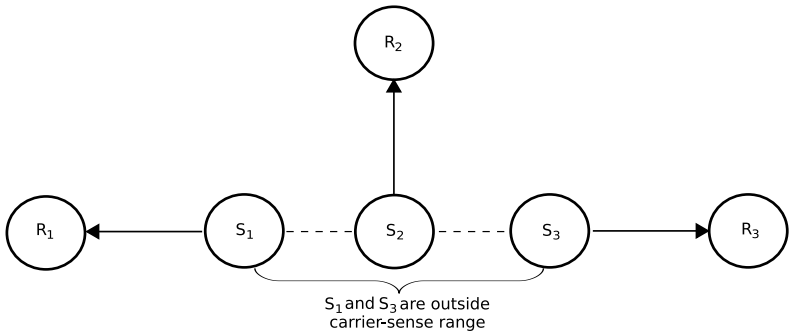

(b) Flow-in-the-middle topology. S_2 is in the carrier sense range of S_1 and S_3. When S_1 and S_3 have backlogged traffic, S_2 starves for transmission opportunities.

Figure 3.3: Illustrative topologies showing DCF performance limitations in multi-hop networks.

likely to start transmitting before S_1; even if S_1 waits a maximum of its 64 time slots, the probability of collision is still 1. S_1 doubles its contention window yet again, but even in this third backoff stage, the probability of collision is 0.6. Thus, the 802.11 MAC steadily builds up the contention window for the disadvantaged node S_1, while allowing S_2 to keep capturing the channel with a lower contention window; the two transmitters develop an inconsistent, asymmetric view of the state of the wireless channel that they share [39].

We note that the information asymmetry topology in Fig. 3.3a is an extension of the hidden terminal problem described in Section 2.3.1. However, floor-acquisition mechanisms such as RTS/CTS cannot completely solve this problem. First, even the RTS frames are susceptible to a collision probability of 0.55 when both transmitters are in the first backoff. Second, when the RTS frames do not collide, R_1 will not respond to S_1's RTS if it has already been silenced by a prior RTS from S_2 to R_2. From S_1's perspective, this is no different from when its RTS frame collided at R_1 because of S_2's transmission. Finally, this scenario is valid even when R_1 is outside transmission range but still within interference range of S_2.

Starvation from Lack of Transmission Opportunities

Collisions are not the only reason for nodes sharing an inconsistent view of the channel state; this may occur even in an ideal CSMA/CA protocol in which all transmissions are successful. Consider the flow-in-the-middle [39] topology in Fig. 3.3b where S_2 is in carrier sense range of both S_1 and S_3, but S_1 and S_3 are outside carrier sense range of each other. With all senders backlogged, throughput for nodes S_1 and S_3 equals the channel capacity with node S_2 starving. This happens because S_2 is always deferring its transmissions to one of the other senders.

3.3 TCP Performance in DCF-based WMNs

TCP's reliable delivery mechanisms were engineered for wired networks with a low bit-error rate (BER) [10]. In contrast, the BER in a wireless network is orders of magnitude higher (typical BER of 10^{-15} to 10^{-12} in wired vs. 10^{-5} to 10^{-3} in wireless networks [72]), resulting in suboptimal TCP performance. These performance issues are compounded when a TCP stream traverses multiple wireless links. Further, DCF MAC makes distributed scheduling decisions based on local channel conditions, and this introduces additional challenges for multihop TCP streams

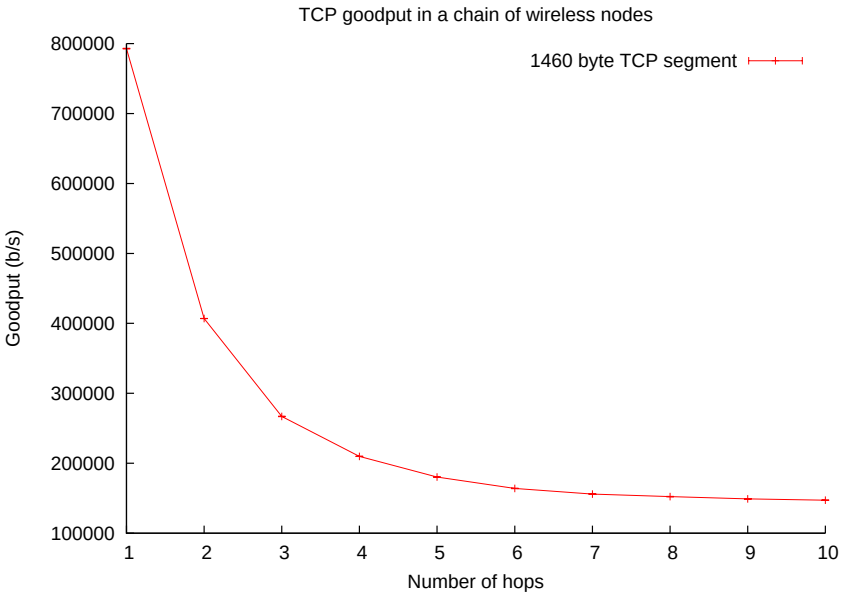

Figure 3.4: TCP goodput as a function of flow length

that traverse multiple contention regions. We first analyze the end-to-end performance of a single multihop TCP stream. We then consider multiple TCP streams that contend for access to the shared channel.

3.3.1 Single Multihop Flow

Li *et al.* [76] showed that even a single multihop TCP stream exhibits a suboptimal performance behavior due to inter-flow contention in a multihop network. We reproduce their results through a series of simulations, analyzing the end-to-end throughput of a TCP stream over a chain of wireless nodes, progressively increasing the chain length in each experiment. These results are summarized in Figure 3.4.

A 1-hop TCP stream has a throughput close to the nominal MAC layer capacity of 800 Kb/s for a 1 Mb/s wireless link. The measured throughput drops to a half and a third over 2 and 3-hops, respectively. This behavior is expected in a single-channel WMN. The throughput stabilizes at 140 Kb/s, approximately $\frac{1}{6}$ the nominal MAC layer capacity. This is much less than the optimal spatial reuse of $\frac{1}{3} - \frac{1}{4}$ of the link capacity based on theoretical analysis [131]. Li *et al.* showed that spatial (location-dependent) contention for channel access is responsible for this behavior. Relay nodes in the middle of a chain experience greater channel contention than the source node at one end of the chain. Consequently, the source injects more packets that get dropped at intermediate nodes, reducing throughput.

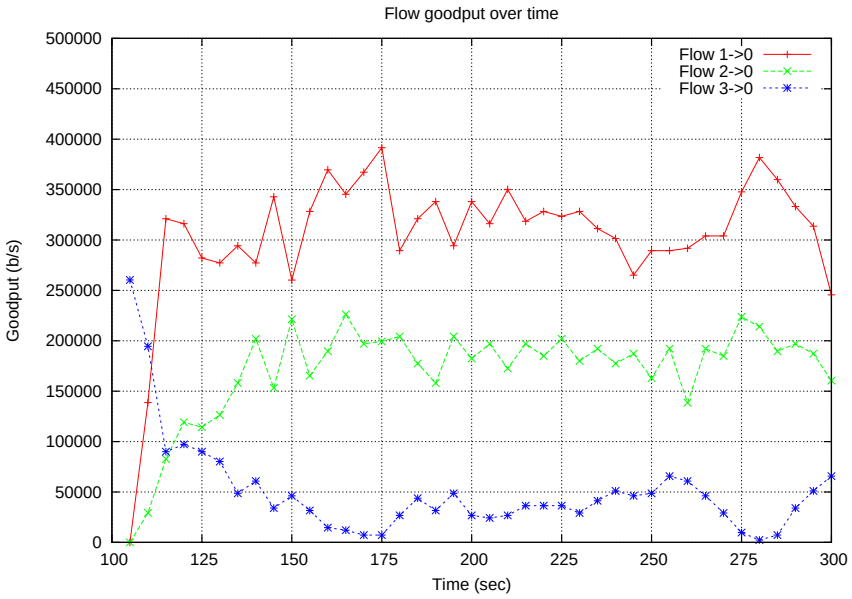

Figure 3.5: Goodput over time with upstream TCP flows in a 3-hop chain. The average goodput of node 1, 2, and 3 is approximately 305 Kb/s, 170 Kb/s, and 50 Kb/s, respectively.

3.3.2 Multiple Multihop Flows

The impact of inter-flow contention on TCP transmission rates in a multihop network has been described in prior work ([38, 53, 107, 108, 129]). We illustrate the impact of this contention using a 3-hop chain (Figure 3.1) with three upstream TCP flows sourced from nodes 1, 2, and 3 to the gateway node 0. Figure 3.5 shows the measured TCP throughput averaged over a 5 s. interval for the three flows. The average throughput over the experiment is 305 Kb/s, 170 Kb/s, and 50 Kb/s for the 1, 2, and 3-hop flow, respectively. While we used TCP NewReno for this simulation, we note that these results are qualitatively similar to those reported by Gambiroza *et al.* using TCP SACK [38].

Our analysis of the trace data shows that flow 3 experiences a drop rate of approximately 20%, primarily due to collisions with the TCP ACKs transmitted by the gateway node 0. Both nodes 0 and 3 (Figure 3.1) are hidden terminals, outside mutual carrier sense range. We infer the state of the TCP senders using the congestion window size of the three flows as shown in Figure 3.6. The average congestion window size is approximately 63, 45, and 6 packets for flows 1, 2, and 3, respectively (We used a FIFO queue of size 50 packets at the wireless interface of each node). The congestion window for both nodes 1 and 2 continually increase

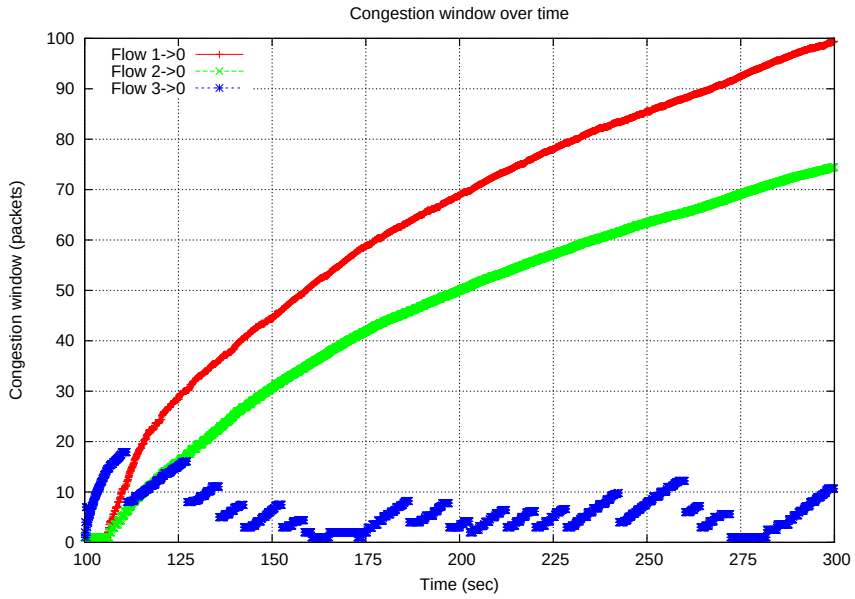

Figure 3.6: TCP congestion window growth in a 3-hop chain using FIFO queues of size 50 packets at each node. The average congestion window size is approximately 63, 45, and 6 packets for flows 1, 2, and 3, respectively.

through the duration of the experiment; thus link-layer retransmissions and the cumulative nature of TCP ACKs shields these flows from the impact of collisions between their TCP ACKs transmitted by the gateway and node 3's TCP segments. Link-layer retransmissions fail to similarly recover node 3 because of *cross-layer interaction* between DCF and TCP. The TCP sender at node 3 times-out while the node is still contending for channel access. TCP interprets this as a sign of packet loss, and invokes its congestion control algorithm by droppings its congestion window to one. On the other hand, contending nodes that successfully transmitted a packet will continue increasing their TCP congestion window under backlogged traffic, till their throughput equals the link capacity. Thus with TCP, the short-term MAC unfairness degenerates to long-term flow rate unfairness and possible starvation for disadvantaged flows.

Finally, we note that node 2 only gets roughly half as much throughput as node 1. This is because the throughput of a TCP flows varies inversely with its RTT. The rate of congestion window increase is higher for node 1 compared to node 2 because of its smaller RTT (1-hop flow vs. 2-hop flow).

3.4 Summary: TCP Performance Analysis

We summarize the reasons for poor performance of TCP in a WMN as follows:

1. TCP's congestion control mechanism is tuned for networks where packet loss occurs primarily due to congestion. However wireless communication is often characterized by sporadic errors and intermittent connectivity. These errors reduce the throughput of a TCP stream below the available capacity. 802.11 uses positive acknowledgments with retransmissions to hide these transient wireless errors from higher layers.

2. The long-term throughput r of a TCP connection in congestion avoidance mode is inversely proportional to its RTT [86]:

$$r = \frac{cwnd}{RTT} \approx \frac{c \times MSS}{RTT\sqrt{p}}$$

   where c is a constant of proportionality, p is the packet loss rate, MSS is the maximum segment size, and RTT is the round trip time. TCP thus exhibits an inherent bias towards flows with a smaller RTT. This puts flows with a longer hop count at a disadvantage when competing with shorter length flows for their share of the channel capacity. This RTT-bias is not present in WMNs where a common link (*e.g.*, wired link to the public Internet) with a large delay is shared by the two flows.

3. TCP's window-based transmission scheme can trigger a burst of packets on receiving a cumulative ACK. Such bursts can generate short-term unfairness between flows. Sustained bursts lead to higher queueing delays, leading to packet loss and subsequent retransmissions.

4. With backlogged traffic, this short-term unfairness can degenerate to long-term unfairness and instability, including flow starvation due to cross-layer interaction with the DCF MAC protocol.

3.5 Summary

In this chapter we illustrated the performance challenges of DCF-based multihop networks. A multihop flow in these networks is susceptible to both intra-flow and inter-flow contention. Intra-flow contention results in suboptimal utilization of the

wireless spectrum, leading to a loss in end-to-end throughput of a flow. Inter-flow contention results in throughput unfairness between different flows. With backlogged TCP sources, this unfairness degenerates to flow starvation. We described this behavior as an artifact of DCF performance in a multihop network, TCP congestion control mechanisms, and the cross-layer interaction between the two protocols under sustained traffic loads.

Chapter 4

Capacity Models of a Multihop Wireless Network

The fair rate allocation of a flow is a function of the network capacity for a given topology. In this chapter, we describe two models for determining the capacity of a multihop wireless network: the *collision-domain* model [61] and the *clique graph* model [88]. These models differ in terms of how the wireless spectral resource is shared between the wireless links. We show how these models can be used as a part of a feasibility-based computational model for computing the optimal fair bandwidth allocation for all active streams in a given network. We then provide an accuracy analysis of these models by comparing their computed fair rates against those achieved by simulations.

4.1 Modeling and Estimating Per-flow Fair Share

We first state the assumptions necessary to our approach. We presume that routing is relatively static, based on the fact that the WMN nodes are stationary, and likely quite reliable. By "relatively static" we mean that changes in routing will be significantly fewer than the changes in stream activity. This assumption implies a few things, including that network membership changes (such as node additions or hardware failures) are few and far between, and that load balancing is not used in the network. While the first assumption is certainly valid, the second assumption is a simplification that we hope to address in the near future.

We also assume that the WMN has a single gateway. Though this is generally not true in large deployments, given static routing, for each node there will be a

single gateway. We thus partition a multi-gateway WMN into disjoint WMNs, each with a single gateway. While there may be interference between the resulting set of WMNs, this is a problem that must already be dealt with insofar as there may be interference from any number of other sources.

Given these assumptions, we consider a WMN with N nodes that are arbitrarily located in a plane. Let d_{ij} denote the distance between nodes n_i and n_j. Let T_i be the transmission range of node n_i. We model this network as a labeled graph, where the mesh nodes are the vertices, and a labeled edge exists between two vertices n_i and n_j iff

$$(d_{ij} \leq T_i) \wedge (d_{ij} \leq T_j)$$

In other words, the nodes must be within transmission range of each other. An edge in this connectivity graph is also referred to as a *link*. A *stream* is defined by an exchange of data packets between a mesh node and its corresponding gateway. An *active stream* is one for which data is currently being exchanged.

4.1.1 Computational Model

The fair-share computation model is an optimization problem subject to the feasibility model for the network, the network state, and the fairness criterion adopted.

The feasibility model reflects the throughput constraints imposed by the network. It consists of a set of constraints determined by how streams use the links, and then how these links contend for the wireless channel. The former is a function of the routing protocol; for the latter, we describe two variations (bottleneck clique vs. collision domain) in the following section below.

This feasibility model is extended by the network state, which is simply the desired rate, $G(s)$, for each stream, s. We consider only binary activity: the stream is either silent ($G(s) = 0$) or never satisfied ($G(s) = \infty$). This corresponds to TCP behavior, which either is not transmitting or will increase its transmission rate to the available bandwidth.

Finally, the fairness criterion implements the selected fairness model. In this dissertation we deliberately restrict our analysis to max-min fairness, so as to focus on the accuracy of the model for 802.11-based WMNs and the efficacy of the gateway as a control point. However, we note that the computation model can be extended to any feasible, mathematically-tractable fairness criterion that can be expressed as a set of rate allocation constraints.

4.1.2 Network Feasibility Models

We now describe the details of the two network feasibility models. Both models start by dividing the problem into one of *link constraints* (*i.e.*, usage of links by streams) and *medium constraints* (*i.e.*, usage of the medium by links). The former is the same for both models, as it is a function of the routing together with the demands placed on the network. The latter is where the two models differ.

Link-resource Constraints

Let $R(s)$ be the rate of stream s, and $C(l)$ be the maximum allowed aggregate throughput that link l can carry. For each link l the link resource constraint is specified as:

$$\sum_{i:s_i \text{ uses } l} R(s_i) \leq C(l) \tag{4.1}$$

Since a stream uses all the links on its route, the above usage information can be inferred directly from the routing information. This usage information can be encoded in a 0-1 link-usage matrix $\mathbf{L}$ [65] as follows:

$$\mathbf{L}[i,j] = \begin{cases} 1 & \text{when stream } s_j \text{ uses link } l_i \\ 0 & \text{otherwise} \end{cases}$$

Let $\mathbf{C}$ be the link-capacity vector, where $\mathbf{C}[j] = C(l_j)$. Also let $\mathbf{R}$ be the stream throughput vector, where $\mathbf{R}[i] = R(s_i)$. Then the stream-link usage constraint can be expressed as:

$$\mathbf{LR} \leq \mathbf{C} \tag{4.2}$$

$$\mathbf{R} \geq 0 \tag{4.3}$$

Medium-resource Constraints

The basic problem in developing medium-resource constraints is that contention is location-dependent, with the medium conceptually divided into overlapping resources of limited capacity. The clique model computes mutually incompatible sets of links, all but one of which must be silent at any given time for collision-free transmission. The collision-domain model considers the medium-resource unit to be the link, and determines the set of links that must be silent for a given link to be used. We formalize these two models below.

Clique Model of Medium-Resource Constraints In the clique model, two links *contend* if they cannot be used simultaneously for transmission of packets. Link contention is captured by a set of link-contention graphs $G = (V, E)$, where V is the set of all links, and $\{u, v\} \in E$ iff links u and v contend. Define $B(u)$ to be the available bandwidth in each such distinct region u (*i.e.*, in each clique). Since all links in a clique contend with each other, only one link in the clique can be active at any instant. We can thus define the medium-resource constraints of the clique model as:

$$\sum_{i:i \text{ in clique } u} C(l_i) \leq B(u) \tag{4.4}$$

Note that if each wireless router transmits at the same rate, the value of $B(u)$ can be reasonably approximated as the throughput that can be achieved at the MAC layer in a one-hop network with infrastructure [59]. If routers transmit at different rates, a weighted contention graph may be used.

The resulting set of medium-resource constraints can be written down as matrix equation. First, define the 0-1 medium-usage matrix $\mathbf{M}$ as:

$$\forall i, j \; \mathbf{M}[i, j] = \begin{cases} 1 & \text{when link } l_j \in \text{clique } u_i \\ 0 & \text{otherwise} \end{cases}$$

Let the medium-capacity vector be $\mathbf{B}$, where $\mathbf{B}[i] = B(u_i)$. The medium-resource constraint is then:

$$\mathbf{MC} \leq \mathbf{B} \tag{4.5}$$

The clique model requires the (NP-complete) computation of cliques within the contention graph and, as a more practical matter, the determination of which links contend. While the former problem is, to some degree, amenable to careful analysis potentially enabling more-efficient computation [43], the latter problem is extremely difficult to deal with. Specifically, determining which links interfere with which other links in a wireless mesh network is not, in general, feasible, in part because interference is experienced by a receiver, not by a link, and thus depends on traffic direction [119].

Collision-domain Model of Medium-resource Constraints We therefore examine the efficacy of a simpler model of collision domains [61]. This model both reduces the computation requirements as well as being practically determinable. In this model, two links contend if one endpoint of a link is within transmission range of an endpoint of the other link. The collision domain of link l_i is defined as the set

of all links that contend with link l_i. Note that this is equivalent to the set of all vertices adjacent to vertex l_i in the link-contention graph, modulo the definition of "contend". In this case we define $B(u)$ as the available bandwidth in each collision domain. In single-rate routers this will be the same value as that in the clique model. The medium-resource constraints for the collision-domain model are then:

$$\sum_{i:l_i \text{ in } u} C(l_i) \leq B(u) \tag{4.6}$$

Note that since transmission range is often much less than interference range, this model underestimates the level of contention. However, each collision domain will, in general, contain links that do not contend with each other, thus overestimating the number of contending links compared to the more-accurate cliques. As a result, the combined model has the potential of offering acceptable accuracy, with computational simplicity and practical feasibility. We must emphasize that in this model it is possible for nodes within the WMN to identify the set of contending links, which is difficult, if not infeasible, with the clique model.

As with the clique model, we can define a 0-1 medium-usage matrix $\mathbf{M}$ as follows:

$$\forall i, j \; \mathbf{M}[i,j] = \begin{cases} 1 & \text{when link } l_j \in \text{collision domain } u_i \\ 0 & \text{otherwise} \end{cases}$$

Similarly, the medium-capacity vector $\mathbf{B}$ can be redefined as $\mathbf{B}[i] = B(u_i)$, where $B(u_i)$ is the available bandwidth of collision domain u_i. Equation 4.5 then remains unaltered, though using the collision-domain definitions of $\mathbf{M}$ and $\mathbf{B}$.

In both cases, the network feasibility model is the combination of the link (Equations 4.2 and 4.3) and medium (Equation 4.5) resource constraints, and can be represented in the following manner:

$$\mathbf{MLR} \leq \mathbf{B} \tag{4.7}$$

$$\mathbf{R} \geq 0 \tag{4.8}$$

4.1.3 Network State Constraints and Fairness Criterion

Any rate allocation specified in $\mathbf{R}$ has to satisfy the linear constraints in equations 4.7 and 4.8, together with those imposed by the network state constraints and the fairness model.

The network state constraints require that no flow be allocated a rate higher than its desired rate. Thus, if the bandwidth requested by a stream s is $G(s)$, then $\forall_s R(s) \leq G(s)$. As previously discussed, in this model we only consider either inactive streams ($G(s) = 0$) or TCP streams with infinite backlog ($G(s) = \infty$).

Finally, the fairness criterion that we consider is max-min fairness. This imposes an additional constraint that no rate $R(s_i)$ can increase at the expense of $R(s_j)$ if $R(s_i) > R(s_j)$.

The resulting computational problem is to maximize the bandwidth allocation vector $\mathbf{R}$, while satisfying the set of constraints described in the above sections.

4.1.4 Model Accuracy

Having described the two computation models, we now wish to evaluate their accuracy within 802.11-based WMNs. To achieve this we have devised experiments that would determine, for a given topology and a set of active streams, the max-min fair-share points. We compare these experimentally-determined values to those computed using the two models to determine the accuracy of the computation. Given enough topologies and stream variations, we can then determine the statistical accuracy of the models.

The experiment we created is as follows. For a given set of streams in a given network topology, we simulate, using ns-2 [2], source-rate limiting those streams over a range of rates from 50% of the computed fair-share rate to 150% of the computed fair-share rate. To avoid TCP complications, UDP data is used, with 1500 byte packets. This simulation is executed 5 times, with a different random seed each time. The 5 results are averaged to give an expected throughput for each stream for any given input rate.

Plotting these results yields graphs such as that shown in Figure 4.1. This particular figure is a 36-node network arranged in a 6x6-grid topology with 15 streams. The vertical line labeled "o+cl" represents the computed value for the clique model, where "o" is for omniscient, since it requires omniscient knowledge to know which links interfere with which other links. This is feasible in the simulator, though not in practice. Similarly, the vertical line "r+cd" represents the computed value for the collision-domain model, where "r" is for "realistic" as it is computable within a physical network.

To determine the accuracy of the computational models we define the fair-share points as follows. The fair-share point for bottleneck i is that point at which the

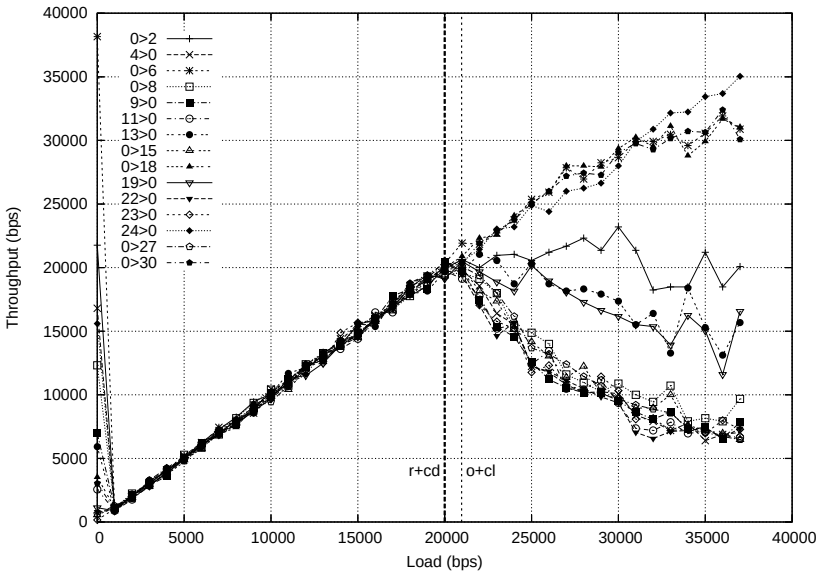

Figure 4.1: Plot of Input Rate vs. Throughput for a Sample Topology, without RTS/CTS

throughput of more than one-third of the streams that are constrained by bottleneck i is less than the input source rate by more than 5%. All streams that are constrained by a lesser bottleneck must be capped when running the relevant simulation. We determine a drop of more than 5% by requiring this to be true for four successive data points, and then taking the first of those four points as the point of loss for that stream. While this definition may seem somewhat arbitrary, when trying several variations (*e.g.*, 8% loss by 20% of the stream, *etc.*), all pointed to approximately the same fair-share point, and visual inspection of plots has suggested that this definition is fairly reasonable.

Given this definition, we executed this experiment over 50 random topologies in a 1000x1000 m area with between 25 and 40 streams for each topology, both with and without the RTS/CTS protocol. We then compute the average error in each computation model, together with the standard deviation.

Our results are shown in Table 4.1. The value "Ocl" is the computed value of the clique model, "Rcd" is the computed value of the collision domain model, and "fp" is the experimentally-determined fair-share point.

As is apparent, both models are reasonably accurate at predicting the first fair-share point, generally slightly under-estimating the capacity, and within about 10% deviation. The simpler collision domain model is only marginally less accurate than the more-complex clique model, and thus seems quite sufficient for estimating

Measured Entity	No RTS/CTS	With RTS/CTS
Avg. of (Ocl - fp)/fp	0.000077	0.183
Std. Dev. of (Ocl - fp)/fp	0.11	0.357
Avg. of (Rcd - fp)/fp	0.027	0.212
Std. Dev. of (Rcd - fp)/fp	0.12	0.361

Table 4.1: Computational model accuracy analysis

the fair rates for a given topology. Finally, we note that while the experiment in Figure 4.1 was performed on a 36-node network, we have corroborated this observation and found it consistent across a large number of random, chain, and grid topologies.

4.2 Summary

In this chapter we described two models for computing the capacity of a multihop wireless network – the collision-domain model and the clique graph model. We showed how these models can be used to determine the optimal fair share rate for a given network. Further, we evaluated the accuracy of these models using simulations in ns-2. Our results showed that the rate allocation computed using the simpler collision-domain model is reasonably accurate to the behavior observed via simulation analysis.

Chapter 5

Previous Work

Fair resource allocation has been extensively studied in the context of wired networks. However, the resource allocation constraints are significantly different in a wireless environment, necessitating investigation of new and novel approaches. In this chapter our goal is to introduce broad categories of the solution space, and we refer the interested reader to more comprehensive manuscripts where available.

The challenges in using CSMA/CA-based MAC protocols for multihop networks have been discussed previously [76, 99, 108, 127]. In general, a flow not only experiences inter-flow contention with other flows sharing the spectrum, but may even interfere with its own transmissions along the path to the destination, *i.e.*, intra-flow contention [130]. The degree of contention increases with increasing traffic loads. Related work in the literature addresses it from different perspectives:

1. MAC-layer enhancements
2. TCP enhancements
3. Higher-layer rate-control algorithms.

5.1 MAC-layer Enhancements

By far the largest body of literature specifically devoted to wireless network fairness is that of MAC-layer solutions (see [12, 83, 82, 88, 114], among others). Such approaches tend to assume that contending flows span a single-hop and fairness may be achieved by converging the MAC contention windows to a common value.

Single-hop fairness, however, does not translate to end-to-end fairness in a multihop network [75].

We now provide a summary of prior work proposed for addressing various MAC-layer challenges in wireless networks.

5.1.1 Hidden and Exposed Terminals

The impact of hidden terminals in degrading network capacity and producing flow rate unfairness has been described in prior work [126]. RTS/CTS handshake works well in a BSS architecture where any two stations are at most two hops apart. However, it does not resolve all hidden terminals when multiple BSS are co-located in a given space [128], and hidden nodes may now exist in the interference range of a receiver. Typically, such hidden nodes are mitigated by assigning non-overlapping channels to neighboring BSS. This does not work in single-radio WMNs where all radios operate on a common channel to ensure connectivity.

Haas and Deng [44] have proposed Dual Busy Tone Multiple Access (DBTMA) that solves both the hidden and the exposed terminal problem. DBTMA builds on to the idea of Receiver-Initiated Busy-Tone Multiple Access (RI-BTMA) scheme [122] in which the receiver broadcasts an out-of-band busy tone during the reception of data. This allows neighboring nodes to detect an ongoing communication at the receiver, thus preventing them from transmitting. In addition to this receive busy tone, DBTMA introduces an out-of-band transmit busy tone. A transmitter initiates this tone when sending out an RTS packet, thus protecting this packet and increasing the probability of its successful reception at the intended receiver.

This design allows exposed terminals to initiate a new communication because they do not listen on the shared data channel for receiving acknowledgment from the intended receiver [44]; this acknowledgment is instead sent as a receive busy tone. Similarly, hidden terminals can respond to RTS requests by enabling the receive busy tone.

While DBTMA MAC design is simple, its practical implementation remains a challenge. First, it needs extra transmitting and sensing circuitry per node for generating and receiving the two busy tones. Second, there needs to be a considerable spectral separation between the data channel and the control channel for the tones to prevent any co-channel interference. However coordinating radios across widely separate frequency bands is hard because of frequency-dependent radio propagation characteristics [9]. Finally, though both transmit and receive busy tone are

narrowband tones, yet they still incur an overhead by consuming a finite amount of bandwidth that cannot instead be used by the data channel.

5.1.2 Prioritized MAC Access

CSMA/CA based MACs provide each node with an equal opportunity to transmit. However, in WMN, nodes closer to the gateway have to transmit their own traffic along with the aggregate traffic from other nodes in the network towards the gateway. As such, congested nodes higher in the connectivity graph should have prioritized access to the medium compared to its child nodes.

There are different mechanisms for prioritizing access to the wireless medium. If the fair share of a flow is already known, nodes along the multihop link can set their contention delays so as to achieve the desired rate [129]. Hull *et al.* [47] recommend using the scheme first outlined by [5]; a node higher in the connectivity graph has its randomized backoff window set to $\frac{1}{2N}$ the size of each of its N children, as on average this gives the parent node as many transmission opportunities as each of its children. In [30], the authors propose adjusting TXOP and CWmin values as described in 802.11e enhancements (see Section 2.3.2) to restore fairness amongst multihop flows. We note that such schemes do not provide fairness amongst the same access category and can only scale to small networks.

5.1.3 Receiver-initiated/Hybrid MAC

The contention resolution mechanism in CSMA/CA is sender-initiated. We have seen that when the channel state at the sender is incomplete, its transmissions result in collisions at the receiver. To resolve this, receiver-initiated transmission protocols have been proposed [111]. However, these schemes work well only when the intended receiver is aware of the exact traffic load information.

Hybrid MAC protocols that combine both sender and receiver-initiated transmissions have also been proposed [17, 120]. Results show that such hybrid schemes can only improve fairness in some scenarios without significantly degrading the network capacity [120].

Receiver-initiated extensions to traditional CSMA/CA protocol have also been proposed. MACAW [12] uses a receiver-initiated Request-for-Request-To-Send (RRTS) control packet. It handles the use case when a receiver receives a RTS but cannot

immediately respond with a CTS till its NAV counter expires. At NAV expiration, the receiver transmits a RRTS frame to the original sender, requesting that RTS packet be retransmitted. Note that this works only when the initial RTS is decodable at the receiver. If this RTS is non-decodable due to a collision (lasting the duration of RTS frame), the receiver can decide to broadcast a RRTS frame based on a given probability distribution [74]. We note that while RRTS control frame can resolve some scenarios with missed transmission opportunities, the overhead associated with the probabilistic use of an additional control frame can be a performance challenge for wireless networks.

5.1.4 Overlay MAC

Overlay MAC Layer (OML) [100] is a software-based TDMA overlay implemented as a *Click* [68] module that sits between the IP and 802.11 MAC layers. It requires only lose synchronization between the nodes, relying instead on using large slot sizes to account for synchronization errors, *i.e.*, their slot size is equivalent to the time required for transmitting 10 maximal size packets. These large slot sizes significantly deteriorate the short-term fairness of the network.

SoftMAC [123] is another overlay over 802.11 MAC, targeted towards supporting real-time traffic through distributed admission control and rate-control mechanisms in a network with a mix of real-time and best-effort traffic. In general, however, admission control is at best an ineffective proposition in a wireless network where link and channel capacity varies over time [57].

5.1.5 Multi-channel MAC protocols

Asynchronous Multi-channel Coordination Protocol (AMCP) [108] addresses the fairness problem through use of separate data and control channels. Using RTS/CTS handshake in the common control channel, nodes negotiate the data channel they will use for the data transmission. This improves fairness because nodes contend for channel access only for the smaller control packets whose lengths are comparable to the backoff period. There are, however, practical challenges in using AMCP with 802.11 hardware. IEEE 802.11b/g networks have only 3 non-overlapping channels, and it is unclear if non-overlapping data channels can be assigned to all contending links in a large network. Second, the mandatory use of RTS/CTS, even for small data frames, is an overhead that limits the network performance.

5.1.6 Challenges: MAC-layer Modifications

Modifying MAC-layer protocols to support multihop flow fairness involves the following challenges:

1. Schemes requiring MAC-layer modifications have incremental deployment challenges, as the MAC-layer is fundamental for establishing link-level connectivity amongst the network nodes. This clearly limits its practical utility for the type of broadband wireless access networks based on heterogeneous node configurations that we consider in this dissertation.

2. Only a subset of the MAC-layer modifications described above can be practically implemented on 802.11 radio chipsets. This is because some functionality of these radios (such as carrier sensing) is inherent to the firmware which is often not exposed by the manufacturers. Switching to a different radio platform may often be infeasible because the cost dynamics of commodity 802.11 hardware is a significant factor in making WMNs an attractive last mile access technology.

5.2 TCP Enhancements

There is extensive literature on understanding and improving the performance of TCP in wireless networks. We provide a brief overview of broad categories of this research relevant to our work, referring the reader to [80] for a comprehensive survey.

The performance of TCP in one-hop wireless networks has been studied extensively. The congestion control mechanisms of TCP have been optimized for wired networks. Wireless networks have fundamentally different characteristics in terms of bandwidth, propagation delay, and link reliability. As a result, packet loss can no longer be treated simply as an artifact of congestion in the network, disrupting the foundations of TCP's congestion control mechanisms [21].

Balakrishnan *et al.* [10] classified the research work addressing TCP performance limitations in a one-hop wireless network into three major categories: end-to-end proposals, split-connection proposals, and link-layer proposals [10].

The end-to-end protocols attempt to make TCP senders differentiate between losses from congestion or from other errors through the use of Explicit Loss No-

tification (ELN) mechanism. They also use variants of selective acknowledgments (SACKs) to enable the sender to recover from multiple packet losses in a window.

The split-connection protocols hide the wireless link from a wired TCP sender by terminating its TCP connection at the wireless base station (BS), and using a separate reliable transport protocol on the wireless link between the BS and the wireless client.

Finally, the link-layer protocols attempt to shield the TCP sender from wireless losses by implementing local retransmissions and forward error correction.

5.2.1 TCP Pacing

TCP's window-based congestion control algorithm can trigger a burst of packet transmissions on receiving an ACK (*e.g.*, a cumulative ACK) or several back-to-back ACKs. Such bursts can lead to higher queueing delays, packet losses, and subsequent drop in throughput. TCP pacing [133] addresses this by spacing out the transmission of a *cwnd* worth of packets over the estimated RTT interval, *i.e.*, the packets are injected into the network at a rate $\frac{cwnd}{RTT}$. Aggarwal *et al.* [6] performed a detailed simulation study to show that while pacing improves fairness characteristics, it can also lead to lower throughput compared to unmodified TCP because of delayed congestion signals and synchronized losses. They also showed that paced TCP performs poorly competing with bursty TCP when a paced packets encounters congestion along the path.

ElRakabawy *et al.* [32] observe that the inherent variability in the RTT of a multihop wireless flow may offset the synchronization issues discussed above. They propose a rate-based transmission algorithm over TCP called TCP with Adaptive Pacing (TCP-AP): instead of spacing the transmission of *cwnd* worth of packets over the RTT of a flow, the transmission rate is computed using four-hop propagation delay (determined by spatial reuse in a chain of wireless nodes) and coefficient of variation of recent RTTs (to identify incipient congestion along network path). They further extended this work to hybrid wired/wireless networks [33]; flows sourced at a wireless node are rate limited using TCP-AP, while wired-to-wireless flows are rate limited at the gateway before entering the wireless medium. The authors also introduce Goodput Control at the gateway that can further throttle wired-to-wireless flows so that they share bandwidth fairly with wireless-to-wired flows. We have earlier shown that in some topologies wired-to-wireless flows have already better fairness characteristics than upstream flows (see Section 3.2). In this

dissertation we establish that gateways can be used to enforce a desired rate allocation for both upstream and downstream flows, independent of their path lengths, and without requiring modifications to individual mesh routers.

5.2.2 TCP Window Sizing

As described in Section 2.4, TCP uses sliding windows and acknowledgments to provide reliable, in-order delivery of data. The congestion window *cwnd* associated with a TCP sender determines the amount of data it may have in the network at a given time. A number of studies [37] have associated the inter-flow contention experienced by a TCP flow to its *cwnd* exceeding its optimum size. *cwnd* is ideally set to the bandwidth-delay product (BDP) of the network pipe to keep it 'full'; a smaller value leads to under-utilization, and a larger value results in queueing and subsequent packet drops, invoking the penalty of congestion avoidance.

Chen *et al.* [19] show that computing the BDP of a wireless network is fundamentally different from that of a wireline network; while a wired network can push back-to-back frames in a pipe at a given time, wireless MAC protocols like 802.11 require the transmitter to wait for an ACK before it can contend for channel access for its next frame. Further, for a multihop flow, transmissions cannot be pipelined over adjacent, interfering links. Based on these constraints, the authors determine an upper-bound on the BDP for a chain of wireless nodes as $k\,H \times S$, where $\frac{1}{8} \leq k \leq \frac{1}{4}$, H is the number of round-trip hops, and S is the size of the TCP segment. $k = \frac{1}{4}$ is the optimal MAC-layer spatial reuse possible in a chain of 802.11-based nodes with interference range twice the transmission range. This value of k reduces due to the interference by TCP's ACK segments traveling in the opposite direction. This upper-bound on BDP represents the maximum carrying capacity of the path, beyond which no additional throughput can be obtained. The authors contend that the *cwnd* of a TCP sender should not be allowed to exceed this upper-bound.

Similar constraints on limiting the *cwnd* size have been proposed in other work, though there is no consensus on a value that works across all scenarios, *e.g.*, *cwnd* may be set to $\frac{1}{4}$ [37] or even $\frac{3}{2}$ of the path length [63]. Koutsonikolas *et al.* [69] show via experimental evaluation that RTS/CTS also impacts the choice of an appropriate *cwnd* value, and when enabled, the optimal *cwnd* size is 1 MSS.

We note that adjusting *cwnd* value impacts only the intra-flow contention experienced by a multihop flow; it does not resolve any inter-flow contention, and

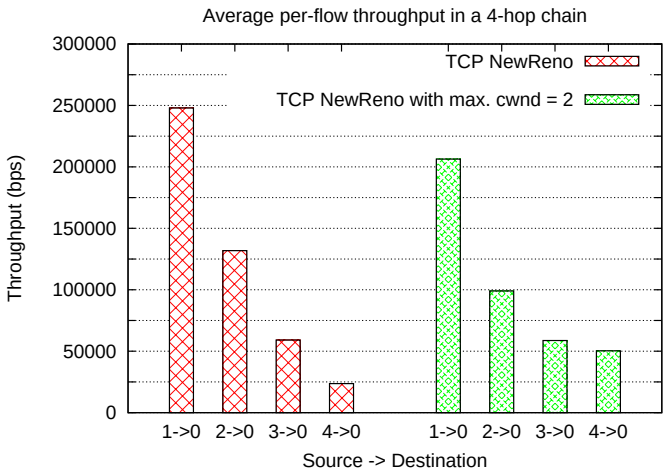

Figure 5.1: Limiting TCP congestion window size does not eliminate inter-flow contention, and has little impact on flow rate fairness.

subsequent unfairness and starvation may still ensue. We have validated this on a 4-hop chain (Fig. 3.1) with uploads from nodes 1, 2, 3 and 4 to the gateway node 0. The TCP congestion window limit was set to a maximum of 2. Fig. 5.1 shows that limiting congestion window size shows only a minor improvement over the base case with no such arbitrary limits.

5.2.3 Challenges: TCP Enhancements

TCP enhancements to provide improved fairness for multihop wireless flows have the following challenges:

1. TCP enhancements require modifications to the network protocol software stack on the end-hosts. This is an impractical proposition considering the large deployed base of TCP on millions of hosts on the Internet. Even split-connection approaches that require modifications only to the client devices on the wireless network are infeasible from a service providers perspective as they would have to develop and maintain software patches for supporting all types of client devices used by their subscribers.

2. TCP modifications also have incremental deployment challenges, *e.g.*, fairness considerations need to be evaluated for the case where only some users in the network use a wireless-optimized TCP variant.

5.3 Mechanisms

Rate-control mechanisms that operate independently of the transport-layer protocols have also been proposed. We provide a summary of this work below.

5.3.1 Router-assisted Control

In general, router-assisted resource management encompasses a set of mechanisms including congestion signaling, packet scheduling, and queue management. Active Queue Management (AQM) protocols like Random Early Detection (RED) [35] are examples of such router-assisted congestion control mechanisms. RED gateways are typically used at network boundaries where queue build-ups are expected when flows from high throughput networks are being aggregated across slower links. RED gateways provide congestion avoidance by detecting incipient congestion through active monitoring of average queue sizes at the gateway. When the queue size exceeds a certain threshold, the gateway can notify the connection through explicit feedback or by dropping packets. RED gateways require that the transport protocol managing those connections be responsive to congestion notification indicated either through marked packets or through packet loss.

We observe that there has been little work exploring the applicability (or lack thereof) of AQM techniques in multihop wireless networks. One noticeable exception is Xu *et al.*'s [125] Neighborhood RED (NRED) scheme that drops packets based on the size of a virtual distributed"neighborhood" queue comprising all nodes that contend for channel access. NRED only identifies a subset of these contending nodes, as it misses the flows that are outside the transmission range but still interfere. Additionally, this proposed mechanism is closely tied with a particular queue management discipline required on all mesh routers.

5.3.2 Rate-based Protocols

In contrast to window-based protocols, rate-based protocols require the receiver or the network to inform the sender of the rate at which it can support that connection [93]. EXACT [18] is a end-to-end rate-based flow control technique for ad hoc networks. It requires each router to periodically estimate its local capacity and use that to compute the fair share of all egress flows. A special IP header (called flow control header) is then populated with the lowest end-to-end rate along the path

of a flow. This rate is communicated back to the source where it is enforced locally. However, maintaining per-flow state at intermediate routers is a challenge in scaling EXACT to large multihop networks. Further, EXACT only defines a rate-based flow control scheme; additional mechanisms like Selective Acknowledgments (SACK) need to be separately overlaid on EXACT for reliable data transmission.

Stateless rate-based protocols have also been proposed in the literature. ATP (Ad hoc Transport Protocol) [110] uses packet delay feedback from intermediate routers to allow a source to compute its rate. The routers maintain the average delay (sum of queueing and transmission delays) experienced by all egress packets. These routers can then update the header of a passing packet such that the header always carries the largest delay encountered along the path of a packet. The receiver aggregates these delay values over a time interval, computes a new rate, and communicates it to the sender. Results in [99] show that while ATP improves the average rate allocation compared to TCP, the fairness index was no better than TCP and some flows still experienced starvation.

5.3.3 Alternative Distributed Protocol Designs

Distributed algorithms for enforcing fairness in multihop networks have been proposed in [38, 52, 75, 99, 125, 132], amongst others. In general, distributed computation of fair rates requires periodic signaling between contending senders. For example, a change in the status of a stream activity needs to be propagated to all nodes along the path of the stream *and* as well as their contending neighbors [52]. Further, contending nodes need to periodically synchronize their estimate of the network capacity. This may be done by interpreting the queue size as indicators of local contention, but when this contention is asymmetric, explicit signaling is required [99]. All nodes in the network need to understand and correctly interpret these signaling messages. Jain *et al.* [52] and Raniwala *et al.* [99] have proposed distributed algorithms to achieve these requirements based on this conflict graph approach. Gambiroza *et al.* [38] propose a time-fairness reference model that removes the spatial bias for flows traversing multiple hops, and propose a distributed algorithm that allows them to achieve their fair-rate allocation.

TCP has a link-centric view of congestion that works well for wired networks. In wireless networks, however, congestion is a neighborhood phenomenon, *i.e.*, it is not local to a single node but common to all nodes sharing the radio channel. IFRC [97] is a distributed protocol for a set of sensor nodes to detect incipient

congestion, communicate this to interfering nodes, and to follow an AIMD rate-control mechanism for converging to the fair-rate. IFRC supports the many-to-one communication paradigm of sensor networks, but fails to identify and signal all set of interfering nodes in one-to-many traffic scenarios (typical downloads in WMNs). Using a clean-slate approach, the authors extend this work and propose WCP [98], a new rate-based protocol that shares congestion information with interfering nodes and uses synchronized AIMD of flow rates to achieve fairness. With WCP the rate of a flow is inversely proportional to the number of congested neighborhoods it traverses. We note that this allocation criterion is not consistent with any of the commonly used fairness notions described in Section 2.1.2. Further, WCP identifies the congestion neighborhood of a link based on transmission ranges, while it is known that nodes in the interference range (which is typically larger than transmission range) may interfere with a transmission.

Other recent work propose rate control measures that also require modifications to the MAC layer. Zhang *et al.* [132] transform the global max-min fairness objectives into a set of conditions locally enforceable at each node, and propose a rate adaptation algorithm based on these conditions. This work assumes a modified 802.11 MAC that transmits a packet only when a receiver has buffer to store it.

5.3.4 Challenges: Rate-control Mechanisms

Rate-control mechanisms described above face the following challenges:

1. Many of the protocols described above provide rate-control functionality only. Separate reliable delivery mechanisms are required if these protocols are to be an effective replacement for TCP.

2. It is not clear how the clean-slate approach adopted by many of these rate-control mechanisms can be retrofitted on top of TCP, the dominant transport protocol used on the Internet.

5.4 Standardization Efforts

Working Groups (WG) in both IEEE and Internet Engineering Task Force (IETF) are involved in standards development work for various facets of multihop (ad hoc) wireless networks. In this section we provide a summary of their work on congestion control in these networks.

5.4.1 IEEE 802.16

The IEEE 802.16 [25] family of standard specifications define PHY and MAC layer air interfaces for fixed and mobile metropolitan area networks. Various revisions of the standard were last consolidated in 802.16e specifications. It defines a PMP mode for communication between a Base Station (BS) and Subscriber Stations (SSs), and an optional Mesh mode that allows traffic to be routed across SSs. Recent amendments introduced as a part of 802.16j relay specifications replace the Mesh mode with Mobile Multihop Relay (MMR) mode [41] and introduce Relay Stations (RS) that relay information between BS and SS.

The WiMAX Forum is an industry consortium leading the efforts to promote and establish the 802.16 technology. The forum has established a certification process for ensuring interoperability between 802.16 systems from different vendors. This process verifies conformance with the base standard specifications as well as interoperability based on system profiles established by the Forum. While the original standard was designed to cover a wide spectrum of possible applications, these profiles establish the baseline for mandatory or optional PHY and MAC-layer features based on realistic market requirements.

Packet Scheduling in 802.16

802.16 standard specifications support both time division duplexing (TDD) and frequency division duplexing (FDD). The current set of WiMAX profiles are primarily TDD-based as it supports higher spectral efficiency by dynamically allocating uplink and downlink bandwidth to better reflect asymmetric nature of Internet centric applications.

TDD systems use the same wireless channel for downlink and uplink traffic, spacing the transmissions apart in time. An 802.16 frame is thus divided in two subframes, downlink (DL) and uplink (UL), with transition guard bands in between for switching the radio circuitry operation. TDD mode requires tight time synchronization to minimize duration of these guard bands. Most current 802.16 hardware uses highly accurate GPS receiver clocks for synchronization.

There are two modes of scheduling specified for MMR: centralized and distributed. In centralized scheduling, the BS determines the bandwidth allocation for an RS's downlink stations; in distributed scheduling, RS determines this allocation in conjunction with BS. Centralized scheduling is useful in small topologies

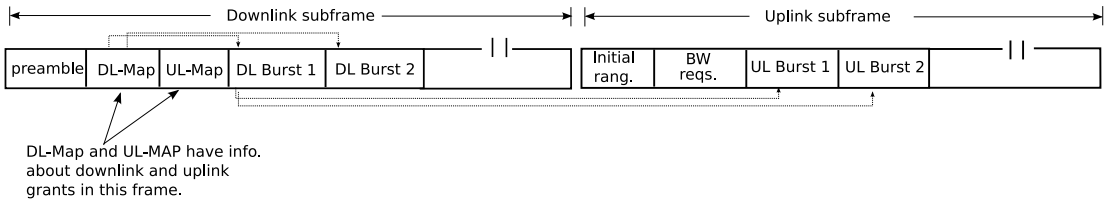

Figure 5.2: Simplified WiMAX frame structure transmitted by a BS.

(up to 2-hop networks), as the overhead for a BS to specify the scheduling profile becomes prohibitive with an increasing number of connections.

The BS is responsible for managing the scheduling of transmissions so to achieve traffic QoS requirements. It allocates usage time to SSs through information embedded in the DL-MAP and UL-MAP headers shown in Figure 5.2 [106]. Initial ranging contention slot allows a SS to discover optimum transmission power settings and timing offsets. Bandwidth request contention slots allow a SS make bandwidth requests to the BS for subsequent frames. The time slot allocated to a node can constrict and enlarge over a period of time. In these scheduling aspects, WiMAX borrows heavily from DOCSIS/HFC cable modem technology standards and applies them to wireless settings.

5.4.2 Hybrid Networks: WiMAX and 802.11 WMNs

While WiMAX MMR specifications have only recently been ratified, 802.11 radios have become a commodity platform with over 387 million chipset sales reported in 2008 alone [7]. This economy of scale has resulted in 802.11 becoming the preferred radio platform for developing last mile access networks for a large number of commercial entities. It is expected that as WiMAX matures, the two technologies will be used in a complementary manner, with WiMAX providing a long distance wireless backhaul for a last-mile distribution network which is primarily based on 802.11-based WMNs [15].

5.4.3 IEEE 802.11s

The IEEE 802.11 Task Group s is working on standardizing a set of amendments to the 802.11 MAC to create an Extended Service Set (ESS) of Mesh Points (MPs) that are connected via a multihop Wireless Distribution System (WDS).

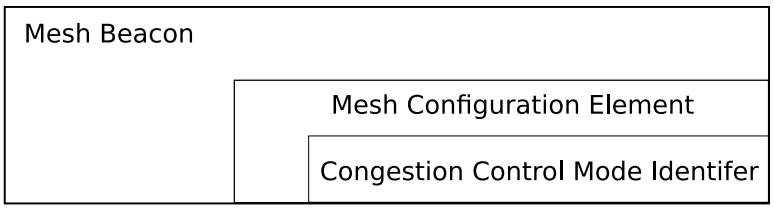

Figure 5.3: Congestion Control Mode Identifier field in a Mesh Beacon announces the supported congestion control protocol.

Congestion Control in 802.11s

Intra-mesh congestion control is based on three mechanisms: congestion monitoring and detection, congestion notification, and congestion resolution via local rate-control algorithms. The 802.11 standard only provides for a signaling framework for exchanging congestion notification messages; congestion monitoring and detection as well as subsequent rate-control algorithms are considered out of scope. This reflects the fact that while congestion control is necessary, there is no single solution that can be optimized for all the different mesh applications. The standard thus allows for an extensible congestion control framework.

Mesh Points (MPs) can support multiple congestion control protocols, though only a single protocol may be active at a given time in a network. This protocol is identified by the Congestion Control Mode Identifier (CCMI) field that is a part of the mesh beacon (Figure 5.3) [104]. A null value for this identifier means that the network does not support any congestion control scheme. An identifier may be reserved for an open, standardized congestion control protocol or may even be vendor specific.

The draft 802.11s standard specifies a congestion control signaling protocol. When an MP detects local congestion, it may transmit a Congestion Control Notification (CCN) frame. This frame may either be sent to neighboring MPs or directed to the MP sourcing the traffic causing this congestion. The recipient may then choose to adjust their frame rate to the MP that sent the CCN frame. Each CCN frame contains Congestion Notification Element (CNE). The default CNE described by the standard contains the estimated time the congestion is expected to last for each of the four access categories in 802.11e (Figure 5.4) [104]; a value of zero specifies that there is no congestion detected for that specific access category. However, as previously described, the framework is extensible to accommodate CNEs that contain additional information as required by the new congestion control protocols.

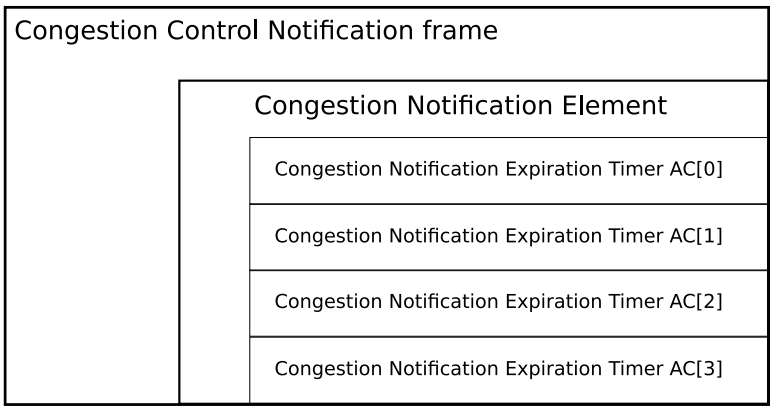

Figure 5.4: The default Congestion Notification Element in a Congestion Control Notification frame contains the estimated congestion duration for each of the four Access Categories.

The congestion control framework in IEEE 802.11s draft specifications sacrifices robustness of the protocol in favor of supporting greater extensibility. Unfortunately, this leaves the framework with little functional specifications to ensure true interoperability across various vendors. It also raises the possibility of new security attacks, *e.g.*, selfish nodes may not adjust their rates in response to CCN frames, or may even generate spurious CCN frames to slow down other MPs unnecessarily.

5.4.4 IETF MANET Working Group

The MANET Working Group in Internet Engineering Task Force (IETF) has standardized a number of routing protocol for both static and dynamic multihop wireless networks. These include Ad Hoc On Demand Distance Vector (AODV) [92] protocol, Dynamic Source Routing (DSR) [58] protocol, Optimized Link State Routing (OLSR) [24] protocol, and Topology Broadcast based on Reverse-Path Forwarding (TBRPF) [89] protocol. To the best of our knowledge, this WG has not yet looked into congestion control protocols for multihop wireless networks.

5.5 Summary

There is extensive literature in the realm of resource allocation, fairness, and congestion control in wireless networks. In our discussion we categorized the relevant work as MAC-layer modifications, TCP modifications, and alternate rate-control

protocols. We note that many solutions across all three classes present incremental deployment challenges.

There is ongoing work within the standard bodies to address congestion control as a part of 802.11s standards specifications. IEEE 802.11s draft standard only specifies a lightweight congestion control signaling framework. It does not specify as to which nodes should receive this notification or how the recipient should respond. Leaving out these critical components of the congestion control framework leaves the network vulnerable to new kind of security attacks.

Part II

Centralized Rate Control: Efficacy and Mechanisms

Chapter 6

The Efficacy of Centralized Rate Control in WMNs

In this chapter we explore the feasibility of using centralized rate control in WMNs. Conceptually, this approach is based on router-assisted rate control mechanisms that are designed for use alongside end-to-end rate control mechanisms in wired networks. We first evaluate the performance of commonly used router-assisted rate control mechanisms previously proposed for wired networks. We discover that fundamental differences between the characteristics of wired and wireless networks render a number of these mechanisms ineffective in a WMN. We show that centralized non-work-conserving rate-based scheduling can effectively enforce a desired rate allocation in WMNs. We evaluate the efficacy of these rate control measures through extensive simulation analysis as well as experiments on our WMN testbed.

6.1 Introduction

In wired networks, router-assisted flow control mechanisms have been proposed for use alongside end-host based congestion control protocols, *e.g.*, [29, 35, 84]. Pure end-to-end flow control schemes cannot provide isolation between flows or ensure rate or delay guarantees; they instead depend on these router-assisted mechanisms for support. We are interested in evaluating the feasibility of establishing similar controls at gateway mesh routers in WMNs. Traffic patterns in these networks primarily consist of flows directed either towards or away from the gateway. This allows the gateway to develop a unified view of the entire network, making it a suitable choice for enforcing various resource allocation policy objectives that may

be required to support a scalable, functional network. In particular, we wish to use gateway-enforced control to address flow rate unfairness challenges described in Chapter 3.

In this chapter, we focus on the efficacy of such a centralized control, rather than the specifics of the controller mechanism design. Given a desired rate allocation policy objective (*e.g.*, max-min fair rate allocation), we evaluate the effectiveness of gateway rate control in enforcing this objective in a 802.11-based WMN. This evaluation is necessary because wireless multihop network characteristics are distinct from wired networks or even one-hop WLANs: competing flows in a WMN may have different path lengths, and a flow experiences varying levels of link contention along each hop; further, transmissions along individual links are scheduled based only on the localized view of the CSMA/CA transmitters. We discover that these characteristics render many commonly used router-assisted wired network mechanisms ineffective as gateway-enforceable solutions in WMNs. Work-conserving scheduling techniques, such as Fair Queueing (FQ) or Weighted Fair Queueing (WFQ) [29] are inadequate on their own as they assume independence of links. Similarly, router-assisted probabilistic packet drop techniques including Active Queue Management (AQM) [35] are ineffective because packet losses in a multihop network are spatially distributed and cannot be accurately predicted using the queue size at the gateway router. We describe these fundamental differences in Section 6.3.1 and 6.3.2.

We show that simple non-work-conserving rate-based centralized scheduling techniques can enforce fairness in 802.11-based WMNs. Link layer retransmissions in 802.11 MAC allow it to recover from wireless-specific packet losses. Combining this with rate-based scheduling results in managing spectral resources in a way that allows all nodes to obtain their share of the network capacity. We show that even course-grained rate control on net-aggregate traffic passing through the gateway is effective in eliminating unfairness. Further improvement in fairness is obtained when we provide isolation between flows using FQ alongside aggregate rate-based scheduling. Finally, rate-based scheduling can be enforced on a per-flow basis, allowing fine-grained control over the resource allocation process. We evaluate the efficacy of this centralized control under varying network loads and flow conditions, including short and long-lived adaptive flows for both upstream and downstream traffic.

The remainder of this chapter is organized as follows. In Sections 6.2 below, we describe a number of techniques for enforcing centralize rate control. We evaluate their effectiveness in Section 6.3 using a simulation framework based on the computational model approach described in Chapter 4. We then evaluate the efficacy of

centralized non-work-conserving rate-based schedulers via experimental evaluation on our WMN testbed.

6.2 Centralized Flow Rate Control in WMNs

Router-assisted congestion control mechanisms have been extensively studied for wired networks. Congestion in Internet routers occurs due to statistical multiplexing or link speed mismatch across different network interfaces. Gateway nodes in WMNs interface the high-speed wired backhaul link with the shared-spectrum wireless resource that is often the system bottleneck, creating opportunities for reusing existing wired solutions in this new domain. In the following sections, we consider three categories of algorithms: work-conserving scheduling-based algorithms (Section 6.2.1), preferential packet-drop algorithms (Section 6.2.2), and traffic-shaping algorithms (Section 6.2.3).

6.2.1 Work-conserving Scheduling-based Algorithms

Work-conserving packet scheduling algorithms like FQ and WFQ are approximations of the Generalized Processor Sharing (GPS) scheduler that is the theoretically ideal mechanism for providing fair bandwidth allocation [29]. Their work-conserving nature allows them to maintain high network utilization. They use flow or class-based queueing that provides isolation between the units of scheduling. WFQ, in addition, may also provide differential service to a flow i based on its weight w_i, guaranteeing it to receive $\frac{w_i}{\Sigma w_j}$ fraction of the output bandwidth, where the sum of weights in the denominator is calculated over all flows that have packets queued up. These algorithms maintain high network efficiency because of their work-conserving nature.

We note that while distributed FQ protocols have earlier been proposed for ad hoc networks [81], we are interested in evaluating their impact on fairness when enforced only at the gateway in a WMN. To the best of our knowledge, this has not been evaluated in prior work.

6.2.2 Packet-drop/Marking Algorithms

Packet loss in wired networks primarily occurs as queue drops at the router interface across the bottleneck link. Selective packet drop and/or marking techniques (*e.g.*,

AQM techniques such as Random Early Detection (RED) [35] and its variants) allow these congested routers to respond to signs of incipient congestion by signaling the source nodes to slow down. Since our gateway router is the interface between the high-speed wired links and the shared-spectrum wireless links, it appears that some of these algorithms might also be effective in WMNs.

While RED gateways have proven effective in avoiding congestion, it has been shown that they provide little fairness improvement [79]. This is because RED gateways do not differentiate between particular connections or classes of connections [35]. As a result, when incipient congestion is detected, all received packets (irrespective of the flow) are marked with the same drop probability. The fact that all connections see the same instantaneous loss rate means that even a connection using less than its fair share will be subject to packet drops.

Flow Random Early Drop (FRED) [79] is an extension to the RED algorithm designed to reduce the unfairness between flows. In essence, it applies per-flow RED to create an isolation between flows. By using per-active-flow accounting, FRED ensures that the drop rate for a flow depends on its buffer usage [79].

A brief description of FRED is as follows: A FRED gateway uses flow classification to enqueue flows into logically separate buffers. For each flow i, it maintains the corresponding queue length $qlen_i$. It defines min_q and max_q, which respectively are the minimum and the maximum number of packets individual flows are allowed to queue. Similarly, it also maintains min_{th}, max_{th}, and avg for the overall queue. All new packet arrivals are accepted as long as avg is below the min_{th}. When avg lies between min_{th} and max_{th}, a new packet arrival is deterministically accepted only if the corresponding $qlen_i$ is less than min_q. Otherwise, as in RED, the packet is dropped with a probability that increases with increasing queue size.

We note that Xu *et al.* [125] have proposed the use of RED over a virtual distributed "neighborhood" queue comprising nodes that contend for channel access. This was in the context of wireless ad hoc networks in which flows do not necessarily share traffic aggregation points. In our work we explore the traditional use of AQM as a router-assisted (gateway-enforced) mechanism.

6.2.3 Traffic Policing/Shaping Algorithms

Traffic policing and shaping algorithms are commonly used in scenarios where traffic limits are known or pre-determined in advance (*e.g.*, while enforcing compliance

with a contract). The difference between policing and shaping is minor yet subtle: policing does not implement any queueing and excess packets are immediately dropped. Shaping, on the other hand, can absorb short bursts of packet, where the burst size is determined by the allocated buffer. When the buffer is full, all incoming packets are immediately dropped and traffic shaping effectively acts as traffic policing. Both policing and shaping are examples of non-work-conserving scheduling methods.

Traffic shaping can be enforced at different levels of resource abstraction; it can be applied to aggregate traffic allowed to pass through a network interface, or it may be enforced on individual flows in a traffic stream. We describe these control configurations below.

Interface Aggregate Rate Limit

The fundamental trade-off between total network capacity and flow-level fairness has been identified in prior work [38]. Specifically, aggregate network throughput is highest when all resources are allocated to the least cost flow while starving all others. Since the gateway router injects TCP packets or the subsequent ACKs into the wireless network, it can be used to control the aggregate throughput of a network. We are interested in enforcing a *fair-aggregate* rate limit at the gateway wireless interface. This is the fair-aggregate network capacity, and is simply the sum of fair rate allocation of all flows in the network. This rate is then enforced on the net aggregate data traffic allowed through the gateway using the token bucket mechanism shown in Figure 6.1a.

We note that aggregation of traffic flows has been proposed in prior work (*e.g.*, [105]) for core Internet routers in wired networks to allow Integrated Services architecture (IntServ) to scale for a large number of flows. Such scalability is not a concern for contemporary WMNs; because of the shared wireless channel, these networks are designed to limit their service to tens of nodes per gateway router. Our use of interface aggregate rate limiting is driven by its simplicity of rate allocation heuristics, and we are interested in evaluating the underlying fairness characteristics of 802.11 MAC to distribute the allocated network capacity fairly across all contending nodes.

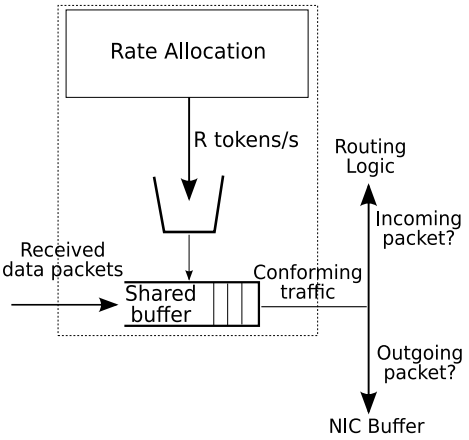

(a) Interface aggregate rate limit

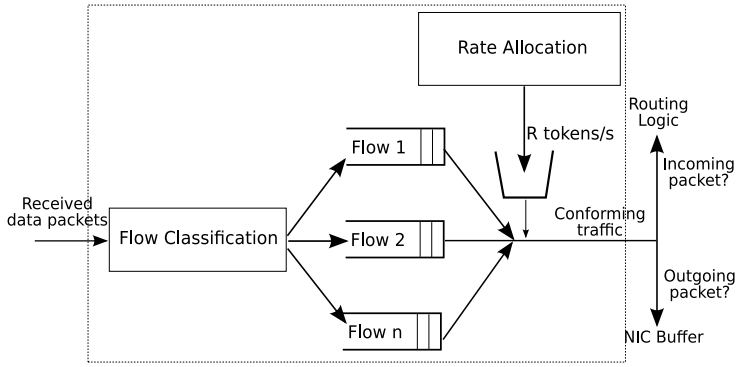

(b) Interface aggregate rate limit with FQ

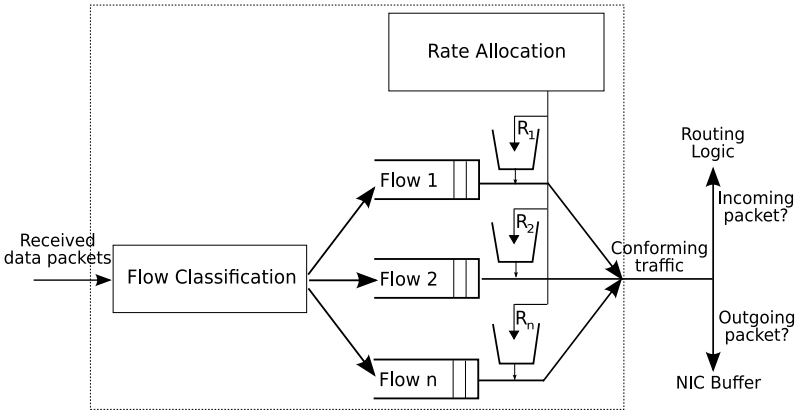

(c) Per-flow rate limit

Figure 6.1: Traffic shaping at gateway router. Figure 6.1a limits the aggregate traffic allowed through the interface to rate R. All flows share a single FIFO buffer. Figure 6.1b provides isolation between flows using per-flow queues and limits the aggregate traffic through the interface. Figure 6.1c enforces per-flow rate limiting, with rate R_1 for Flow 1, R_2 for Flow 2, etc.

Interface Aggregate Rate Limit with FQ

TCP flows sharing a single queue are susceptible to synchronization due to bursty and correlated packet losses. To prevent this, we introduce per-flow queues with fair scheduling between them. By separating flows, we can provide isolation between flows experiencing different levels of contention for network access, *e.g.*, we can separate locally generated traffic at a node from its relayed traffic. This new architecture is shown in Figure 6.1b. Note that while flows are queued separately, rate limits are still enforced for the net aggregate traffic traversing the gateway.

Separating traffic into flows requires a flow classifier. For WMNs providing last mile access, this classification can be based on source or destination mesh routers. Thus a flow f_i represents the aggregate of all micro-flows originating from, or destined to, mesh router n_i in the network. In this context, we use nodes and flows interchangeably in our discussion. We note that this classification is consistent with the common practices employed by ISPs on wired networks, where capacity is managed on a per-subscriber basis.

Per-flow Rate Limit

While the architecture in Figures 6.1a and 6.1b manages aggregate traffic through an interface, there may be a requirement for more fine-grained control over resource allocation between individual flows. This may be necessitated by QoS-enabled mesh networks where the provider wishes to support differentiated services, or provide weighted max-min or proportional fairness. We extend the system architecture to provide per-flow rate limiting at the gateway router as shown in Figure 6.1c. Data traffic through the gateway can be classified into queues, which are then drained out at their specific rate. Note that we are proposing rate-limiting data traffic only; system housekeeping messages like routing updates are not rate limited.

6.3 Simulation Analysis

We perform simulations using ns-2 [2] to evaluate the effectiveness of gateway-enforced control in WMNs. We implement and evaluate each of the control mechanisms described in Section 6.2 at the gateway. Our implementation works between the 802.11 MAC layer and the network layer at the gateway router, and operates transparently across the two layers. No modifications were made on the regular mesh nodes.

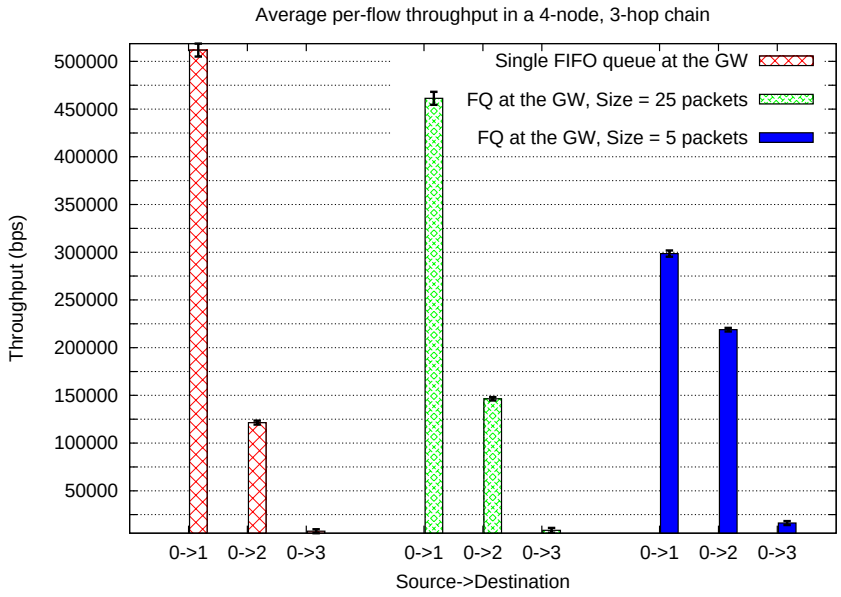

Figure 6.2: Single FIFO queue vs. per-flow queue at the gateway router for a 3-hop chain with download traffic. The error bars are the 95% confidence intervals over 25-runs of the experiments.

6.3.1 Work-conserving Scheduling-based Algorithms

We simulate a TCP source on a wired network sending data to three mesh routers arranged in a 3-hop chain (see Figure 3.1) via the gateway node 0. The wireless interface on the gateway node implements FQ for downstream traffic. We benchmark these results against experiments with a single shared Drop Tail FIFO queue at the gateway.

Figure 6.2 shows that the impact of fair queueing is limited and varies with the size of the buffer allocated to each flow. Node 3's traffic (TCP ACKs) is susceptible to collisions at receiver node 2 because of collisions with node 0's transmissions. This produces an inconsistent view of the channel state between the nodes; while node 3 backs off with repeated collisions, the TCP congestion window for flow $0 \rightarrow 1$ builds up to fill the channel capacity. Smaller buffer size at the gateway limits the growth of this window, but when node 3 is backed up, any leftover capacity is consumed by flow $0 \rightarrow 2$.

FQ, WFQ, and similar router-assisted scheduling techniques assume independence between links and were designed as work-conserving schedulers; they do not allow the output link to remain idle if any of the flows have packets to send. While this maintains high efficiency in wired networks, it creates problems in wireless net-

GW Queue	Flow	$\frac{avg.rate}{fair.rate}$	% Coll. - ACKs	JFI
FIFO	0→1	3.18	0.00	0.63
	0→2	1.73	0.00	
	0→3	0.03	42.4	
FRED	0→1	2.72	0.00	0.66
	0→2	1.96	0.00	
	0→3	0.04	39.6	

Table 6.1: Performance comparisons between a Drop Tail FIFO Queue and a FRED Queue at the gateway router.

works where the contending links are not independent, *i.e.*, transmission on a link precludes successful delivery of data on contending links. In topologies where mesh nodes develop an inconsistent view of the channel state, work-conserving scheduler would schedule packets for advantaged node when it has nothing to send for distant, disadvantaged flows, while on the contrary, the best alternative would have been to defer any transmissions and keep the medium idle to allow for successful transmissions by disadvantaged nodes. The situation deteriorates when work-conserving schedulers are used with backlogged traffic sources using adaptive transport protocols such as TCP due to cross-layer interaction issues described in Chapter 3.

6.3.2 Packet-drop/Marking Algorithms

We simulate a FRED gateway router on the 3-hop chain topology similar to the one used in last section. We use downstream flows in our experiment because a queue build-up (for detecting incipient congestion) only occurs when packets traverse from a high-speed wired link to a shared-medium WMN. The gateway queue size is set at 50 packets. FRED parameters are consistent with the default values in ns-2.

Our results are summarized in Table 6.1. FIFO queue exhibits the unfairness characteristics described in prior chapters, with flow 3 starving. FRED queue does not prevent this starvation. By monitoring queue drops at the gateway, we found that FRED queue did register some proactive packet drops for 1 and 2−hop flows, though it was insufficient to preclude the starvation of flow 3.

Figure 6.3 shows the per-flow data arrival rate (not ACKs) in the FRED queue at the gateway during the simulation run. The queue space is evenly shared between the flows at the start of the simulation, but continues deteriorating during

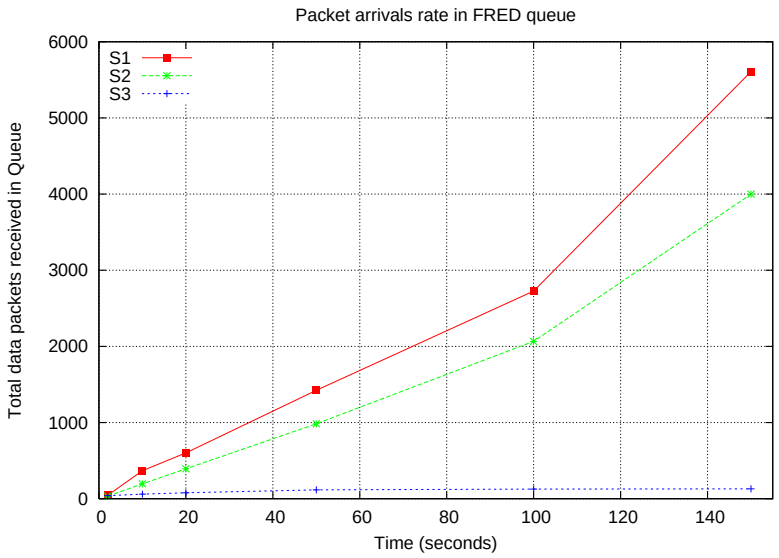

Figure 6.3: New data packet arrival rate in FRED queue.

the simulation execution. New data packets are not seen for flow 3 because ACKs for the previously transmitted ones have not been received (loss rate of 39.6% for flow 3 ACKs with FRED). This is because the gateway acts as a hidden terminal for TCP ACKs generated by node 3. As discussed previously in Section 3.2, this hidden terminal cannot be resolved using RTS/CTS as both GW and 3 have different receivers. Because of frequent collisions, node 3 repeatedly increases its contention window to a point where TCP timeouts occur, and the packets have to be retransmitted by the gateway. Though flow 1 transmits fewer packets with FRED, the extra available bandwidth is acquired by flow 2 because there is very little traffic to be sent out for flow 3 because of the combined effect of the 802.11 contention window and the TCP congestion window.

We conclude that AQM is ineffective as a gateway-enforced technique for improving flow rate fairness in WMNs. This is due to fundamental differences in packet loss characteristics between wired networks and WMNs [54]. In wired networks, packet loss occurs primarily at the queue interface into the bottleneck link. In WMNs, however, these packet losses are spatially distributed over the network topology at various intermediate routers (see Section 3.2) and cannot be accurately predicted by simply monitoring the queue size at the gateway router.

6.3.3 Traffic Policing/Shaping Algorithms

We evaluate the various traffic shaping alternatives described in Section 6.2.3. Our simulations include a number of chains, grids, and random multihop network topologies, including both upstream and downstream flows, with up to a maximum of 35 simultaneously active nodes transmitting via a single gateway. Experiments for a given topology are repeated 25 times with different random seeds and random flow activation sequences, and the results averaged. For each topology, the traffic shaping rate is computed off-hand using the collision-domain network capacity model described in Chapter 4. Other capacity models such as clique graph models [50] may similarly be used. We reiterate that our focus in this Chapter is on evaluating the efficacy of gateway-enforced control, and not on the mechanisms required for computing the desired rate allocation. We propose such mechanisms separately in the subsequent chapters of this dissertation.

The fair rate allocation computed by the model is enforced at the gateway via the traffic shaping architectures described in Section 6.2.3. The collision domain capacity model allows us to compute per-flow rate. The interface aggregate rate limit is then simply the sum of the fair rates of constituent flows. This rate limit is the fair-aggregate capacity of the network.

Long-lived Elastic TCP Flows

Our results are summarized in Tables 6.2 and 6.3 for downstream and upstream TCP flows, respectively. The fairness metrics we use were described in Section 2.1.5. JFI is a quantitative measure of the fairness for a given rate allocation. $\frac{avg.\,min.\,flow\,rate}{fair\,rate}$ and $\frac{avg.\,max.\,flow\,rate}{fair\,rate}$ illustrate the degree of imbalance between the minimum and maximum throughput flows. We use normalized effective network utilization to quantify the spatial reuse for a given allocation and the resulting network capacity. We benchmark our results as follows:

1. We perform the same set of experiments using a single, shared, FIFO Drop Tail queue at the gateway router.

2. We repeat these experiments using FQ at the gateway router with a per-flow buffer size of 5 packets.

3. For upstream flows, we perform additional experiments that source rate limit the flows to their computed fair share rate without any modifications on the

gateway router. For downstream flows, this source rate limit is akin to per-flow gateway rate limit as the gateway is now injecting packets in the wireless medium.

Our results show that simply enforcing rate-based scheduling, even on the granularity of aggregate amount of traffic allowed through the network interface, provides upwards of two-fold improvement in JFI compared to the base case with a shared FIFO queue. We note that rate-based scheduling enforced via traffic shaping is, by nature, non-work-conserving. Thus while underlying topologies may still be susceptible to 802.11 MAC limitations described in Section 3.2, link-layer retransmissions can provide reliable packet delivery as long as non-work-conserving, rate-based scheduling can shield individual flows from effects of cross-layer interaction with TCP.

FQ by itself only provides a marginal improvement in fairness over FIFO Drop Tail queues. However, when FQ is combined with non-work-conserving rate-based scheduling, we see a further improvement of about 15%–20% over interface rate limiting alone. FQ introduces isolation between flows, protecting one flow's traffic from that of another. This leads to better short-term fairness that translates to improved long-term fairness calculated over average flow rates. We highlight this for a 5-hop, 4-flow chain in Figure 6.4. The buffer size at the gateway was 5 packets in experiments with per-flow queueing, 25 packets otherwise (The impact of buffer size is described in the section below). With 1 Mb/s wireless links, max-min fair share per-flow is approximately 65 Kb/s. Simply providing flow isolation using FQ without any rate limiting does not solve the fairness problem. In Figure 6.4b, the work-conserving FQ allows TCP congestion window size to grow to large values even with a per-flow buffer size of 5 packets at the gateway. Interface aggregate rate limiting improves long-term flow rate fairness in Figure 6.4c, though some flows still experience short-term unfairness at time instances when other aggressive flows have built up a large TCP congestion window. This happens because all flows share the same buffer at the gateway. It is the combination of FQ and aggregate rate limiting that improves short-term fairness between flows. TCP congestion window sizes are now bounded as shown in Figure 6.4f, thus considerably cutting down the jitter between packets from different flows. Per-flow rate limiting provides similar qualitative results as it also allocates separate buffers to flows at the gateway.

The quantitative analysis of per-flow rate control in Tables 6.2 and 6.3 show a further improvement in fairness index of about 1%–8% over FQ with interface aggregate rate limiting. We note that these fairness characteristics of per-flow rate-

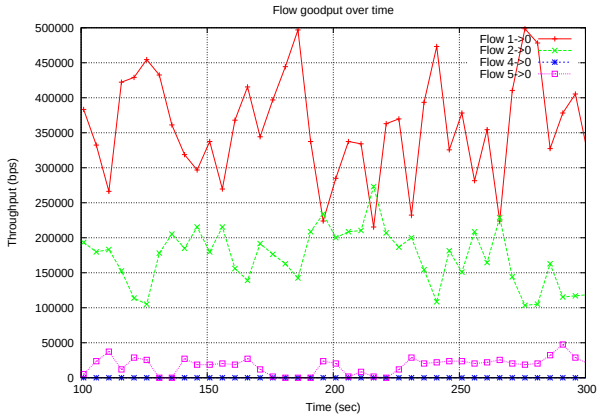

(a) Flow goodput. FQ at GW.

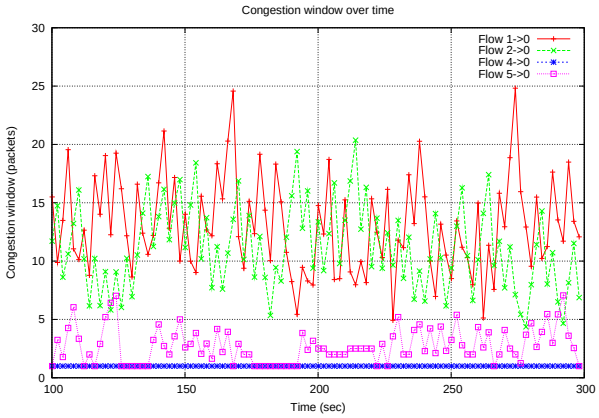

(b) TCP congestion window. FQ at GW.

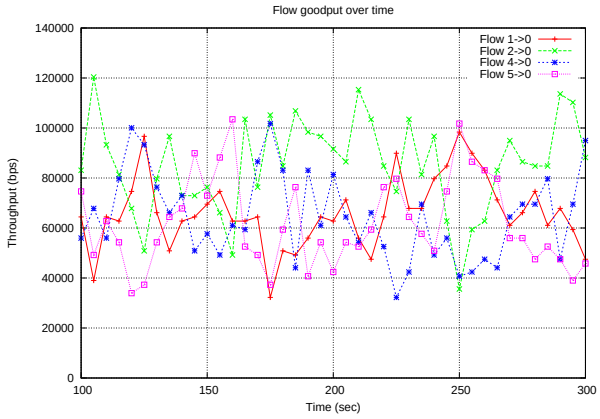

(c) Flow goodput. Aggregate rate control at GW.

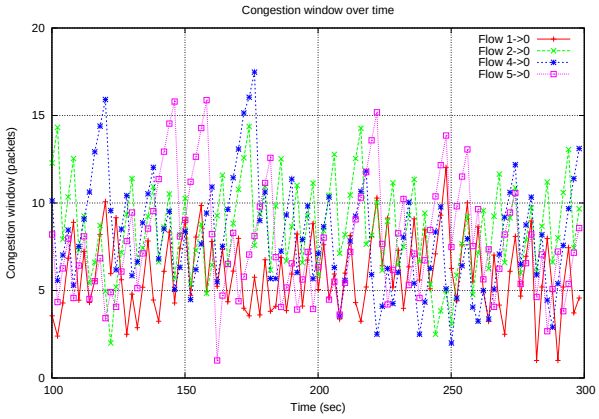

(d) TCP congestion window. Aggregate rate control at GW

Figure 6.4: Goodput over time and TCP congestion window growth over time for a 5-hop, 4-flow chain topology. Continued on next page.

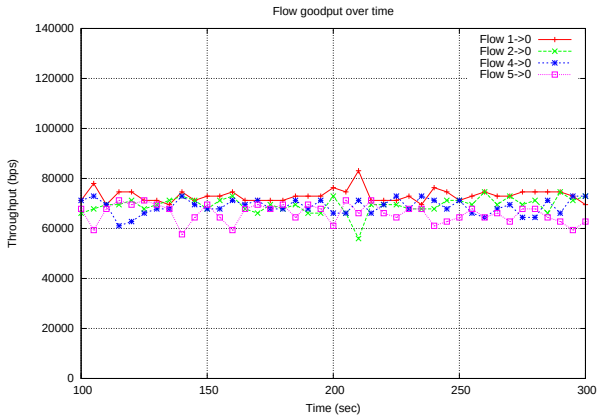

(e) Goodput. Aggregate rate control & FQ at GW.

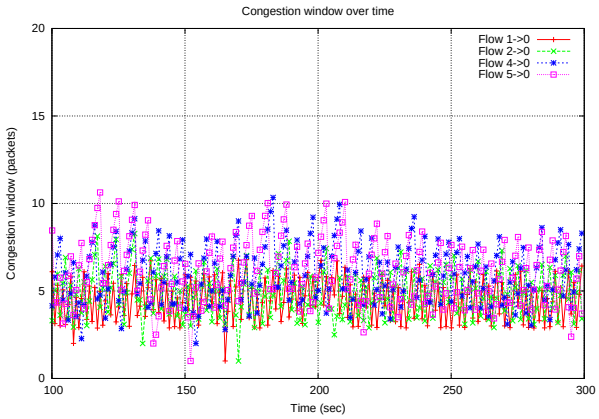

(f) TCP congestion window. Aggregate rate control & FQ at GW.

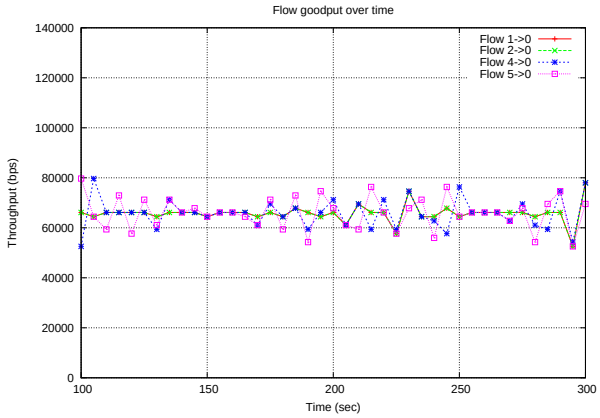

(g) Flow goodput. Per-flow rate limit at GW.

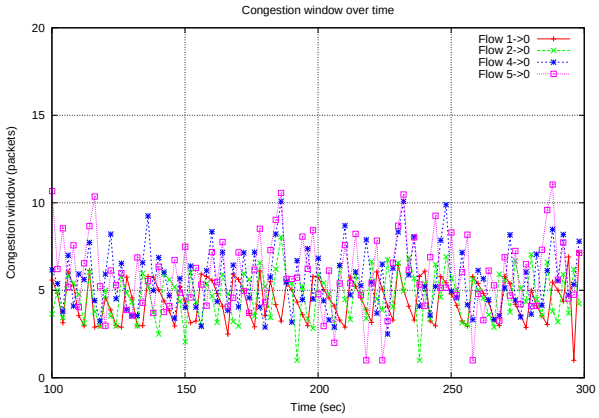

(h) TCP congestion window. Per-flow rate limit at GW.

Figure 6.4: Goodput over time and TCP congestion window growth over time for a 5-hop, 4-flow chain topology. Max-min fair share per flow is approx. 65 Kb/s. For aggregate rate limit (Figure 6.4c and 6.4d), flows shared a single FIFO buffer with size 25 packets. In all other cases, per-flow buffer size was 5 packets.

Scheme	JFI		$\frac{min.\,rate}{fair\,rate}$		$\frac{max.\,rate}{fair\,rate}$		$\frac{U}{U_{opt}}$	
	Avg.	Std.Dev.	Avg.	Std.Dev.	Avg.	Std.Dev.	Avg.	Std.Dev.
Single FIFO queue	0.41	0.24	0.10	0.10	10.86	7.08	0.95	0.09
FQ	0.55	0.20	0.20	0.06	5.36	2.95	1.00	0.07
Aggregate rate limit	0.81	0.15	0.43	0.30	2.02	0.86	0.91	0.11
Aggregate rate limit & FQ	0.98	0.02	0.72	0.31	1.08	0.08	0.98	0.03
Per-flow rate limit	0.99	0.02	0.75	0.26	1.01	0.01	0.95	0.07

Table 6.2: Fairness indices for downstream TCP flows.

Scheme	JFI		$\frac{min.\,rate}{fair\,rate}$		$\frac{max.\,rate}{fair\,rate}$		$\frac{U}{U_{opt}}$	
	Avg.	Std.Dev.	Avg.	Std.Dev.	Avg.	Std.Dev.	Avg.	Std.Dev.
Single FIFO queue	0.31	0.13	0.17	0.16	15.2	11.6	0.95	0.09
FQ	0.32	0.13	0.16	0.15	14.04	0.61	1.00	0.06
Aggregate rate limit	0.79	0.16	0.43	0.34	2.23	0.91	0.99	0.07
Aggregate rate limit & FQ	0.91	0.11	0.59	0.40	1.38	0.37	1.00	0.03
Per-flow rate limit	0.99	0.02	0.76	0.30	1.00	0.06	0.90	0.06
Source rate limit	0.99	0.01	0.77	0.21	1.00	0.01	0.91	0.07

Table 6.3: Fairness indices for upstream TCP flows.

limiting are very similar to those achieved with source rate limiting. Incidentally, perfect fairness cannot be achieved even with source rate limiting. Some network topologies may exhibit inherent *structural unfairness* [78], requiring control action beyond simple rate limiting. Addressing this is beyond the scope of our work.

Finally, we note that normalized effective network utilization $\frac{U}{U_{opt}}$ remains upwards of 90% for all scheduling techniques for both downstream and upstream flows; backlogged TCP flows saturate the spectrum around the gateway in all cases, irrespective of fairness in terms of rate allocation between individual flows.

In summary, our experiments show that centralized rate control cannot be exercised in WMNs using work-conserving scheduling techniques. Using non-work-conserving, rate-based scheduling is equally effective as source rate limiting techniques that require modifying the MAC or the transport-layer on all mesh nodes.

Short-lived elastic TCP flows

In previous section, we considered long-lived node aggregated flows that were active for the duration of the experiment. We now evaluate centralized rate control for

short-lived adaptive flows that are active only for part of the experiment. When these flows terminate, an efficient rate allocation mechanism must allow for distributing the freed resources to other flows in the network. Similarly, when a new flow is born, it should be possible to expeditiously allocate it its share of the network resources.

Flow activation/termination can be detected in multiple ways. TCP stream activation and tear-down can be detected by the exchange of the TCP-specific three-way handshake messages. In our case where a flow bundle constitutes multiple TCP streams, we simply use the presence or absence of packets to determine the current state of stream activity, thus obviating any overhead associated with the distribution of stream activity information. On detecting a new stream, the centralized controller simply computes a new rate per active stream and starts enforcing it. Detecting stream deactivation can be a little tricky, and the controller has to wait some time interval during which no packet is received from a flow. This time interval should be a function of the average delay experienced by the packets from a flow as well as the jitter.

We consider the results of a 7-hop chain (see Figure 3.1) with nodes indexed $0, 1, 2, ...7$, with node 0 being the gateway router. Five flows are active between the time interval 100–150 s. At 150 s., flows 1→0 and 0→5 are terminated. At time 200 s., flow 0→7 is turned off. Finally, at time 250 s, flows 1→0 and 0→7 are turned back on. Flow throughput values are shown in Figure 6.5. Here we show our results with per-flow rate limiting at the gateway. We are particularly interested in the convergence times required for the flows to converge around their new fair rates. We note that this convergence time is a function of the TCP state. A TCP agent starts up in slow start, where its congestion window builds up exponentially over time. This allows flows 1→0 and 0→7 to rapidly approach their fair rate within the 5 s. resolution of the graphs. However, increasing rates for flows in congestion avoidance modes is slower where the congestion window can only increase linearly with time. Because of this, the flows 3→0 and 0→6 take up to 15 s. to approximate their new fair rate at 215 s.

Non-adaptive Flows

Router-assisted rate control mechanisms are targeted at adaptive transport protocols that can react to congestion notification. TCP is the canonical example of such an adaptive protocol and constitutes the bulk of Internet traffic [121]. However, many delay-sensitive applications such as streaming media and telephony that pre-

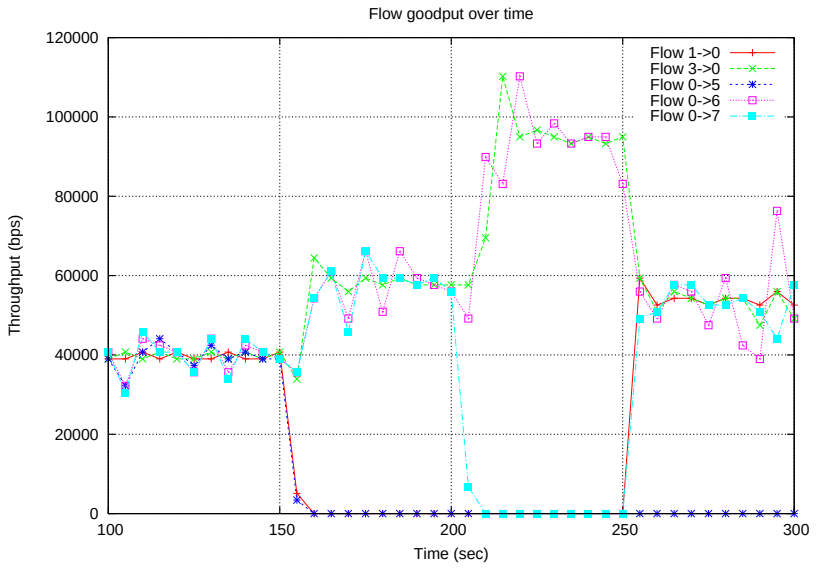

Figure 6.5: Throughput vs. time for a 7-hop chain with per-flow rate limiting at the gateway. Flows 1→0 and 0→5 terminate at 150 s., while flow 0→7 terminates at 200 s. Flows 1→0 and 0→7 are reactivated at 250 s.

fer timeliness to reliability use a UDP-based transport. In this section, we evaluate the performance of centralized rate control for such non-adaptive flows.

We simulate a 3-hop chain topology, with nodes indexed $0, 1, 2, 3$ and node 0 set as the gateway (see Figure 3.1). Our UDP constant bit rate (CBR) application generates a 500-byte payload at 5 ms. intervals, for a total load of 800 Kb/s. We considered both upstream and downstream flows, with a UDP stream originating/terminating per mesh node respectively. With 1 Mb/s wireless links, the max-min fair rate is approximately 124 Kb/s. Thus our UDP sources generate traffic load that is higher than the fair share per-flow, but is still low enough to prevent complete channel capture by any single flow. Our results with per-flow rate limiting at the gateway are shown in Table 6.4.

We observe that gateway-assisted rate control in WMNs can only successfully contain downstream flows. In this case, it effectively acts as source rate control, limiting each stream to its fair share on the wireless network. However, upstream flows continue experiencing unfairness; while we can limit the goodput of flow 1 to its fair share by dropping its excess traffic at the gateway, its non-adaptive transport protocol still sources traffic at 800 Kb/s across the wireless channel, thus keeping the medium busy and starving out other flows.

We note that while gateway-assisted rate control cannot provide protection

Traffic Type	Flow	$\frac{avg.rate}{fair.rate}$	JFI
Upstream UDP	1→0	1.00	0.54
	2→0	0.31	
	3→0	0.02	
Downstream UDP	0→1	1.00	1.00
	0→2	1.00	
	0→3	1.01	

Table 6.4: Per-flow centralized rate control for upstream and downstream UDP flows in a 3-hop chain with gateway node 0.

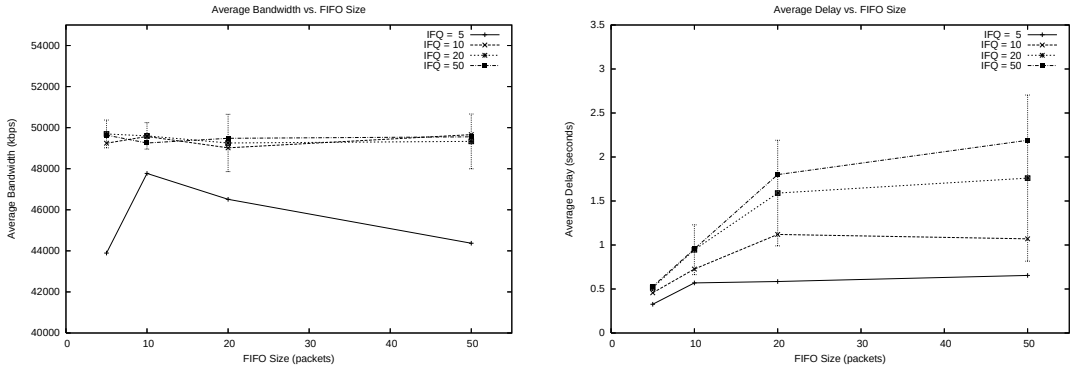

(a) Bandwidth vs. FIFO size

(b) Delay vs. FIFO size

Figure 6.6: Impact of per-flow queue size at the gateway as a function of the wireless interface FIFO queue (IFQ) size at mesh nodes. The range information corresponds to the IFQ size of 20 packets at all mesh nodes.

against channel capture by greedy upstream UDP flows, the fact that flow 1 sees a loss rate of around 70% means that there is little useful traffic being carried for this flow. If this flow was a multimedia application, this high loss rate will result in unacceptable performance, leading to a user-triggered backoff [14]: *i.e.*, the user will either adjust the application to use a less bandwidth-intensive coding technique (*e.g.*, reduced video resolution), or will simply terminate the application. Either action indirectly improves the fairness for remaining flows.

Impact of FIFO Buffer Size

We experimented with a 5-hop chain to understand the impact of the size of per-flow queue at the gateway on flow bandwidth and delay. We varied this per-flow queue

size from 5 to 50 packets, while adjusting the mesh nodes' wireless interface queue (IFQ) size from 5 to 50 packets. Our results are shown in Figure 6.6, with range information shown for the case of an IFQ of 20. We found that the gateway per-flow queue size of 5 packets yielded minimum delay, with little effect on bandwidth provided the IFQ was 10 or larger. A smaller IFQ of 5 packets results in considerable drop of throughput from buffer overflows at nodes that relay traffic for multiple other nodes in the network.

6.4 Testbed Analysis

In addition to our simulation results described previously, we have also evaluated the performance of gateway-assisted rate control on a multihop wireless testbed. In this section we first describe our testbed implementation and then illustrate the efficacy of gateway control through experimental analysis.

6.4.1 Testbed Implementation

We set up a 9-node WMN testbed on the 4^{th} floor of the E&IT building on the University of Waterloo campus. Node placement is shown in Figure 6.7a. We identify the nodes by alphabets A through I.

Our node configuration is shown in Table 6.5. Each node is retrofitted with two wireless interfaces. We use one interface for the multihop wireless backhaul, and the other interface for the access network. The two interfaces are configured to use orthogonal (non-overlapping) channels. Node E has additional wired connectivity and serves as the gateway mesh router for our testbed.

Software configuration

In addition to the base operating system and relevant drivers, we use the following software in our testbed implementation.

Linux traffic control (tc) Linux traffic control (`tc`) is a utility for configuring the traffic management functionality in the Linux kernel. `tc` is distributed as a part of the `iproute2` package. Here we introduce the three architectural components of this framework used in our implementation: queueing discipline (*qdisc*), classes, and filters. We refer the reader to the relevant documentation [46] for other details.

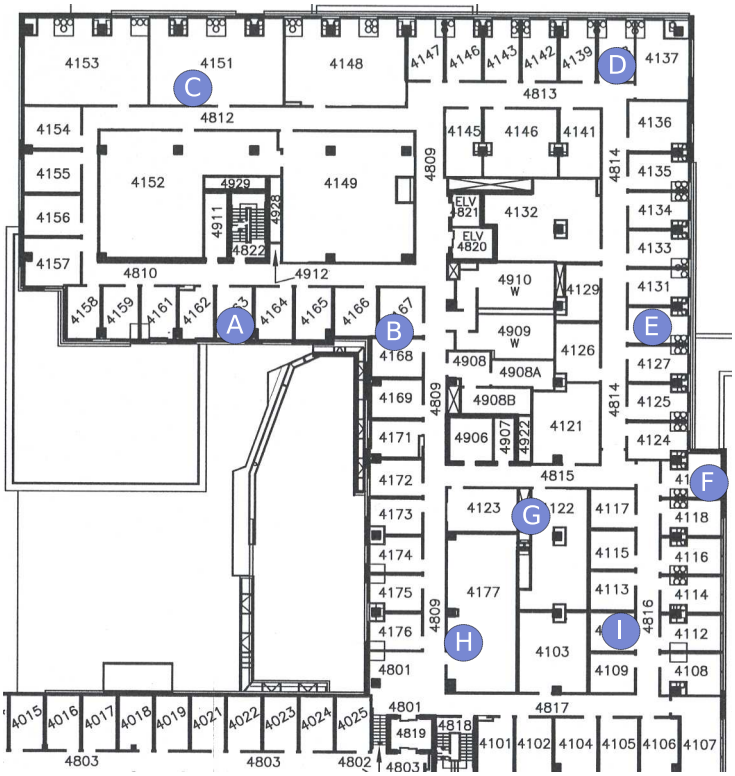

(a) Testbed node placement

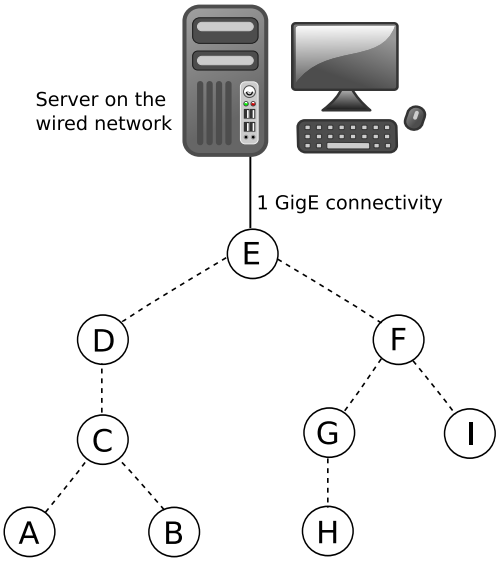

(b) Testbed routing topology

Figure 6.7: A 9-node multihop wireless testbed on the 4^{th} floor of the E&IT building on University of Waterloo campus. Node locations are identified by alphabets A through I. We use ETX routing metric with OLSR on the wireless network. Node E serves as the gateway node and bridges traffic between the wired and the wireless networks through its 1 GigE interface.

Node specifications	1.2 GHz VIA C7 fanless processor, 1 GB RAM, 40 GB HDD
Wireless interface	Two EMP-8602 PLUS-S 802.11a/b/g radios (Atheros 5006 chipset) per node
Antennas	Tri-band rubber duck antennas. 5 dBi gain in 5 GHz band
PHY link	802.11a with link rates up to 54 Mb/s
Radio channel	Channel 48 (5.24 GHz) for multihop backhaul. Channel 52 (5.26 GHz) for access network. Both channels are unused by the production network
Operating system	Arch Linux distribution (kernel 2.6.28) patched for Web100
Wireless drivers	Open source MadWifi v0.9.4.1
Routing	olsr.org v0.5.6-r3 with ETX metric

Table 6.5: Attribute summary of testbed configuration

A qdisc is a scheduler that manges the queue associated with a device. Most devices have one or more qdiscs (one exception is the loopback device that does not have any qdiscs). The *root* qdisc is directly attached to the network device. In Linux, the root qdisc is, by default, a FIFO queue. This is an example of a *classless* qdisc, *i.e.*, the qdisc does not internally subdivide or discriminate between packets. *Classful* qdiscs, on the other hand, may contain multiple classes, each corresponding to a traffic type. Each class has its own qdisc, which may also be classful, thus creating a tree-like hierarchy of classes. *Filters* may be used to classify traffic into classes; a filter is a set of rules corresponding to the conditions for packet classification. Note that the network device communicates only with the root qdisc to enqueue or dequeue a packet. This root qdisc is then responsible for invoking the correct operation on the relevant classes.

The qdiscs we use in our implementation are FIFO (called *pfifo-fast* in Linux terminology), *Token Bucket Filters* (TBF), *Stochastic Fair Queueing* (SFQ), and *Hierarchical Token Bucket* (HTB). FIFO and TBF are classless, while HTB is a classful qdisc. SFQ is also considered a classless qdisc [46] since its internal classification mechanism cannot be configured by the user. The TBF qdisc is a rate limiter that passes the packets at a rate that is smaller of the packet arrival rate or the administratively set rate for this qdisc. SFQ is a simple implementation of the fair queueing algorithms. It identifies a flow using source and destination IP addresses and ports. HTB is a classful TBF that uses a combination of filters for classification and TBF for rate enforcement.

Routing protocol We use the *olsr.org* [3] implementation of the popular Optimized Link State Routing (OLSR) [24] protocol. OLSR is a proactive link state routing protocol: each mesh node maintains a table of routes to all other nodes it has discovered via periodic exchange of control messages. OLSR uses two types of control messages: HELLO messages between one-hop neighbors are used for local discovery, while Topology Control (TC) messages are used to diffuse link-state information throughout the network. Optimizations introduced in OLSR use a controlled flooding mechanism in which only select nodes called *multipoint relays* (MPRs) broadcast this link-state information.

We use OLSR with Expected Transmission Count (ETX) [27] routing metric. ETX is an estimate of the number of transmissions required to send a unicast packet over a wireless link. It is calculated by broadcasting a predetermined number of short probe packets and counting the number of packets successfully received over a wireless link. This is used to determine forward and reverse packet delivery ratios (d_f and d_r, respectively) for the link. The ETX value for this link is then calculated as follows:

$$ETX = \frac{1}{d_f \times d_r}$$

The routing protocol then selects a path with the smallest sum of ETX values along the constituent links.

The routing protocol sets up our 9-node testbed in a multihop configuration shown in Figure 6.7b. The routing tree is rooted at the gateway node E which bridges traffic between the wired and the wireless networks through its 1 GigE interface.

Web100 We use the Web100 suite of software [4] to access the TCP statistics on a mesh node. Web100 consists of a kernel patch that collects and exposes these statistics through a set of instruments known as Kernel Instrument Set (KIS)[85], as well as a library that defines an API for reading these statistics. Under Linux, these statistics are accessible through the `/proc` file system.

iperf We use `iperf` [1] to perform network traffic measurements in our testbed. `iperf` operates in a client/server mode where a client transmits a test stream to a server. We typically run each experiment for a duration of 100 s. to capture the stable, long-term behavior of a TCP stream.

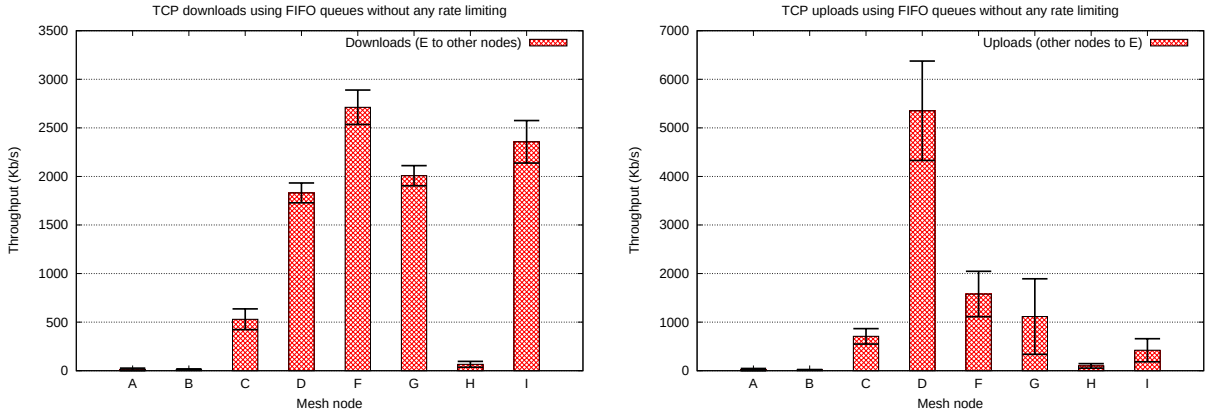

(a) Download flows

(b) Upload flows

Figure 6.8: Flow rates distribution with FIFO queues for downstream and upstream flows in our WMN testbed. Error bars are the 95% confidence intervals.

6.4.2 Evaluation

We evaluate the performance of both upstream and downstream TCP flows between the mesh routers and the wired server. The gateway node E bridges traffic between the wireless and the wired networks through its 1 GigE interface. Thus the traffic flows in our testbed are bottlenecked by the shared wireless spectrum.

FIFO Queues with no Rate Limiting

We first present our results using a shared FIFO queue at the gateway. These results are summarized for both download and upload flows in Figure 6.8. Error bars are the 95% confidence intervals.

Generally, one-hop flows have a higher throughput compared to flows traversing two or more hops which exhibit unfairness, including starvation. For gateway-in-the-middle chain, we find that the available capacity is unfairly shared between the two one-hop nodes, B and D. This is partly due to the fact that node D relays traffic for twice as many nodes compared to node B (Nodes B and D obtain equal throughput for both upstream and downstream flows if they are the only flows transmitting to the gateway C). JFI is better for gateway-in-the-middle chain compared with gateway-in-the corner: 0.46 vs. 0.27 for download flows, and 0.61 vs. 0.28 for upload flows, respectively. We note that a distribution in which the network capacity is assigned to a single flow with all others starving yields a JFI of 0.2 in a network with 5 flows (see Section 2.1.5).

Efficacy of Gateway-enforced Control

We characterize the efficacy of gateway-enforced rate control through a series of experiments similar to those used in Section 4.1.4, albeit this time using TCP with gateway rate control. We gradually increase the rate allocated at the gateway using one of the enforcement mechanisms in Figures 6.1b and 6.1c, and measure the corresponding throughput of the TCP streams. We characterize the resulting network response by plotting the allocated rate vs. the measured flow rate. Our results are discussed below.

Figure 6.9 shows our results for both download and upload flows. The vertical axis is the measured per-flow rate, while the horizontal axis is the rate allocation at the gateway (per-flow or aggregate).

Our main observation is that initially all flow rates (both uploads and downloads) increase in parallel with increasing rate allocation at the gateway. Increasing this allocation beyond the fair share point, however, produces increasing throughput for smaller-hop flows at the expense of flows traversing a larger number of hops. Thus, the gateway control mechanism can effectively enforce fairness in rate allocation as long as the allocated rate at the gateway does not exceed the fair rate for the network. This observation is consistent with the simulation results described earlier in this chapter in which we used a computational model to determine the fair share point for a given network topology.

We further note that the fair share point for download flows is approximately twice that of upload flows for the same topology. We suspect that this is due to asymmetric wireless links in our network. We characterized this asymmetry by performing bulk TCP transfers between the gateway and individual mesh nodes in isolation with other flows turned off. Our results are show in Figure 6.10. We observe that a download flow from the gateway E to node C gets approximately 65% more throughput than an upload flow from C to the gateway E. Similarly, the download flow from E to D gets about 18% more throughput that the upload from D to E. We note that since the wireless links exhibiting this asymmetry are also the transit link for traffic between nodes A and B and the gateway., it considerably improves the total network capacity with download flows.

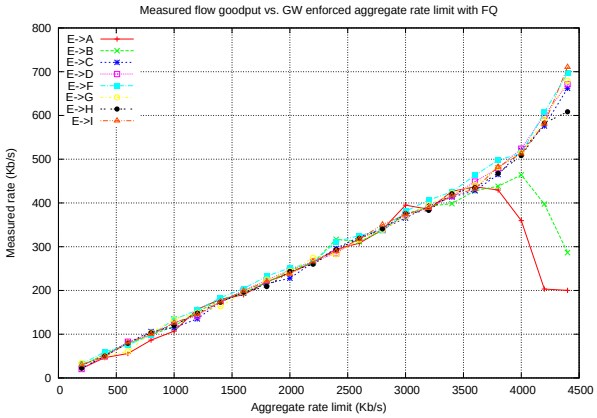

(a) Downloads. Gateway aggregate rate limit

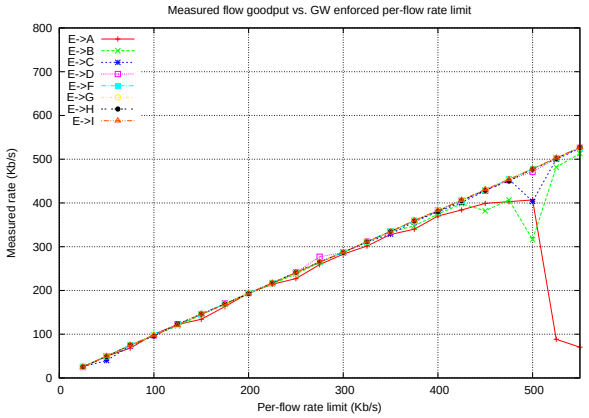

(b) Downloads. Gateway per-flow rate limit

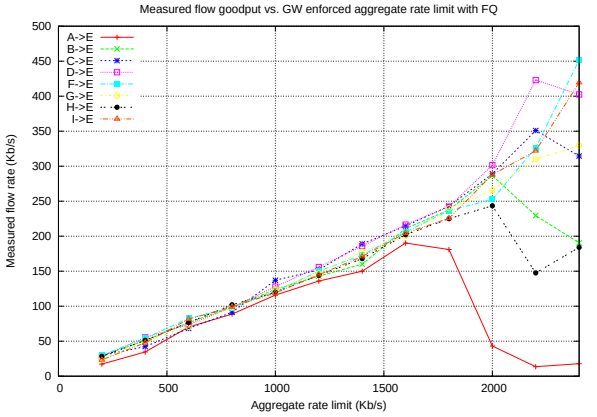

(c) Uploads. Gateway aggregate rate limit

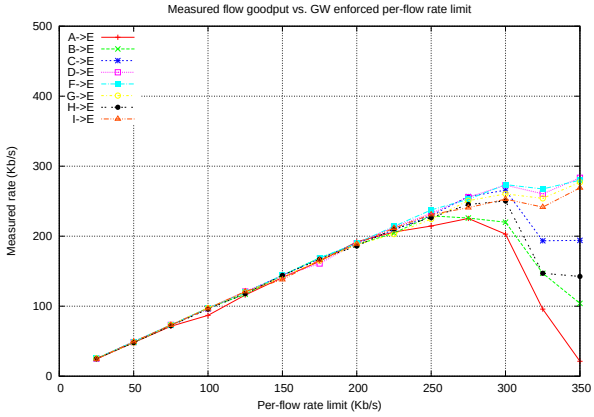

(d) Uploads. Gateway per-flow rate limit

Figure 6.9: Measured flow goodput as a function of the gateway rate limit for the testbed nodes

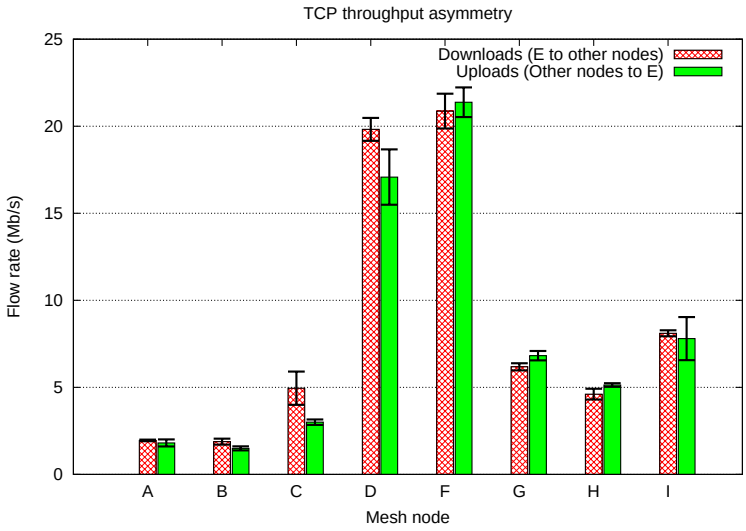

Figure 6.10: Asymmetric wireless links in our testbed. We show the average download and upload throughput between the mesh node and the gateway. Nodes C and D shows maximum asymmetry between download and upload flows.

6.5 Summary

In this chapter we explored the feasibility of using centralized rate control that can be enforced at traffic aggregation points such as gateway routers. We show that router-assisted techniques in wired networks, including work-conserving packet scheduling (such as FQ and its variants) and probabilistic packet-drop techniques (such as AQM and its variants) are inadequate as centralized rate control techniques in WMNs. This is because of fundamental differences in the abstraction of wired and wireless networks: (1) transmissions on wired links can be scheduled independently, and (2) packet losses in wired networks occur only as queue drops at bottleneck routers. Our experiments indicate that non-work-conserving rate-based centralized scheduling can be used effectively in WMNs. Even rate-limiting the aggregate traffic passing through the gateway router improves the fairness index by a factor of 2 over the base case with a shared FIFO queue. Further granularity in rate allocation control can be obtained by isolating flows using per-flow queueing and by exercising per-flow rate limiting. The fairness indices achieved with these modifications are comparable to source rate limiting techniques that require modifying the MAC or the transport-layer on the end-hosts.

Having established the feasibility of gateway-assisted rate control in WMNs, our next goal is to move away from the computational model used in this chap-

ter for determining rate information. We are interested in developing heuristics and mechanisms to estimate flow rates based strictly on the information available locally at the gateway. The remaining chapters in this dissertation describe our measurement-based approach in which the rate controller adapts its behavior in response to changing network and flow conditions.

Chapter 7

Aggregate Rate Controller

Having established the efficacy of gateway nodes in enforcing rate control for adaptive traffic flows, we now turn our attention towards designing *practical* centralized rate controllers, *i.e.*, we wish to move away from the computational model based approaches, and instead develop a framework of heuristics that are practically feasible for deployment by an ISP operating a WMN. In this chapter we propose Aggregate Rate Controller (ARC), that can enforce approximate max-min rate allocation using only the information locally available at the gateway. ARC manages the net amount of traffic allowed through the network, relying on the underlying max-min fairness characteristics of DCF to apportion this capacity fairly amongst all contending flows. This chapter discusses the implications of max-min fairness in WMNs, the design considerations governing our proposed controller, as well as its performance evaluation using simulations and testbed analysis.

7.1 Introduction

In Chapter 6, we proposed and verified the efficacy of using traffic-aggregation points like gateway nodes in enforcing rate control for adaptive traffic flows. The computational model that we used required both the network topology and link interference information to compute the fair rate vector. In general, gathering this information requires distributed coordination amongst the nodes. In this chapter we remove these requirements and propose a framework of gateway-enforced heuristics that can enforce approximate max-min rate allocation only using the local information available at the gateway.

Our proposed controller exploits the underlying max-min fairness characteristics

of 802.11 MAC. Using simulations, we establish that the rate allocation vector in a WMN is a function of the aggregate capacity of that network. We define this *aggregate capacity* as the sum of end-to-end rate of all active flows. Similarly, the *fair-aggregate capacity* is the sum of end-to-end max-min rates of all active flows. We show that when the aggregate capacity of a network is limited to its fair-aggregate capacity, the 802.11 MAC apportions this allocated capacity in an approximate max-min manner across all flows. This aggregate capacity does not need to be managed by a large set of distributed source rate limiters; instead, it can simply be managed by a single rate limiter at the gateway node.

This forms the basis of our Aggregate Rate Controller (ARC), named because it allocates rate to data traffic as an aggregate bulk, relying on the underlying MAC to distribute it fairly across contending flows. We propose heuristics that allow ARC to search for fair-aggregate capacity of the network amongst the set of feasible allocations. Our measurement-based, closed-loop feedback-driven heuristic uses existing data traffic as capacity probes, thus minimizing control overhead. While ARC singularly improves fairness indices, we show that combining it with FQ provides isolation between different flows, further improving fairness.

Our contributions in this chapter are as follows: First, we show that distributed bottlenecks can exist even in a WMN where traffic patterns are skewed towards the gateway. Max-min rate allocation allows us to saturate these bottlenecks and efficiently utilize the available capacity. Second, we characterize the response of TCP flows in a 802.11 multihop network as a function of the aggregate capacity allowed through its traffic aggregation points. We show that it is possible to achieve approximate max-min flow rates simply by regulating the *net* amount of data traffic allowed through the gateway to its fair-aggregate capacity. Third, based on this behavior, we propose ARC, an aggregate rate-based scheduler that uses a measurement-based approach to determine this fair-aggregate capacity of a network, leading to approximate max-min allocation across contending flows.

This remainder of this chapter is organized as follows. In Section 7.2, we illustrate the differences between the bottlenecks in a wired and a wireless network and describe the conditions necessary for generating max-min rate allocation vectors with lexicographically different components. In Section 7.3, we describe the network response as a function of the aggregate network capacity and the circumstances under which it leads to approximate max-min fairness. We then propose a framework of heuristics for determining this fair-aggregate capacity. We evaluate these heuristics using simulations in Section 7.6 and using our WMN testbed in Section 7.7, respectively.

7.2 Understanding Max-Min Fairness

The classical max-min rate allocation described in Section 2.1.2 is a commonly used fairness criterion in wired networks. Its implications, however, are not well understood in the context of multihop networks with a shared wireless spectrum. In particular, it is deemed unsuitable for multi-rate wireless networks [45, 96, 118]. 802.11 MAC provides max-min throughput fairness to all single-hop flows that are within carrier sense range. It has been shown that this behavior degenerates to equal rate allocation determined by the flow getting the least rate. We contend that this is simply the well-known efficiency versus fairness trade-off that is also seen, albeit with less severity, in wired networks. Further, in multihop networks, these slower links constrain only the set of flows in their neighborhood; in networks where there is another set of flows that do not share this neighborhood, max-min fairness with its Pareto optimality allows us to make efficient use of the available capacity. In this section we show how such distributed bottlenecks can exist even in a WMN where the dominant traffic pattern is directed either towards or away from the gateway, *i.e.*, unlike the common perception that gateway is the common bottleneck, flows may actually be bounds by distributed bottlenecks in different parts of the network [56].

7.2.1 Max-min Fairness in Wired Networks

We characterize max-min fairness using the notion of bottleneck links as described in [11]. Interconnected links in a network may have heterogeneous capacities. The *utilization* of a link is defined as the sum total of rates for all flows traversing it. A link is *saturated* when its utilization equals its capacity. A saturated link becomes a *bottleneck* for a flow if that flow has a maximal rate amongst all other flows using this link. When all flows experience such a bottleneck, the resulting rate allocation is max-min fair [11]. This forms the basis of the water-filling algorithm used for determining max-min rates. It works as follows: starting from zero, all flow rates are increased in unison till one or more links gets saturated. This link then becomes a shared bottleneck for all flows traversing it. Each of these flows have the same rate as all other flows sharing this link. These set of flows are all capped at this rate; flow rates for remaining uncapped flows are then increased in parallel till some other link gets saturated. The procedure is repeated until rates are assigned to all flows.

Figure 7.1 shows four nodes connected via wired tandem links. Link capacities

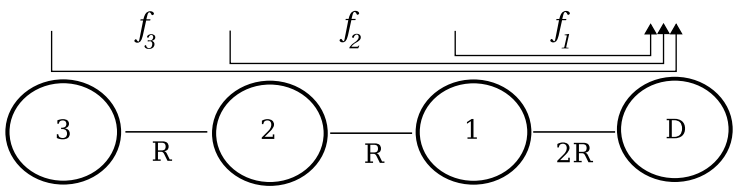

Figure 7.1: With wired, tandem links (capacities as shown), the max-min rates are $(f_1, f_2, f_3) = (R, \frac{R}{2}, \frac{R}{2})$.

are R and $2R$, as shown. Each node sources a flow terminating at destination D. Using the water-filling algorithm, link $2 \leftrightarrow 1$ saturates when a rate of $\frac{R}{2}$ is allocated to all three flows. At this point, link $2 \leftrightarrow 1$ becomes the shared bottleneck for flows f_2 and f_3. However, the rate of flow f_1 can be further raised to R before it saturates the link $1 \leftrightarrow D$. Thus the max-min rate vector is $(f_1, f_2, f_3) = (R, \frac{R}{2}, \frac{R}{2})$.

7.2.2 Max-min Fairness in Wireless Networks

Directly extending this notion of max-min fairness to wireless networks is a challenge because resource allocation constraints are fundamentally different in a shared wireless environment. A wired link has fixed, known capacity and can be scheduled independently of other links. A wireless link, on the other hand, is an abstraction for a shared spectrum between communicating entities and their neighbors, only one of which can successfully transmit at a time. The capacity of a wireless link is thus determined by the channel contention in this neighborhood, which in turn, is spatially dependent on the node distribution around the sender or receiver. We use the collision-domain model (Section 4.1.2) to capture this contention.

The *utilization* of a collision domain is the sum total of transmission times for all links in a collision domain. The feasibility constraints on scheduling require that this utilization cannot exceed 1. Mathematically, we represent it as follows: Let $R_{(m,n)}$ be the link rate between neighboring nodes (m, n) in the network and let $r_{(m,n)}$ be the traffic carried by this link. Let r_i be the end-to-end rate for flow f_i. Then $r_{(m,n)} = \sum_{i:f_i \text{ traverses } (m,n)} r_i$. Let $\mathbf{C} = \{C_1, C_2, ..., C_j\}$ be the set of j collision domains in this network. Ignoring physical and MAC layer headers, the feasibility constraints require

$$\sum_{\forall\,(m,n)\,\text{in}\,C_p} \frac{r_{(m,n)}}{R_{(m,n)}} \leq 1,\ \forall p \in \{1, 2, ..., j\}$$

A *saturated* collision domain is defined as a collision domain which is fully utilized. A saturated collision domain becomes a *bottleneck* for a flow if that flow has a maximal rate amongst all other flows using this collision domain. A multihop flow may be part of one or more collision domains; its end-to-end rate is then bound by the collision domain that assigns it the lowest rate.

Using these definitions we adapt the iterative water-filling algorithm as for wireless environments as follows: starting from zero, we increase the rate of all flows in parallel till a collision domain gets saturated. We then cap the rates for all flows that traverse this collision domain. We update the residual capacity of remaining collision domains based on rates already assigned to these saturated flows, and then continue increasing the rates of remaining uncapped flows till another collision domain gets saturated. The process is repeated until a rate has been assigned to all flows.

7.2.3 Max-min Fairness in WMNs

WMNs used for Internet backhauls have a dominant traffic pattern in which flows are directed either towards or away from the gateway. This increases the spectrum utilization around the gateway, eventually becoming a bottleneck for flows that are not already bottlenecked elsewhere in the network. We know that the max-min algorithm described above assigns equal rate to all flows sharing a common bottleneck. Thus when the spectrum around the gateway constitutes the single bottleneck shared between all flows, max-min fairness results in equal rate allocations.

Despite this skewed traffic pattern in a WMN, topological dependencies can create bottleneck collision domains other than those including the links around the gateway. We show how multi-rate links and node distributions create such distributed bottlenecks.

Multi-rate Links Figure 7.2 shows two variations of a simple chain topology with two backlogged flows f_1 and f_2 transmitting through a common gateway GW. The link rates are a mix of R and $2R$, as shown. An equivalent wired network would yield a rate vector of $(f_1, f_2) = (2R, R)$ in both of these topologies. With wireless links, however, the rate vector depends on the position of the slower link.

- Link f is the slower link in Figure 7.2a. Here f_1 and f_2 are bottlenecked by the collision domain of links c and d, respectively. The slower link is a part of

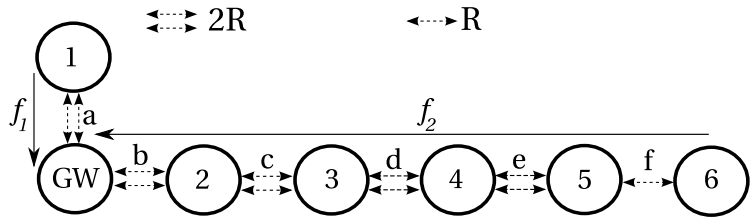

(a) $(f_1, f_2) = (\frac{2R}{3}, \frac{R}{3})$

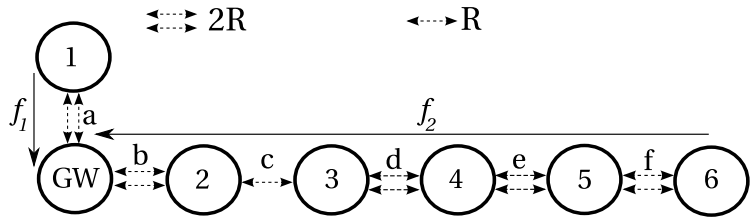

(b) $(f_1, f_2) = (\frac{R}{3}, \frac{R}{3})$

Figure 7.2: Max-min rate depends on the location of the slower link with capacity R. If this slower link is one of links a, b, c, d, or e, the max-min fair rate vector is $(\frac{R}{3}, \frac{R}{3})$. If the slower link is at position f, the max-min rate vector is (f_1, f_2) = $(\frac{2R}{3}, \frac{R}{3})$. An equivalent wired network would always produce an allocation of $(R, 2R)$, with the lower rate for the flow traversing the slower link.

d's collision domain. The max-min rate allocation for this scenario is $(f_1, f_2) = (\frac{2R}{3}, \frac{R}{3})$.

- If the slower link is one of the links b, c, d, or e, the max-min rate allocation is $(f_1, f_2) = (\frac{R}{3}, \frac{R}{3})$. The collision domains of links c and d are fully saturated at this rate and form the bottleneck for flows f_1 and f_2 respectively.

- If the slower link is a, the max-min allocation is still $(f_1, f_2) = (\frac{R}{3}, \frac{R}{3})$. However, in this case the two flows are both bottlenecked by a common collision domain of link c.

Node Distribution Multi-rate links are not necessary to create distributed bottlenecks; these may even exist in a network with uniform rate wireless links. Figure 7.3 shows three flows f_1, f_2, and f_3 transmitting to a common gateway node over wireless links with uniform capacity R. f_2 and f_3 are bottlenecked by the collision domain for link d, and hence share equal rates. f_1 is bottlenecked by collision domain of link c. The max-min fair share in this topology is $(f_1, f_2, f_3) = (\frac{R}{5}, \frac{R}{10}, \frac{R}{10})$.

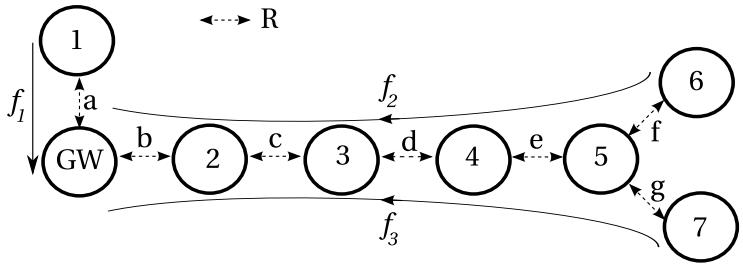

Figure 7.3: Max-min fair rates because of bottlenecks associated with node density $(f_1, f_2, f_3) = (\frac{R}{5}, \frac{R}{10}, \frac{R}{10})$

7.3 Network Response to Aggregate Rate Control

In this section, we analyze the flow goodput response as a function of the aggregate network capacity, *i.e.*, if the network is allowed to transport an aggregate of x units of traffic, how does the 802.11 MAC distribute these x units of capacity between multihop TCP flows all contending for channel access? In this work we experiment with managing this aggregate capacity via a single token bucket at the gateway router.

We experiment with the two rate limiting mechanisms in Figure 7.4. The differences between the two architectures were described in Section 6.2.3. To recap, in Figure 7.4a, all received data is stored in a shared buffer till there are enough tokens to send it out. This simple architecture has known performance problems: it does not provide any isolation between flows and a shared FIFO queue can cause synchronization between TCP connections carrying bursty traffic. We address these issues by using per-node queueing at the gateway as shown in Figure 7.4b. This allows us to separate data from different subscribers irrespective of the number of TCP micro-flows a subscriber generates.

Using ns-2 [2], we simulate a number of network topologies with gateway rate limiting the aggregate TCP traffic it bridges between the wired and the wireless network. Figure 7.5 shows the measured flow goodput as a function of the aggregate capacity for the network in Figure 7.3 with 1 Mb/s 802.11 links. Each data point for a given rate limit represents the average of 5 experimental runs. Recall that the optimal max-min fair rate computed for this topology is $(f_1, f_2, f_3) = (\frac{R}{5}, \frac{R}{10}, \frac{R}{10})$. The nominal capacity of a 1 Mb/s 802.11 link is approximately 800 Kb/s, assuming a perfect channel and no collisions. This translates to (f_1, f_2, f_3) = (160 Kb/s, 80 Kb/s, 80 Kb/s) and a fair-aggregate capacity of 320 Kb/s.

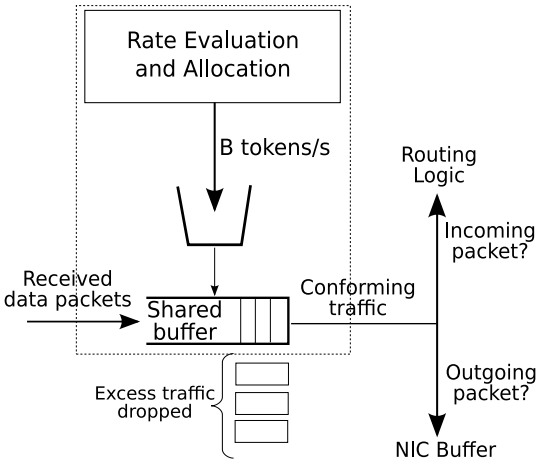

(a) Aggregate rate limit with a shared queue

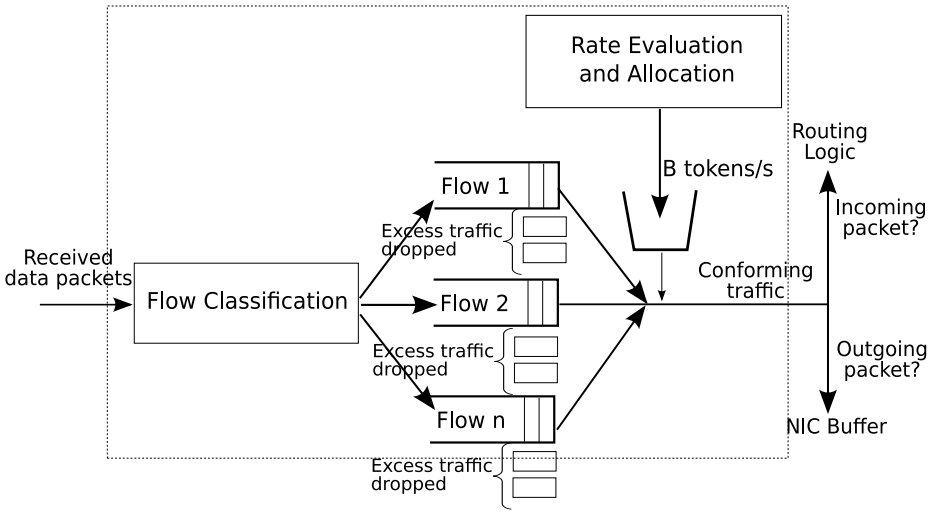

(b) Aggregate rate limit with a per-node queue

Figure 7.4: The main architectural components of ARC

We make the following observations from Figure 7.5. First, both plots show an initial increase in rate of *all* flows with increasing rate limit. These rate increases are prolonged (up to an aggregate rate limit of 225 Kb/s) and more uniform (all rates within 2% of each other up to this rate limit) in Figure 7.5b where we use a per-destination node queue at the gateway. In contrast, Figure 7.5a shows a deviation of up to about 50% between the maximum and the minimum rate flows between $0-150$ Kb/s rate limit. This deviation increases with increasing aggregate rate limit. Thus separating flows while rate limiting at the gateway shows improved fairness characteristics. Second, increasing the rate limit beyond 225 Kb/s in Figure 7.5b only increases the rate of flow f_1 while the rate of flows f_2 and f_3 taper off. Between

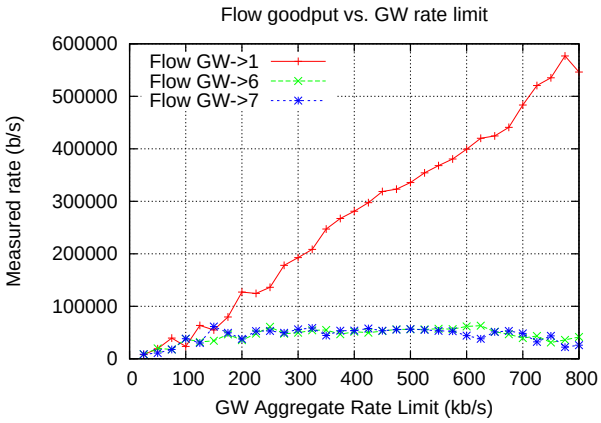

(a) Shared queue with GW rate limiting

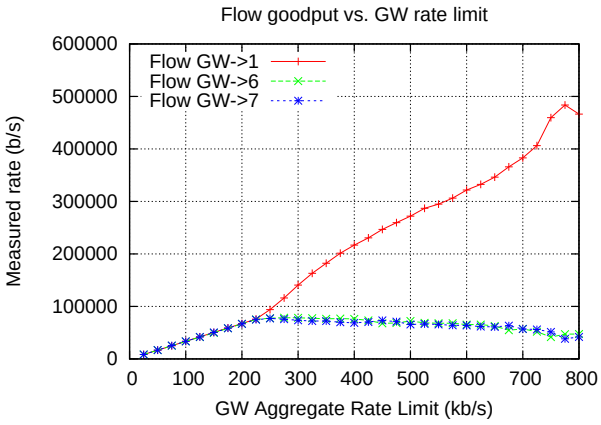

(b) Per-destination queue with GW rate limiting

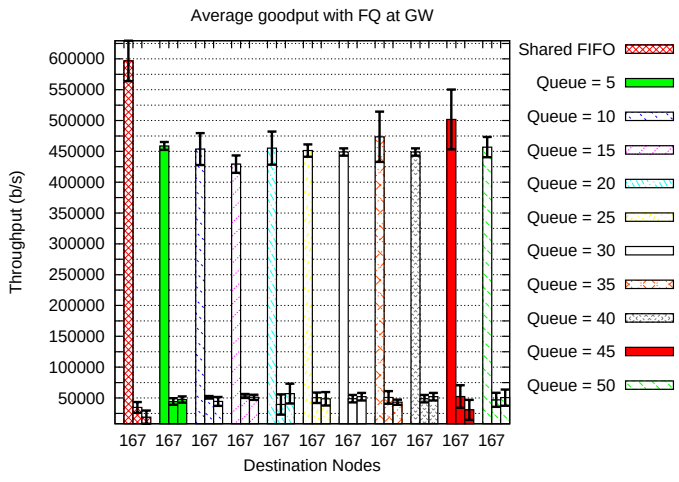

(c) FIFO vs. FQ at the GW

Figure 7.5: Flow goodput vs. gateway aggregate rate limit for the network topology in Figure 7.3 with 1 Mb/s 802.11 links. Figs. 7.5a and 7.5b use the enforcement mechanism in Figs. 7.4a and 7.4b respectively at the gateway router. Figure 7.5c shows average goodput for the same network with FQ at the gateway without any rate limiting.

a rate limit of $250-350$ Kb/s, for example, f_1 approximately doubles its rate while registering a drop of only 4% in the average rate of f_2 and f_3. This drop in rate increases with increasing aggregate capacity, *e.g.*, at 400 Kb/s, the drop in average goodput of f_2 and f_3 is approximately 7% compared to the highs seen at a rate limit of 250 Kb/s. Third, at the computed fair-aggregate capacity of 320 Kb/s, the measured rates of flows f_1, f_2, and f_3 are all within 10% of their optimal max-min rates computed assuming no collisions.

Similar to fair-aggregate capacity which is the sum of optimal max-min rates, we define *measured* fair-aggregate capacity as the sum of measured individual flow rates where the lexicographically lowest rate in the rate vector is no less than θ times the maximum rate previously recorded for that flow. The intuition behind the θ cutoff benchmark is that we are willing to tolerate a marginal decrease of $1-\theta\%$ times the maximum possible rate of the slowest flow as long as it results in an increase in total network capacity. In this experiment, setting θ to 95% sets our measured fair-aggregate capacity to 350 Kb/s. This is within 8% of the optimal fair-aggregate capacity computed using the iterative max-min fair rate algorithm.

The role of per-node queueing at the gateway is important, though it alone is insufficient to enforce flow rate fairness. In Figure 7.5c, we show rate allocations achieved by varying the size of this per-node buffer. For comparison, we also show our results with a shared FIFO queue of 50 packets. The error bars are the 95% confidence intervals. In all cases f_1 achieves a goodput in excess of 425 Kb/s, at the cost of reduced goodput for distant flows.

We have validated this behavior for both upstream and downstream flows on a number of topologies. The network in Figure 7.6a yields an optimal max-min rate vector with three lexicographically different components. Its response characteristics with upstream flows in Figure 7.6c are consistent with those seen in Figure 7.5b with downstream flows. Between a rate limit of $0-400$ Kb/s, all flow rates increase *equally* in parallel (within 10% of each other), irrespective of the hop count or the degree of contention. With the rate limit between $400-600$ Kb/s, only the rate of flows f_1, f_2, and f_3 increase while f_4, f_5, f_6, and f_7 taper off; f_1 registers an approximate increase of 200%, f_2 and f_3 about 80%, while there is a decrease of less than 5% in average rate of flows f_4, f_5, f_6, and f_7. Increasing the aggregate capacity beyond 600 Kb/s increases the rate of flow f_1 only with all other flows tapering off initially and later registering a decrease in goodput as rate limits are increased beyond 700 Kb/s. Using our $\theta = 95\%$ cutoff benchmark, we find the measured fair-aggregate capacity of 625 Kb/s. This is approximately within 20% of the fair-aggregate capacity computed considering optimal scheduling across a 802.11 link.

Apart from the increased collisions due to a larger network, this reduced efficiency is partly also due to the fact that measured TCP goodput across a 2 Mb/s 802.11 link is less than two-times the corresponding goodput across a 1 Mb/s link.

We conclude from these experiments that the network response is a function of the aggregate traffic transported by the network. In earlier chapters we have shown that flow rate fairness characteristics are maximized when individual flows are rate limited to their fair share of the network capacity. We show, that by extension, these fairness characteristics similarly improve when the aggregate traffic transported by the network is limited to its measured fair-aggregate capacity. Up to this traffic load, the underlying 802.11 MAC can provide max-min rate allocation amongst the contending nodes. Unlike prior work that requires a distributed set of source rate limiters, the aggregate capacity of a network can be managed simply by a single, centralized rate-based scheduler for both upstream and downstream flows in a WMN.

7.4 Aggregate Rate Controller

Our results from the previous section show that if we limit the aggregate capacity of a WMN to its measured fair-aggregate capacity, the resulting rate allocation with TCP flows is approximately max-min fair. We now propose heuristics that allow the gateway node to determine this fair-aggregate capacity.

We imposed the following set of practical constraints on a feasible solution:

- The mechanisms are limited to using information available locally at the gateway. This includes information available at the driver level, *e.g.*, which mesh nodes are directly associated with the gateway as well as the data rate used for communication with each of those nodes.
- Mesh nodes use the standard 802.11 radios for the multihop backhaul. Control messages beyond those required by the standard may not be correctly interpreted by a node.
- Client devices use the standard TCP network stack.

Our proposed heuristic ARC uses a simple measurement-based adaptive rate allocation approach. It measures the rate obtained by all flows over a fixed interval called *epoch*. If all flow rates are equal, it assumes the network is underutilized and

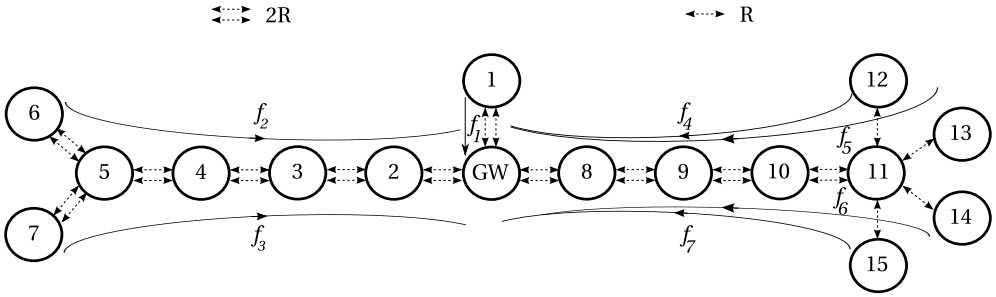

(a) $(f_1, f_2, f_3, f_4, f_5, f_6, f_7) = (\frac{R}{3}, \frac{R}{6}, \frac{R}{6}, \frac{R}{12}, \frac{R}{12}, \frac{R}{12}, \frac{R}{12})$

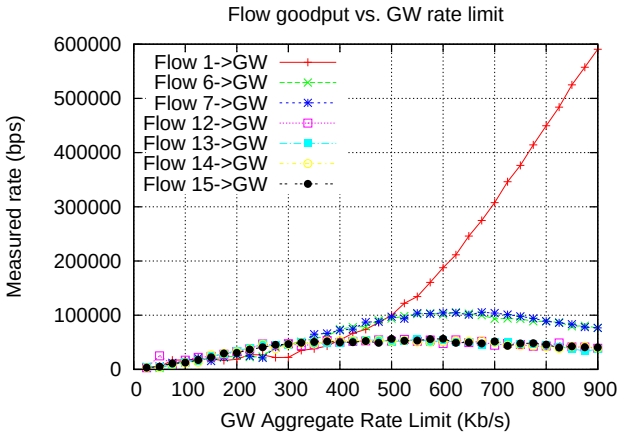

(b) Shared queue with GW rate limiting

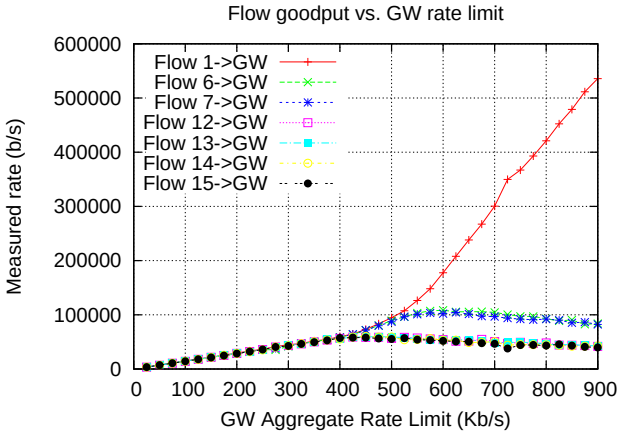

(c) Per-source queue with GW rate limiting

Figure 7.6: A topology with 7 flows that yield 3 lexicographically different components in the optimal max-min rate vector.

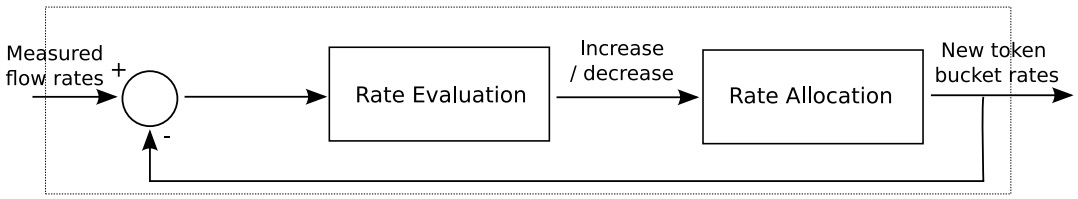

Figure 7.7: Rate evaluation and allocation work in a closed-loop feedback control.

increases the aggregate capacity allocated at the gateway. If the rates are unequal, then the flows with lower rate are either bottlenecked locally or are experiencing unfairness. We differentiate between the two by maintaining state on historic flow rates. The aggregate capacity allocated at the gateway is decreased only when we suspect unfairness. Our heuristic thus mimics the behavior of adaptive protocols like TCP by probing the network for capacity information and adjusting its behavior in response. This closed-loop feedback system allows ARC to adapt to changing network and traffic conditions.

We now describe the ARC heuristic in detail. ARC is a system module on the gateway mesh router. It sits between the MAC layer and the network layer, operating transparently between them. Its three main components perform the following functions:

1. Flow classification
2. Rate evaluation and allocation
3. Flow rate enforcement

7.4.1 Flow Classification

In this first step, ARC performs flow classification for all data traffic (ingress and egress) through the gateway. Here flow refers to any suitable classification of traffic and its precise definition is left as a policy decision for the network operator. In this dissertation we have classified flows based on the source or destination mesh router. Thus a flow f_i represents the aggregate of all micro-flows originating from, or destined to, node n_i in the network. In this context, we use nodes and flows interchangeably in our discussion. Our classification methodology requires a simple lookup of the packet header given a known offset, and can be performed efficiently. We note that such a classification is consistent with the common practices employed

by ISPs on wired access networks, where capacity is managed on a per-subscriber basis.

7.4.2 Rate Evaluation and Allocation

Rate evaluation This component measures the flow rate of all flows in a given epoch τ_t. These measured rates determine the aggregate capacity allocated at the gateway for the next epoch τ_{t+1}. Let the duration of the epoch be δ. This value is configurable, though for stability it should operate at different timescales than the control action of TCP senders. For instance, δ can be set to multiples of round-trip time so that TCP sources can react to changes in rate allocation and stabilize around their new values.

After every epoch, the mechanism compares the measured rate r_i for flow f_i with the rate r_j obtained by some other active flow f_j. Two possibilities exist:

1. If $r_i \approx r_j$ for $\forall i, j \in N$, the mechanism assumes the network capacity is underutilized, *i.e.*, the current estimate of aggregate network capacity ($C_{meas} = \sum_{i=1}^{N} r_i$) is low. It signals the rate allocation component to increase the aggregate rate allocated to the network.
2. If $r_i < r_j$ for any $i, j \in N$, the flow f_i may be limited by its saturated local bottleneck or it may be experiencing unfairness. We differentiate between these cases by comparing r_i to its previously recorded maximum value r_{imax}. If $r_i < r_{imax}$, then the flow is experiencing unfairness and we reduce the aggregate rate limit at the gateway. On the other hand, if $r_i \approx r_{imax}$, then f_i is bound by some local bottleneck. We increase the aggregate rate limit since it may be usable by other flows that have not yet saturated their respective bottlenecks.

The pseudo-code for this rate evaluation component is shown in Algorithm 1.

Rate Allocation The rate allocation component adjusts the token generation rate B (see Figure 7.4) based on its estimate of the current network capacity., C_{est}. It adjusts this capacity estimate based on feedback from the rate evaluation component. After every epoch, it adjusts C_{est} such that the new estimate $C_{est} > C_{meas}$ when signaled to increase rates, or $C_{est} < C_{meas}$ otherwise. As described earlier, $C_{meas} = \sum_{i=1}^{N} r_i$. B is then set to C_{est}. This allocation is derived from the

Input: Epoch duration δ, inter-flow unfairness threshold γ, intra-flow rate cutoff threshold θ, measured rate r_i and historical r_{imax}, $\forall i \in N$

Output: Rate increase or decrease decision

```
1 while once every δ time units do
2 |   if r_i/r_j < γ and r_i/r_imax < θ  for ∀i,j ∈ N then
3 |   |   decAggRate;
4 |   else
5 |   |   r_imax = r_i ;
6 |   |   incAggRate;
7 |   end
8 end
```

Algorithm 1: Rate evaluation algorithm

network response in epoch τ_t and is enforced for the epoch τ_{t+1} with the help of the enforcement mechanism described in Section 7.4.3.

The rate allocation component may use any number of heuristics to determine the new C_{est}. It has to search through the space of feasible allocations for the new capacity estimates. A simple algorithm using exponential increase/decrease in aggregate capacity is shown in Algorithm 2. In Section 7.5 we propose a heuristic that uses binary search within upper and lower aggregate network capacity bounds to allow for faster convergence to the fair rate values.

Input: $C_{meas} = \sum_{i=1}^{N} r_i$

Output: New aggregate rate limit C_{est}.

```
1 incAggRate begin
2 |   C_est = α × C_meas;                    /* α > 1 */
3 end
4 decAggRate begin
5 |   C_est = β × C_meas;                    /* β < 1 */
6 end
```

Algorithm 2: Estimating network capacity using a simple exponential increase/decrease algorithm

7.4.3 Flow Rate Enforcement

ARC uses a single token bucket at the gateway to control the aggregate network capacity. The token generation rate B is controlled by the rate allocation mechanism above. Note that ARC can be used with either of the two enforcement mechanisms in Figure 7.4. Our evaluation in this chapter uses ARC with FQ since it provides better isolation between flows leading to improved fairness characteristics.

7.5 Design Considerations

7.5.1 Dynamic Flows

Our flow bundles are aggregates of micro-flows, and we expect them to be long-lived for durations lasting tens of seconds. However, when they do terminate, any unused capacity needs to be fairly allocated. Similarly, when a new flow emerges, the rate allocation of existing flows will be adjusted. In particular, this impacts r_{imax}, the maximum achievable fair rate that we have observed for a flow. We therefore modified Algorithm 1 to reset the r_{imax} value on detecting a change in the status of a stream.

We had described two flow activation/termination mechanisms in Section 6.3.3. In our case where a flow bundle may contain multiple TCP streams, we simply use the presence or absence of packets to determine the current state of stream activity. In contrast to prior approaches [33], this reduces the complexity as well as the state information maintained by the centralized controller. We evaluate ARC with dynamic flows in Section 7.6.

7.5.2 Rate Increase/Decrease Heuristics

These heuristics help the rate allocation component explore the space of feasible allocations in search of the fair-aggregate network capacity. We prefer heuristics with quick convergence characteristics. Algorithm 2 outlined a simple heuristic with exponential increase/decrease in capacity estimates. We now propose a binary search heuristic within pre-computed aggregate capacity bounds to provide faster convergence. Binary search can converge C_{est} to approximate fair-aggregate capacity in logarithmic time (approximately $log_2 K$ steps, where K is the set of feasible aggregate capacity values between the lower and the upper capacity bounds).

This heuristic works as follows: we first determine lower and upper bounds on feasible C_{est} (In Section 7.5.2 below, we provide an outline of how the initial upper and lower bounds on C_{est} can be determined for WMNs with many-to-one traffic patterns.) Then using binary search, we use the rate feedback in epoch τ_t to determine C_{est} for epoch τ_{t+1}. The pseudo-code for this modified rate allocation component is shown in Algorithm 3.

Input: $C_{meas} = \sum_{i=1}^{N} r_i$ and upper and lower aggregate capacity bounds C_{up} and C_{low} respectively.

Output: New aggregate rate limit C_{est}.

```
incAggRate begin
    C_low = C_meas;
    C_est = (C_meas + C_up)/2;
end
decAggRate begin
    C_up = C_meas;
    C_est = (C_low + C_meas)/2;
end
```

Algorithm 3: Estimating network capacity using binary search within feasible aggregate capacity bounds

Efficient and Fair Transport Capacity Bounds

The binary search heuristics described above search through the space of feasible values for network capacity to determine the capacity for a given topology. In this section we show how to determine the initial upper and lower capacity bounds to jump-start the binary search heuristic. Note that the gateway is only aware of the number of active flows at a given time and does not know the network topology. Further, by symmetry, the capacity bounds computed for upload traffic (many-to-one paradigm) also hold for download traffic (one-to-many).

Consider a network with N mesh routers exchanging data via the gateway. We assume that each router has a single wireless interface connected to an omni-directional antenna with unit gain. For simplicity, we assume that all nodes transmit with a uniform power, obtaining a transmission range of d units. Let the interference range associated with a receiver be m units, where $m \geq d$. Let k denote the distance that allows concurrent transmissions along a path. For CSMA/CA radios, $k \geq m$.

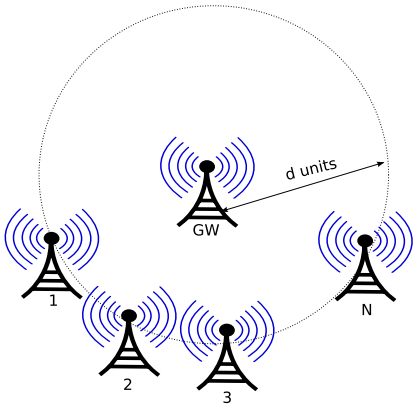

Figure 7.8: Aggregate capacity is maximized when *all* flows consume minimal spectral resource.

Optimal Upper Capacity Bound

With Perfect Scheduling The aggregate transport capacity is maximized when the gateway is either receiving or transmitting data all the time. This happens when all active nodes are one-hop away (*i.e.*, within d units) from the gateway. If the wireless links have a uniform capacity of W bits/s, the upper bound on the aggregate send/receive capacity at the gateway is also W bits/s.

For multi-rate links, suppose that mesh router $n_1, n_2, ..., n_N$ connect to the gateway with link-rate vector $\mathbf{W} = \{W_1, W_2, ..., W_N\}$. Let $T(i)$ be the fraction of time required for a node n_i to transmit or receive a packet of size s_i. If the underlying MAC provides all nodes with equal transmit opportunities, then

$$T(i) = \frac{\frac{s_i}{W_i}}{\sum_{j \in N} \frac{s_j}{W_j}}$$

When all nodes exchange equal-sized packets, then the rate $r(i)$ of node i is given by

$$r(i) = \frac{1}{\sum_{j \in N} \frac{1}{W_j}}$$

and the aggregate send/receive capacity at the gateway is

$$\sum_{i=1}^{N} r(i) = \frac{N}{\sum_{j \in N} \frac{1}{W_j}}$$

It is trivial to see that when $W_i = W_j = W$, $\forall\, i, j \in N$, this expression reduces to an aggregate capacity of W bits/s as described above.

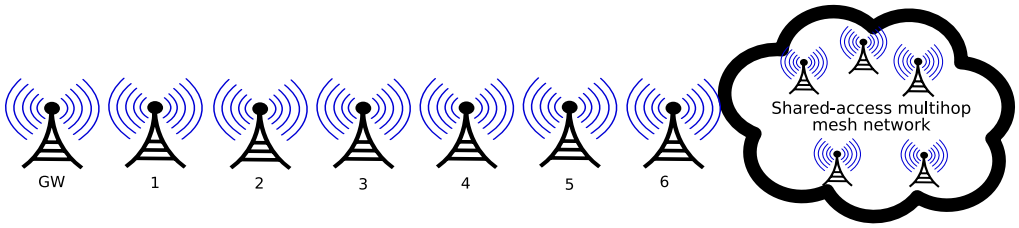

Figure 7.9: Aggregate capacity is minimized when *all* flows consume maximal spectral resource.

With 802.11 Scheduling: 802.11 lowers the capacity bound in two ways: MAC overhead and packet loss. First, 802.11 MAC reduces capacity well below link rates as it incurs a fixed overhead per packet due to backoff contention windows, link-level ACKs for every successful data transmission, optional RTS/CTS exchange, *etc.* Second, packets are susceptible to loss due to collisions from hidden terminals or when multiple transmitters simultaneously countdown their backoff window to zero.

The upper capacity bound we use in our simulations in Chapters 7 and 8 accounts for MAC overhead (we assume 1500-byte Ethernet-friendly MTU), while we ignore loss from collisions. This is a trade-off between accuracy and computational complexity. We accept reduced accuracy by using information that is readily available at the gateway. The number of active mesh nodes N can be determined through flow classification, while the link rate information used for each transmission is available at the radio interface driver.

Optimal Lower Capacity Bound

With Perfect Scheduling: The upper bound on aggregate capacity is obtained when all active nodes consume minimal resource (*e.g.*, spectrum) to communicate with the gateway. Conversely, an efficient lower bound on aggregate capacity is obtained when all active nodes consume *maximal* resource to reach the gateway.

A multihop flow consumes increasing spectral resource with each additional hop, till the number of hops reaches k and the resulting spatial reuse allows transmissions to be pipelined. At this point, the flow is consuming maximal spectral resource as any additional hop will still allow for concurrent, pipelined transmissions. Thus the lower bound of a network is a function of the spatial reuse allowed by the MAC.

A perfect scheduler allows for a fine-grained control of the spatial reuse. In

a chain of wireless nodes in Figure 7.9, transmissions from GW $\rightarrow$ 1 and 3 $\rightarrow$ 2 can occur in parallel while links 1 $\leftrightarrow$ 2 and 3 $\leftrightarrow$ 4 are kept idle. However, note that transmissions GW $\rightarrow$ 1 and 2 $\rightarrow$ 3 cannot occur concurrently, and neither can transmissions 3 $\rightarrow$ 2 and 1 $\rightarrow$ GW. Thus in a network with an equal mix of upstream and downstream traffic, the lower bound on aggregate send/receive capacity is $\frac{W}{2}$ bits/s; with all unidirectional flows (upstream or downstream), the aggregate send/receive capacity reduces to $\frac{W}{3}$ bits/s.

With multi-rate links, the aggregate capacity is lowest when *all* active flows traverse the slowest link. We assume that the link-rate vector $\mathbf{W}$ is lexicographically ordered, *i.e.*, $W_i \leq W_{i+1}$, $\forall i \in N$. Then the lower bound on the aggregate capacity is $\frac{W_1}{2}$ for bidirectional and $\frac{W_1}{3}$ for unidirectional traffic.

With 802.11 Scheduling: The spatial reuse possible with perfect scheduling and tight synchronization cannot be achieved with 802.11 scheduling. DCF's bidirectional handshake (DATA-ACK) requires the interfering nodes around *both* the transmitter and the receiver to be disabled for the duration of the message exchange. In Figure 7.9 when there is an ongoing transmission from 1 $\rightarrow$ 2, links GW $\leftrightarrow$ 1 and 2 $\leftrightarrow$ 3 need to stay idle. This spatial reuse sets the optimal lower capacity bound to $\frac{W}{3}$.

This spatial reuse can also be confirmed analytically. We use the physical model of radio interference to identify the interfering nodes. In this model the packet error rate (PER) at a receiver is a monotonically decreasing function of the Signal-to-Interference-plus-Noise Ratio (SINR). In practice, we can define thresholds such that probability of packet reception is approximately 1 when SINR exceeds a threshold ψ.

$$SINR = \frac{\frac{P_{TX}}{d^{\omega}}}{P_N + \sum_i \frac{P_i}{d_i^{\omega}}} \geq \psi$$

where P_N is the ambient noise, P_{TX} and P_i are the transmit power of the transmitter and interfering nodes respectively, d and d_i are the distance of the receiver from the transmitter and interfering nodes, and ω is the path-loss exponent ranging from 2 (free-space path loss) to 4 (two-ray ground reflection path loss). Measurements have indicated that the path loss exponent of 4 is more accurate [101] when $d \gg \sqrt{h_t h_r}$, where h_t and h_r are the antenna height of the transmitter and receiver respectively.

Ignoring ambient noise P_N and assuming all nodes transmit with equal power, the interfering nodes that can transmit simultaneously without disrupting current

transmission are those at least d_i units apart, where

$$d_i \geq \sqrt[4]{\psi} * d$$

Lee *et al.* [73] empirically show that SINR threshold ψ is around 10 dB to achieve a Frame Reception Ratio (FRR) of 0.90. Substituting this value, we obtain $d_i \geq 1.78 \times d$. This means 802.11 radios up to 2-hops away from the transmitter or receiver may interfere with its reception. In Figure 7.9 when there is an ongoing transmission from $3 \rightarrow 4$, links $1 \leftrightarrow 2$, $2 \leftrightarrow 3$, $4 \leftrightarrow 5$, and $5 \leftrightarrow 6$ are required to stay idle. However, the transmission from GW $\leftrightarrow$ 1 can proceed concurrently, giving a spatial reuse of $\frac{1}{3}$. This sets a lower bound of $\frac{W}{3}$ on the theoretical aggregate send/receive capacity of the gateway.

With multi-rate links, the aggregate capacity is lowest when all flows traverse the slowest link. Consistent with our observations in Section 7.5.2, this bounds the lowest aggregate capacity to $\frac{W_1}{3}$, where W_1 is the first element of the lexicographically ordered rate vector $\mathbf{W}$.

Practically achievable bounds may be lower due to packet losses, non-optimal carrier sense threshold, and other MAC-specific overheads.

7.6 Simulation Evaluation

We have implemented ARC in ns-2 [2]. Our module sits directly on top of the wireless MAC layer, and can rate limit both upstream and downstream flows. A gateway router with multiple wireless interfaces may use an ARC module per interface to avoid synchronization between the flows on different interfaces. We rate limit data packets only; system housekeeping messages such as routing updates bypass ARC and are not rate limited.

We simulated ARC with the binary search heuristics from Section 7.5 (We use the exponential rate increase/decrease heuristics for our testbed evaluation in Section 7.7). Our various control parameters were as follows. The epoch duration δ was set to 10 s.; choosing a value larger than the control action of TCP is important for stability. Our inter-flow unfairness threshold was set to 0.9 and our intra-flow rate cutoff threshold θ set to 0.95. We simulated elastic flows using an infinite file transfer with TCP NewReno [34].

7.6.1 Long-lived Elastic TCP Flows

We compare the performance of ARC against the following:

1. A single, shared FIFO queue at the gateway.
2. An aggregate static rate limit (Static RL) that is the fair-aggregate capacity of the network computed using the iterative max-min algorithm and applied at the gateway using the enforcement architecture in Figure 7.4a.
3. Combining the Static RL with FQ at the gateway as shown in Figure 7.4b.
4. Dynamic ARC where the rate limit is recomputed every epoch using Algorithm 1 and enforced by the mechanism shown in Figure 7.4b.
5. TCP Adaptive Pacing (TCP-AP) [33] rate-based scheduling mechanism that requires modifications to all mesh routers (see Section 5.2 for details). We use the ns-2 TCP-AP implementation of ElRakabawy *et al.* [32] and integrate it in our simulation framework.
6. Source Rate Control (SRC) with the per-node rate pre-computed with the iterative max-min algorithm and enforced via distributed source rate limiters. It represents a performance upper-bound as individual max-min rates are computed using an omniscient knowledge of network topology and enforced at the source nodes without incurring any signaling overhead.

We first tested the topology in Figure 7.6a, substituting 1 Mb/s and 2 Mb/s 802.11 links for R and $2R$, respectively. Our measured flow rates normalized to their *optimal* max-min fair share are shown in Table 7.1. The actual measured rates for the five mechanisms of our interest are shown in Figure 7.10. We see roughly a two-fold improvement in JFI by simply introducing a static rate limit compared to the shared FIFO queue. Combining this rate limit with FQ shows an additional improvement. Ideally, Dynamic ARC would converge to the same results as Static RL with FQ. Our results show that Dynamic ARC further improves the fairness index, but at the cost of reducing the rate of the flows with the highest throughput. This is partly because Dynamic ARC allocates the highest goodput amongst all schemes for flows traversing the 1 Mb/s wireless links (An average increase of 7%, 28%, 22%, and 11% against SRC, Static RL, Static RL+FQ, and TCP-AP for flows 12, 13, 14, and 15.) This behavior of Dynamic ARC can be adjusted using the control parameters γ and θ that trigger rate allocation decisions.

Scheme	JFI	f_1	f_2	f_3	f_4	f_5	f_6	f_7
Shared FIFO	0.45	3.08	0.41	0.46	0.49	0.52	0.42	0.47
FQ	0.45	3.09	0.39	0.46	0.48	0.51	0.46	0.48
Static RL	0.84	1.67	0.67	0.67	0.67	0.66	0.64	0.67
Static RL+FQ	0.87	1.57	0.69	0.69	0.70	0.70	0.69	0.67
Dynamic ARC	0.97	0.55	0.61	0.61	0.85	0.86	0.85	0.84
TCP-AP	0.96	1.21	0.68	0.67	0.75	0.82	0.74	0.70
SRC	0.99	0.96	0.85	0.86	0.80	0.79	0.79	0.79

Table 7.1: Flow rate distribution Normalized flow rates for Figure 7.6a. TCP-AP and SRC require changes on all mesh routers; all other scheduling techniques were implemented at the gateway only

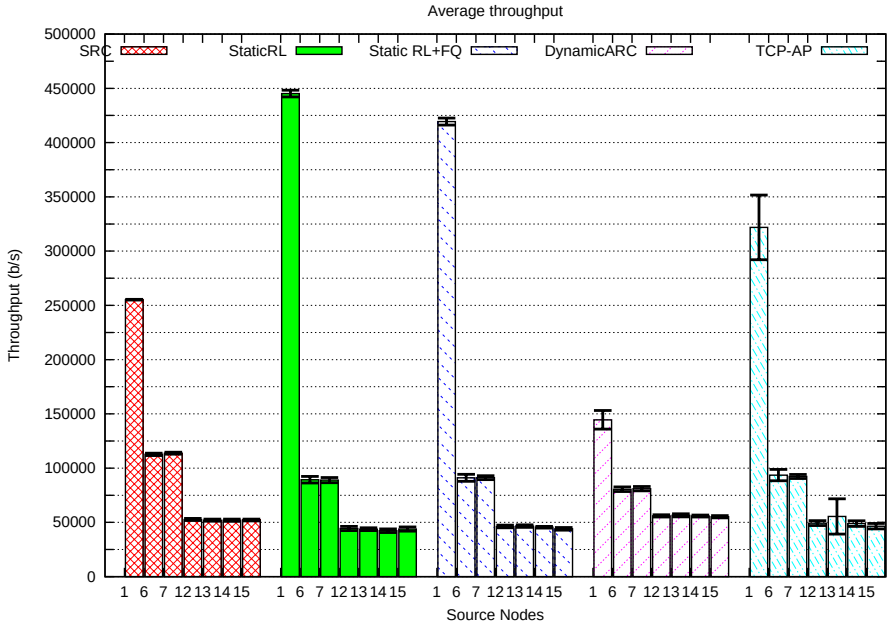

Figure 7.10: Average throughput with 95% confidence intervals for the network in Figure 7.6a.

Scheme	JFI		$\frac{min.\,rate}{fair\,rate}$		$\frac{max.\,rate}{fair\,rate}$		$\frac{U}{U_{opt}}$	
	Avg.	Std.Dev.	Avg.	Std.Dev.	Avg.	Std.Dev.	Avg.	Std.Dev.
Shared FIFO at GW	0.48	0.19	0.34	0.21	4.53	3.05	0.85	0.06
FQ at GW	0.51	0.16	0.36	0.20	3.34	1.36	0.86	0.05
Static RL at GW	0.94	0.03	0.61	0.17	1.26	0.41	0.81	0.10
Static RL & FQ at GW	0.94	0.04	0.60	0.20	1.14	0.14	0.83	0.08
Dynamic ARC	0.84	0.14	0.56	0.17	1.53	0.68	0.85	0.08
TCP-AP	0.82	0.14	0.53	0.25	1.33	0.17	0.87	0.04

Table 7.2: Comparative analysis of ARC fairness indices for downstream flows

Finally, we note that the JFI obtained with Dynamic ARC is within 2–3% of that obtained with TCP-AP and SRC mechanisms. These distributed rate-based scheduling mechanisms are challenging to deploy in WMNs built with commodity mesh routers where the ISPs have limited control over the subscriber equipment.

We have extensively evaluated these set of mechanisms on a number of different topologies, including chains (up to 10-hops) and grids (up to 6x6 node configurations) with a random number of flows transmitting via a common gateway. Our experiments included both upstream and downstream flows. For a given topology, each experiment was repeated 25 times with different random seeds and random flow activation sequences, and the results averaged. These results are summarized in Table 7.2 for downstream and Table 7.3 for upstream flows. We omit SRC results for downstream flows as that is equivalent to gateway rate control. On average, Dynamic ARC shows a fairness improvement by a factor of 3 for upstream flows and by a factor of 2 for downstream flows when compared to the base case with a shared FIFO queue at the gateway with no rate limiting. In addition to these improved fairness characteristics, Dynamic ARC achieves a normalized effective network utilization of more than 80% for both downstream and upstream flows. These results show close resemblance to TCP-AP and SRC mechanisms that require uniform enforcement of rate-based scheduling at individual mesh routers. SRC uses a static rate limit for a given topology that was computed off-hand using the iterative max-min fairness algorithm. In contrast, TCP-AP determines this rate dynamically, and thus can react to changes in network and traffic conditions.

Scheme	JFI		$\frac{min.rate}{fair\ rate}$		$\frac{max.rate}{fair\ rate}$		$\frac{U}{U_{opt}}$	
	Avg.	Std.Dev.	Avg.	Std.Dev.	Avg.	Std.Dev.	Avg.	Std.Dev.
Shared FIFO at GW	0.31	0.13	0.12	0.43	4.34	1.34	0.74	0.11
FQ at GW	0.31	0.12	0.12	0.13	4.32	1.37	0.74	0.11
Static RL at GW	0.93	0.04	0.64	0.13	1.27	0.11	0.87	0.07
Static RL & FQ at GW	0.95	0.03	0.64	0.15	1.18	0.09	0.87	0.05
Dynamic ARC	0.94	0.05	0.60	0.19	1.12	0.25	0.81	0.08
TCP-AP	0.88	0.06	0.59	0.15	1.53	0.27	0.87	0.05
SRC	0.99	0.01	0.81	0.17	0.99	0.01	0.90	0.07

Table 7.3: Comparative analysis of ARC fairness indices for upstream flows

7.6.2 ARC Responsiveness with Short-lived TCP Flows

We evaluated the short term fairness and responsiveness of ARC. Figure 7.11 shows our results with a 5-hop chain where rate allocation is made using binary search. Initially, all five flows are active. We terminate flow 5→0 at time 75 s. and bring it back up at time 150 s. As described in Section 6.3.3, we observe that the flow convergence time is a function of the TCP state. When flow 5→0 reactivates, its slow start phase allows it to rapidly approach its fair share within two averaging intervals of our plot. ARC allows new flows to quickly ramp up their rates to their allocated share of the network capacity. Finally we note that the short-term unfairness at flow activation/termination in Figure 7.11 is an artifact of the binary search heuristic employed by our rate allocation component.

7.7 Testbed Evaluation

We have implemented ARC with FQ using the HTB qdiscs with the Linux traffic control framework `tc` [46]. Our implementation architecture is shown in Figure 7.12. Our root qdisc is a HTB. We use filters to classify `iperf` traffic to a SFQ which is then drained by a single TBF. The token generation rate is a periodically adjusted based on the aggregate rate limit we wish to enforce for the network. Every epoch δ, we poll the statistics exposed by the `Web100` framework to read in the bytes transferred for our test streams. This measurement is then used to adjust the token generation rate per Algorithm 1.

We implemented and evaluated the exponential increase/decrease heuristic (Algorithm 2) for our testbed. We used the exponential increase/decrease factors of α

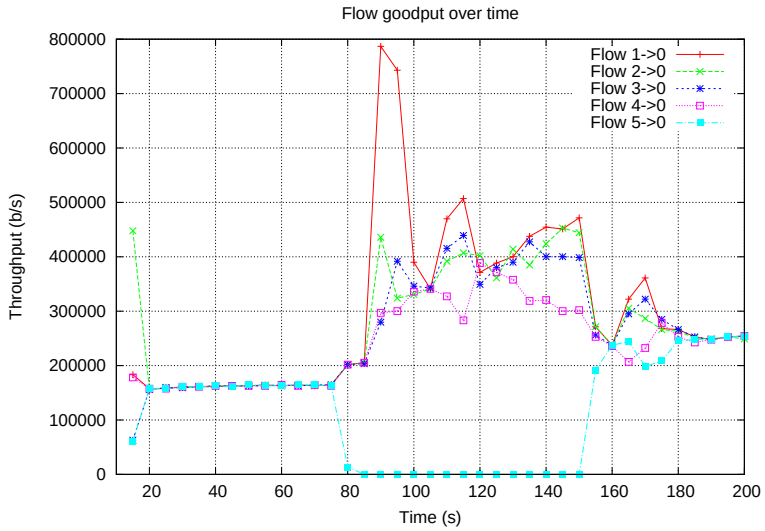

Figure 7.11: Throughput over time for a 5-hop chain. Flow 5→0 terminates at 75 s. and then comes back up at 150 s. The plot shows data averaged over 5 s. Epoch duration was 10 s.

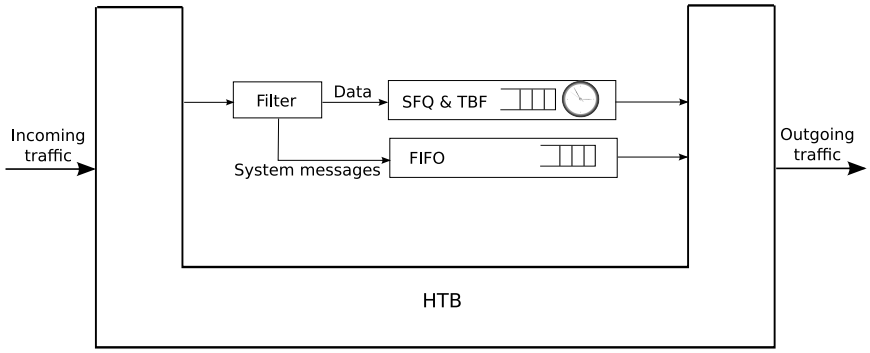

Figure 7.12: Implementation architecture for ARC with FQ at the gateway.

$= 1.1$ and $\beta = 0.9$. Our epoch duration δ was set to 10 s. Our inter-flow unfairness threshold γ was set to 0.85.

Our results for download flows are shown in Figure 7.13. To provide a basis of comparison, we also show in parallel the relevant results for FIFO queues previously described in Section 6.4. Our results show over a two-fold improvement in JFI using PFRC compared to the flow rate distribution obtained with using Drop Tail FIFO queues.

The average throughput of the flow distribution with ARC and FQ is approximately 470 Kb/s. This is within 10% of the fair share points observed with download flows in Figures 6.9a and 6.9b. This is primarily an artifact of the exponential

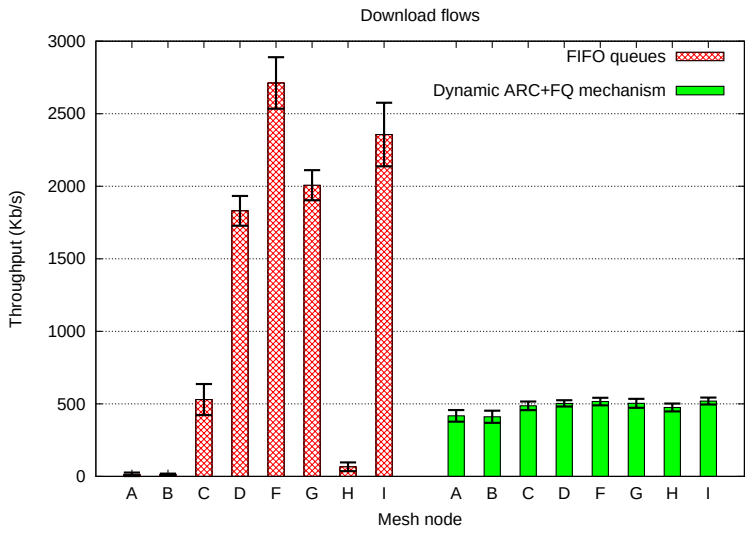

Figure 7.13: Throughput distribution for download flows using our proposed ARC+FQ mechanism at the gateway router E. With FIFO queues, JFI = 0.39. With ARC and FQ, JFI = 0.99.

increase/decrease multiplicative factor used in our experiments (we use α and β of 1.1 and 0.9, respectively). Using larger values allows for quicker convergence to the fair rate allocation; however, this can introduce short-term instability where larger jumps in rate allocation can lead to short-term unfairness between flows.

7.8 Simulation/Testbed Validation

In prior sections, we evaluated the performance of our proposed ARC mechanisms individually via simulations as well as testbed experiments. Our results across both these two frameworks show a similar degree of improvement in fairness indices by a factor of 2–3 when compared to networks with simple FIFO scheduling with no rate limiting. To further validate and strengthen the confidence in our simulation results, we now perform a direct, head-to-head comparison across these two environments.

Validation of wireless network simulations is particularly challenging because in addition to the proposed protocol, we must also abstract the low level behavior of the wireless channel with a reasonable degree of accuracy across the two environments. To simplify this task, we limit the parameter space of network configuration using uniform (static) link rates and static routing as follows:

- Uniform (static) link rates: We configured the PHY link rate for all mesh

routers to the base rate of 6 Mb/s. The modulation scheme used at the base rate provides a high degree of resilience against wireless channel errors, allowing for a strong fidelity between the testbed and simulation environment. This enables us to focus instead on the performance of our transport layer protocols.

- Static routing: We use manual static routing to specify the path traversed by data traffic. We first let OLSR converge to stable routes on the testbed, and then reinforce these routes manually through static routing. Similar static routes are then set up in our simulation framework.

- Nodes within transmission and interference range: We use the association table at each mesh router to determine the mesh nodes within its transmission range. To determine interfering links, we use bandwidth tests by measuring the difference in throughput when a transmitter transmit in isolation and when it transmits in parallel with some other transmitter [90]. Using this information, we carefully reproduced the testbed topology in our simulation framework.

Our parameter configuration for ARC was consistent across the two frameworks. As before, we used the exponential increase/decrease factors of $\alpha = 1.1$ and $\beta = 0.9$. Our epoch duration δ was set to 10 s, and inter-flow unfairness threshold γ was 0.85.

Our results are shown in Figure 7.14, averaged over 25 runs. The error bars are the 95% confidence intervals. The average throughput across all flows in the simulation environment is approximately 150 Kb/s, with a JFI value that rounds off to 1.00. In contrast, the flows in our testbed stabilize to an average throughput of 132 Kb/s. This is within 15% of the average flow throughput observed in the simulations. Our testbed environment is subject to interference and noise on the RF channel, resulting in a lower throughput compared to the simulations.

7.9 Summary

Distributed bottlenecks can exist in a WMN despite its dominant traffic pattern consisting of flows directed towards or away from the gateway. Max-min rate fairness with its Pareto optimality allows us to efficiently utilize these bottlenecks while maximizing the minimum allocation. In this chapter we proposed heuristics

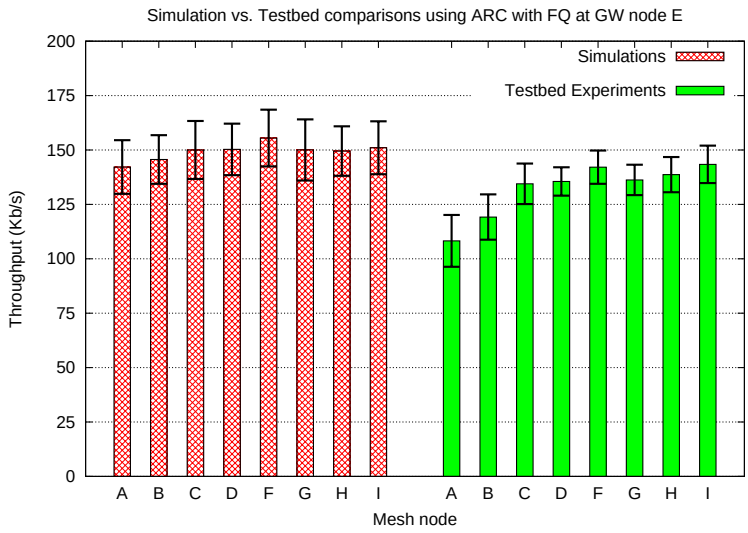

Figure 7.14: Validating ARC simulation results via testbed experiments on equivalent network topologies.

for achieving approximate max-min rate allocation through gateway-enforced rate control in a WMN. We propose ARC, a measurement-based rate controller that can be implemented at the gateway router and manages traffic as a single aggregate bundle instead of distinct flows. Our simulation results, backed by testbed experiments and validation, show that ARC produces improvement in fairness indices by a factor of 2 to 3 when compared to networks using simple FIFO queues without any rate limiting.

Chapter 8

Per-flow Rate Controller

In Chapter 7 we proposed ARC, a framework of mechanisms for enforcing an approximate max-min fair rate allocation using aggregate traffic rate control. To exercise finer-grained control over the resource allocation process, these mechanisms can be extended to support per-flow rate control. Such mechanisms are of interest to a network operator as it enables them to target their subscriber needs by offering differentiated services. In this chapter we extend the controller heuristics proposed for ARC to support weighted flow rate fairness. We conveniently call our new controller Per-flow Rate Controller (PFRC).

In this chapter we first describe the modifications necessary to convert aggregate rate control heuristics to support weighted fairness using PFRC. We then evaluate the performance of PFRC using simulations in Section 8.2 and using our WMN testbed in Section 8.3.

8.1 Per-flow Rate Controller

Per-flow Rate Controller (PFRC) is a derivative of various ARC heuristics proposed in Chapter 7. As in ARC, the three main components of PFRC perform the following operations: (1) Flow classification, (2) Rate evaluation and allocation, and (3) Flow rate enforcement. Our flow classification methodology is consistent with that used in ARC, *i.e.*, we identify a flow as a subset of all micro-flows originating from, or destined to, a given mesh node. However, we need to modify rate evaluation and allocation heuristics to support weighted fairness, and extend the rate enforcement mechanisms to support per-flow control. We describe these modifications below.

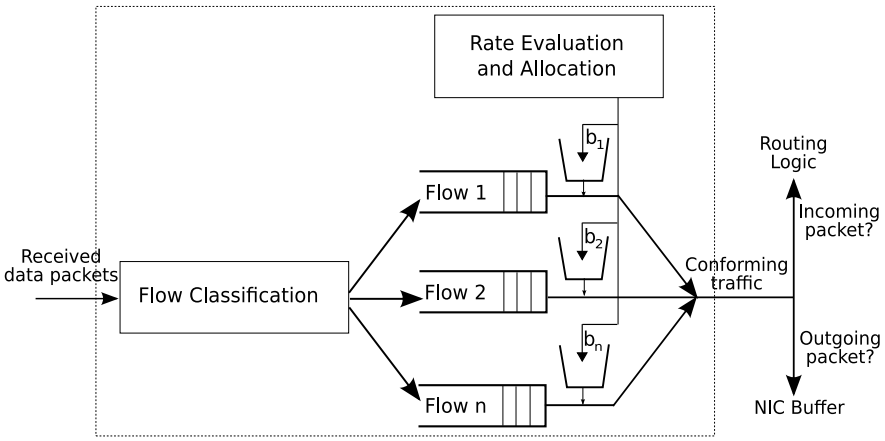

Figure 8.1: The main architectural components of PFRC: flow classification, rate evaluation and allocation, and rate enforcement token buckets.

8.1.1 Rate Evaluation and Allocation

The rate evaluation component uses the measured flow rates to adjust the behavior of the rate allocation component, constituting a closed-loop feedback controller similar to that of ARC shown in Figure 7.7.

Rate evaluation This is based on a simple principle: if all flows obtain their allocated rate, then the network capacity is possibly underutilized (*i.e.*, the network is operating in a regime to the left of the fair share line as depicted by the behavior in Figure 3.2a); the resulting control action is to increase flow rates. However, if a flow obtains less than its allocated rate, then we are likely driving the network beyond its fair capacity (similar to the representative behavior beyond the fair rate in Figure 3.2a). Consequently, the flow rates need to be decreased.

At the end of every time epoch τ_t, PFRC measures the rate r_i obtained by a flow f_i and compares it to the rate b_i allocated for that flow during the epoch τ_t. We associate a weight w_i with a flow f_i, such that b_i equals $\frac{w_i}{\sum_{i=1}^{N} w_i}$ fraction of the available capacity for the N active flows. Two possibilities exist:

1. If $r_i \geq b_i$ for $\forall i \in N$, the mechanism assumes the network capacity may be underutilized, *i.e.*, the current estimate of network capacity ($C_{meas} = \sum_{i=1}^{N} r_i$) is low. It signals the rate allocation component to increase flow rates.
2. If $r_i < b_i$ for any $i \in N$, the mechanism determines that the flow f_i is experiencing unfairness. It assumes that its current estimate of the capacity

$C_{meas} = \sum_{i=1}^{N} r_i$ is too high. It signals the rate allocation component to decrease flow rates to lower the capacity utilization.

The pseudo-code for this rate evaluation component is shown in Algorithm. 4.

Input: Epoch duration δ, unfairness threshold γ ($0 < \gamma \leq 1$), allocated rate vector $[b_1, b_2, ..., b_N]$, and the measured rate vector $[r_1, r_2, ..., r_N]$

Output: Rate increase or decrease decision

```
1 while once every δ time units do
2 |  if r_i/b_i < γ for any active flow f_i then
3 |  |  decreaseRates;
4 |  else
5 |  |  increaseRates;
6 |  end
7 end
```

Algorithm 4: Rate evaluation for PFRC

Rate Allocation The rate allocation component in Figure 8.1 determines new flow rates based on feedback from the rate evaluation component described in Algorithm 4. It may be used with both exponential increase/decrease heuristics (Algorithm 5) or binary search rate increase/decrease heuristics (Algorithm 6). Binary search has faster convergence characteristics and we use it in our simulation analysis in Section 8.2. We evaluate our WMN testbed using exponential increase/decrease in rate allocation in Section 8.3 below.

8.1.2 Flow Rate Enforcement

PFRC implements traffic shaping using per-flow token buckets. The token generation rate vector $\mathbf{B}=[b_1, b_2, ..., b_N]$ for the N active flows is controlled by the rate allocation mechanism described above.

8.1.3 Design Considerations

Dynamic flows Unlike ARC that manages network aggregate capacity, PFRC directly manages individual flow rate allocations. Supporting dynamic flows requires PFRC to reallocate rates when an existing flow terminates or a new flow

Input: $C_{meas} = \sum_{i=1}^{N} r_i$, flow weight vector $[w_1, w_2, ..., w_N]$
Output: New token rate vector $[b_1, b_2, ..., b_N]$

```
1  increaseRates begin
2      C_est = α × C_meas;                                   /* α > 1 */
3      for every active flow f_i do
4          b_i = w_i / Σ_{i=1}^{N} w_i × C_est;
5      end
6  end
7  decreaseRates begin
8      C_est = β × C_meas;                                   /* β < 1 */
9      for every active flow f_i do
10         b_i = w_i / Σ_{i=1}^{N} w_i × C_est;
11     end
12 end
```

Algorithm 5: Exponential increase/decrease rate allocation adapted for PFRC

Input: $C_{meas} = \sum_{i=1}^{N} r_i$, flow weight vector $[w_1, w_2, ..., w_N]$, and upper and lower aggregate capacity bounds C_{up} and C_{low} respectively.
Output: New token rate vector $[b_1, b_2, ..., b_N]$

```
1  increaseRates begin
2      C_low = C_meas;
3      C_est = (C_meas + C_up) / 2;
4      for every active flow f_i do
5          b_i = w_i / Σ_{i=1}^{N} w_i × C_est;
6      end
7  end
8  decreaseRates begin
9      C_up = C_meas;
10     C_est = (C_low + C_meas) / 2;
11     for every active flow f_i do
12         b_i = w_i / Σ_{i=1}^{N} w_i × C_est;
13     end
14 end
```

Algorithm 6: Binary rate allocation adapted for PFRC

emerges. For instance, the procedure `decreaseRates` may be called when a new flow is detected, as the new per-flow allocation will decrease in the presence of an additional flow. Similarly, `increaseRates` may be executed when a flow terminates. We use the presence or absence of packets to determine the current state of stream activity.

8.2 Simulation Evaluation

We have implemented PFRC in ns-2 [2]. Our module sits directly on top of the wireless MAC layer, and can rate limit both upstream and downstream data flows.

We simulated PFRC with the binary search heuristic from Section 8.1.3. We used an epoch duration δ of 10 s. so as not to interfere with the control action of TCP. Our unfairness threshold γ (Algorithm 4, line 2) was set to 0.7. We considered scenarios with both weighted fairness and equal rate fairness.

8.2.1 Long-lived Elastic TCP Flows

We first summarize our results for equal rate fairness with PFRC. We evaluated PFRC on a number of different chain, grid, and random network topologies, with up to a maximum of 35 simultaneously active nodes transmitting via a single gateway. For a given topology, experiments were repeated 25 times with different random seeds and random flow activation sequences, and the results averaged. For performance benchmarks, we repeated the same set of experiments with the following:

1. A single, shared FIFO queue at the gateway without any rate limiting.
2. TCP-AP [33] rate-based scheduling implementation of ElRakabawy *et al.* [32] at individual mesh routers.
3. Using a gateway-enforced per-flow rate limit, where the per-flow rate is statically computed using the computational model described in Chapter 4.
4. For upstream flows, we also list results for source rate limiting the flows to a statically computed fair rate as determined by the computational model described in Chapter 4. No changes were made on the gateway router for these experiments. For downstream flows, this source rate limit is akin to per-flow gateway rate limit as the gateway is now injecting packets in the

Scheme	JFI		$\frac{min.\,rate}{fair\,rate}$		$\frac{max.\,rate}{fair\,rate}$		$\frac{U}{U_{opt}}$	
	Avg.	Std.Dev.	Avg.	Std.Dev.	Avg.	Std.Dev.	Avg.	Std.Dev.
Shared FIFO at GW	0.41	0.24	0.10	0.10	10.86	7.08	0.95	0.09
PFRC	0.99	0.02	0.76	0.28	1.09	0.15	0.99	0.12
TCP-AP	0.80	0.10	0.55	0.12	2.45	0.88	1.01	0.05
Static per-flow rate limit at GW	0.99	0.02	0.75	0.26	1.01	0.01	0.95	0.07

Table 8.1: PFRC fairness indices for downstream flows compared to networks with no rate limiting and networks with centralized rate limiting computed with topology information.

Scheme	JFI		$\frac{min.\,rate}{fair\,rate}$		$\frac{max.\,rate}{fair\,rate}$		$\frac{U}{U_{opt}}$	
	Avg.	Std.Dev.	Avg.	Std.Dev.	Avg.	Std.Dev.	Avg.	Std.Dev.
Shared FIFO at GW	0.31	0.13	0.17	0.16	15.2	11.6	0.95	0.09
PFRC	0.97	0.05	0.76	0.28	1.22	0.18	0.96	0.07
TCP-AP	0.75	0.11	0.45	0.16	2.85	1.18	1.01	0.07
Static per-flow rate limit at GW	0.99	0.02	0.76	0.30	1.00	0.06	0.90	0.06
Source rate limit	0.99	0.01	0.77	0.21	1.00	0.01	0.91	0.07

Table 8.2: PFRC fairness indices for upstream flows compared to networks with no rate limiting and networks with centralized rate limiting computed with topology information.

wireless medium. As described earlier, SRC represents a performance upper-bound of distributed rate limiters in a 802.11 WMN where the rate allocation was computed using the computational mode.

Our results are summarized in Table 8.1 and 8.2 for downstream and upstream flows, respectively. PFRC shows upwards of two-fold and three-fold improvement for downstream and upstream flows, respectively, when compared to a network without any rate control. It provides this improved fairness in rate allocation without any significant loss in network efficiency, achieving upwards of 90% of normalized effective network utilization. In contrast, backlogged TCP flows achieve a high network utilization for shared FIFO queues without any rate limiting only at the cost of severe unfairness and starvation by saturating the spectrum around the gateway with their own traffic. TCP-AP also provides two-fold improvement in fairness indices over the base case without any rate limiting. In general, PFRC exhibits better fairness characteristics while incurring a slight cost in terms of reduced effective network utilization.

8.2.2 Weighted Flow Rate Fairness

Per-flow rate control allows us to exercise fine-grained control over resource allocation for individual mesh nodes. Such control is necessary in a WMN where an ISP wishes to provide differentiated services in terms of bandwidth allocation to various subscribers. In this section we demonstrate how weighted fairness can be enforced using rate allocation via Algorithm 6. Here we show our results for a 6x6 grid topology with 18 upload flows from mesh routers to a host on the wired network via gateway node 0. The network topology is shown in Figure 8.2a. The weight of each active source node is indicated by the number of circles around it, *e.g.*, nodes $30, 31$, and 35 have weights of $3, 1$, and 2, respectively.

Figure 8.2b shows the average rate allocation for the 18 sources achieved by using PFRC at the gateway node 0. The sources are ordered by weight and the error bars are the 95% confidence intervals. Such weighted rate allocation cannot be achieved using work-conserving scheduling techniques such as WFQ at the gateway router.

8.2.3 Short-lived Elastic TCP Flows

We also evaluated the responsiveness of PFRC for dynamic elastic flows. Here we show our results for a 7-hop chain (Figure 3.1). Initially, five flows are active. We terminate flows 1→0 and 5→0 at 200 s, and flow 7→0 at 300 s. Finally, at 400 s, we reactivate flows 1→0 and 7→0. Figure 8.3 plots throughput against time, averaged over 5 s. As described in Section 6.3.3, we observe that the flow convergence time is a function of the TCP state. The slow start phase of TCP allows flows 1→0 and 7→0 to rapidly approach their fair rate within one and three averaging intervals of our plot respectively. Thus PFRC allows new flows to quickly ramp up their rates to their allocated share of the network capacity.

8.2.4 Rate-constrained TCP Flows

PFRC is optimized for continuously backlogged elastic data sources. Here we analyze its performance when rate-constrained TCP flows are introduced in the traffic mix.

The underlying rate increase/decrease heuristics determine how PFRC apportions the network capacity among the flows. Our binary search algorithm uses

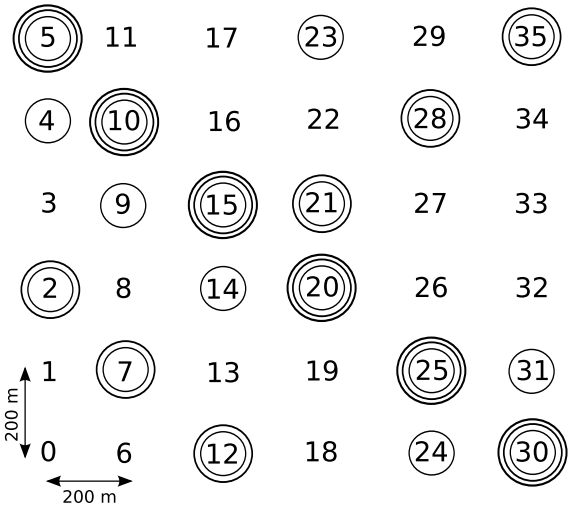

(a) Weighted 6x6 grid topology

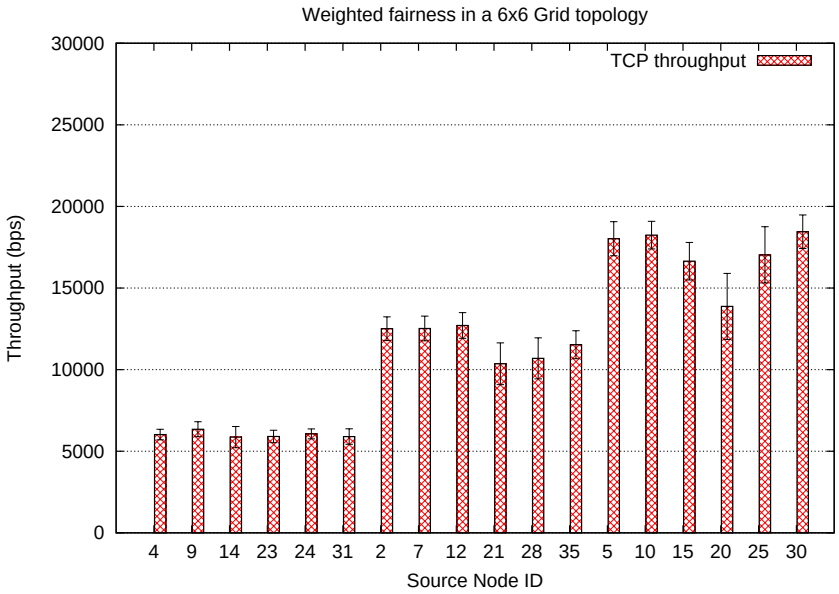

(b) Flow rate distribution using PFRC

Figure 8.2: A weighted 6x6 equidistant grid topology with 18 nodes uploading data to a gateway node 0. The weight of a source node is indicated by the number of circles around it; nodes $4, 9, 14, 23, 24$, and 31 are assigned a weight of 1; nodes $2, 7, 12, 21, 28$, and 35 are assigned a weight of 2; nodes $5, 10, 15, 20, 25$, and 30 are assigned a weight of 3. PFRC achieves the rate allocation shown in Figure 8.2b above. The error bars are the 95% confidence intervals.

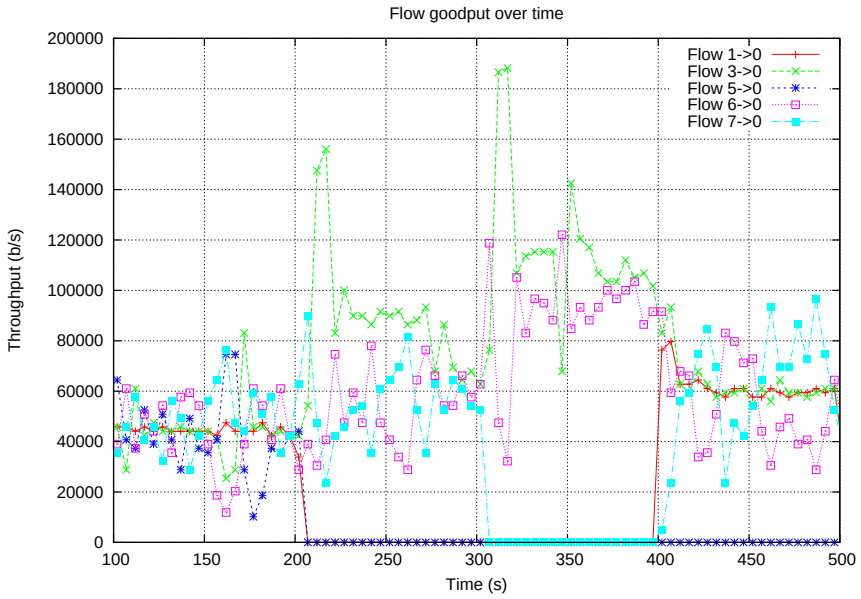

Figure 8.3: Throughput over time for a 7-hop chain. Flows 1→0 and 5→0 terminate at 200 s. 7→0 terminate at 300 s. 1→0 and 7→0 restart at 400 s.

upper and lower aggregate network capacity bounds. When all flows are equally weighted, this can be extended to per-flow upper and lower throughput bounds. From Section 7.5.2, we determine these per-flow upper and lower bounds as $\frac{W}{N}$ and $\frac{W}{3N}$ respectively. Thus irrespective of the traffic mix, PFRC does not allow the rate allocation for elastic, adaptive flows to fall below $\frac{W}{3N}$ or rise above $\frac{W}{N}$. The actual rate allocations are a function of the rate limit of the constrained flow, r_{rl}, as shown below:

1. When $r_{rl} < \frac{W}{3N}$: In this case, the steady-state rate allocation for each unconstrained flow is $\frac{W}{3N}$.
2. When $r_{rl} > \frac{W}{3N}$: Here, the steady-state rate allocation for *all* flows is r_{rl} when $r_{rl} < fairshare$. Otherwise, the rate allocation is the fair share itself. Thus a rate-limited TCP node with a rate limit higher than the fair share cannot obtain a rate higher than its fair share.

We validated this behavior with a 4-hop chain (Figure 3.1). Nodes 1, 2, and 3 use elastic TCP sources with backlogged traffic. Node 4 sources a locally-enforced, rate-limited TCP stream. All streams terminate at the same wired destination accessible *via* the gateway. We successively increase the rate limit of stream 4 from 10 Kb/s to 70 Kb/s in increments of 10 Kb/s. The fair share is approx.

Node 4 rate	$\frac{Node1avg.}{optimal}$	$\frac{Node2avg.}{optimal}$	$\frac{Node3avg.}{optimal}$	$\frac{Node4avg.}{optimal}$
10 Kb/s	0.70	0.70	0.80	1
20 Kb/s	0.74	0.74	0.74	1
30 Kb/s	0.79	0.79	0.79	1
40 Kb/s	0.84	0.84	0.84	1
50 Kb/s	0.90	0.90	0.90	1
60 Kb/s	0.94	0.94	0.94	1
70 Kb/s	1.04	1.03	1.03	1

Table 8.3: PFRC performance with rate-limited TCP.

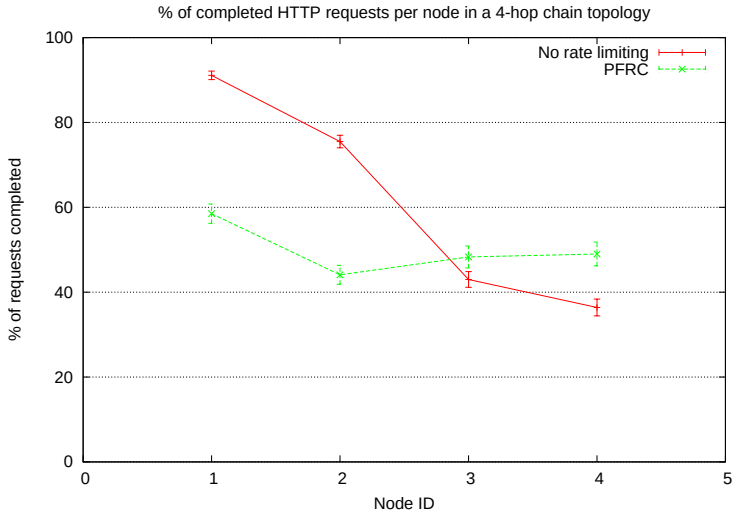

Figure 8.4: HTTP request completion rate with and without gateway-enforced rate limiting. Error bars are the 95% confidence intervals.

75 Kb/s if all flows were unconstrained. The results in Table 8.3 show the average measured throughput of a node normalized to its optimal fair share (calculated after redistributing the leftover capacity of the constrained TCP flow). Our experiments show that irrespective of the rate of a constrained node, the rate allocated to backlogged nodes never dropped below $\frac{W}{3N}$ (around 71 Kb/s in this experiment).

8.2.5 HTTP Flows

HTTP flows constitute a major portion of the Internet traffic. In this section, we describe how this protocol fares in WMNs.

We consider a 4-hop chain (Figure 3.1), where mesh routers 1, 2, 3, and 4 generate HTTP requests at a predefined rate of 5 requests/s. The request messages are uniformly distributed between 200–1000 bytes. These requests are transported to a web server on the wired network *via* the gateway router 0. This server generates normally distributed HTTP response messages with an average size of 50,000 bytes and standard deviation of 10,000. Figure 8.4 shows that without any rate limiting, there is a stark unfairness in terms of the number of requests completed. Node 1 gets around 90% of its requests completed, while node 4 only gets around 35% of its requests completed within the simulation time interval. Using PFRC considerably improves the fairness in number of requests completed amongst the mesh nodes.

8.2.6 Peer-to-peer Flows within Mesh Routers

Our proposed centralized rate allocation framework is targeted towards last mile access networks where the flows traverse the gateway mesh router that bridges traffic across the WMN and the Internet. Despite this dominant traffic pattern, it is instructive to consider the impact of traffic flows *within* the nodes in a WMN, *i.e.*, flows that both originate and terminate at wireless mesh routers. Depending upon the network topology and routing protocols, such peer-to-peer flows may or may not traverse the gateway router in a WMN. In this section we analyze the impact of these flows on rate allocation using centralized enforcement mechanisms such as PFRC.

Impact of peer-to-peer flows that do not traverse the gateway

Our proposed centralized rate allocation mechanisms enforce flow control for adaptive traffic streams at the gateway mesh router. The gateway router passively monitors the rate of traffic flows to infer the network state and adjust rate allocation. This control cannot be exercised over flows that do not traverse the gateway.

We illustrate the impact of such flows using a 7-hop chain topology with flows shown in Figure 8.5. Nodes 1 through 4 have upload flows that traverse the gateway router GW. We introduce a peer-to-peer flow $7 \rightarrow 5$. Both sender and receiver nodes for this flow are outside the carrier sense range of GW. Thus the gateway does not have omniscient knowledge of all network flows that we have previously assumed in our experiments.

Figure 8.5b shows the rate allocation for different flows using PFRC at GW. We also show our results when simple FIFO queues are used at the gateway with-

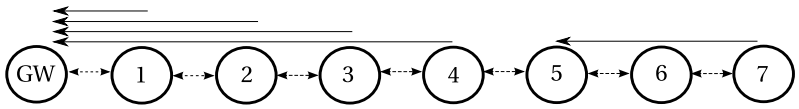

(a) Network topology

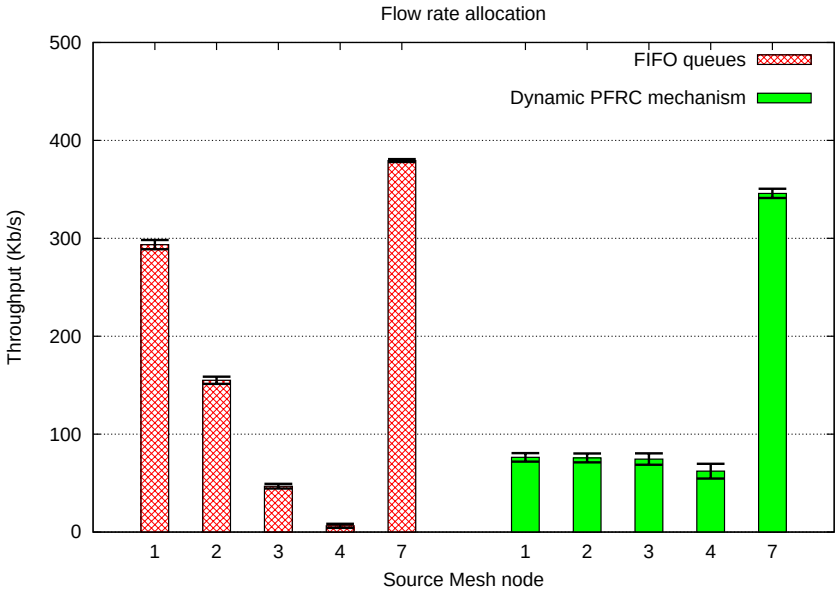

(b) Flow rate distribution

Figure 8.5: Impact of peer-to-peer flows between WMN nodes. Flow $7 \rightarrow 5$ does not traverse the gateway router.

out any rate limiting. In both scenarios, flow $7 \rightarrow 5$ receives a disproportionate share of network capacity. The gateway cannot control the allocation of this flow since it does not traverse it. However, PFRC apportions the remaining network capacity fairly between the flows traversing the gateway, while with FIFO queues we observe unfairness and starvation for nodes 2, 3, and 4 even for this residual network capacity. Finally, we note that with PFRC there is an approximate drop of 10% in throughput of node 7 due to increased channel contention when nodes 3 and 4 obtain a higher throughput.

Impact of peer-to-peer flows through the gateway

We now consider the behavior of PFRC on peer-to-peer flows between mesh nodes that traverse the gateway router. In particular, we are interested in flows that are bound by different bottleneck rates for the ingress and egress through the gateway router. An example network topology is shown in Figure 8.6, with flows between nodes $6 \rightarrow 1$ and $7 \rightarrow GW$. We previously analyzed this topology in Figure 7.3;

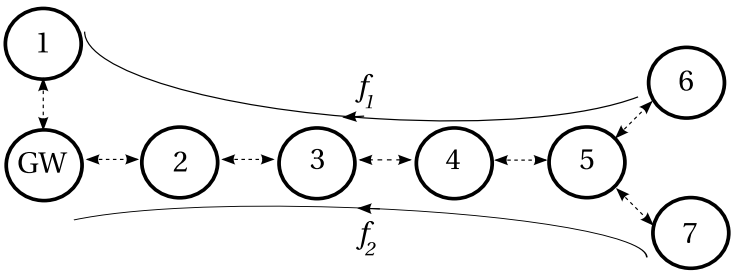

Figure 8.6: Peer-to-peer flow between mesh nodes. f_1 traverses The flow that traverse the gateway

with max-min allocation, the link $1 - GW$ can support a rate of $\frac{R}{5}$, while the links constituting the collision domain bottlenecks for flows f_1 and f_2 saturate at $\frac{R}{10}$, where R is the wireless link rate. It is well-known, however, that the end-to-end rate of a multihop flow is bound by the smallest rate allocated along its path [75]. We observe similar results with PFRC, with flows f_1 and f_2 obtaining a rate of approximately 82 Kb/s each with uniform wireless link rates of 1 Mb/s. This rate allocation provides only 50% utilization of link $1 - GW$. This is an artifact of end-to-end throughput of a flow being limited by its bottleneck collision domain. Similar results will be obtained even with any distributed source rate limiting mechanisms proposed in the literature.

8.3 Testbed Evaluation

We have implemented PFRC using the HTB qdiscs with the Linux traffic control framework `tc` [46]. Our implementation architecture is shown in Figure 8.7. The root qdisc is a HTB. We use filters to classify a flow (using source mesh node IP for uploads and destination mesh node IP for downloads) to a FIFO queue which is drained by a TBF. The token generation rate is a periodically adjusted based on the per-flow rate limit we wish to enforce for the network. The measured flow rate information is polled by reading in the `tc` qdisc statistics every epoch. This measurement is then used to adjust the token generation rate per the Algorithm 4.

Our configuration parameters in this analysis are consistent with those previously used in Section 7.7. We use exponential increase/decrease factors of 1.1 and 0.9 for α and β, respectively. Our epoch duration was set to 10 s. Our inter-flow unfairness threshold γ was set to 0.85.

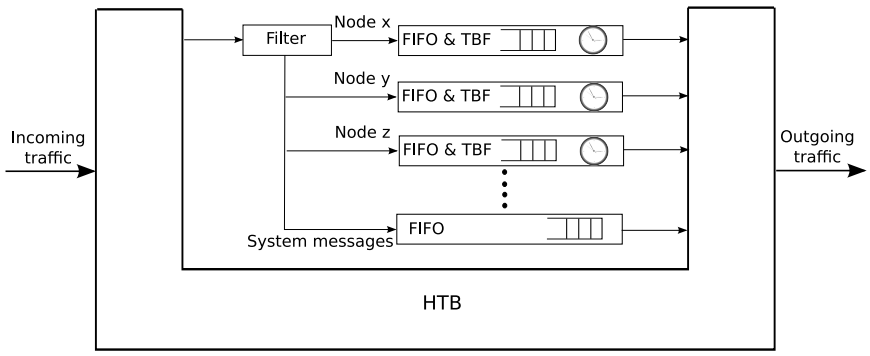

Figure 8.7: Implementation architecture for PFRC at the gateway

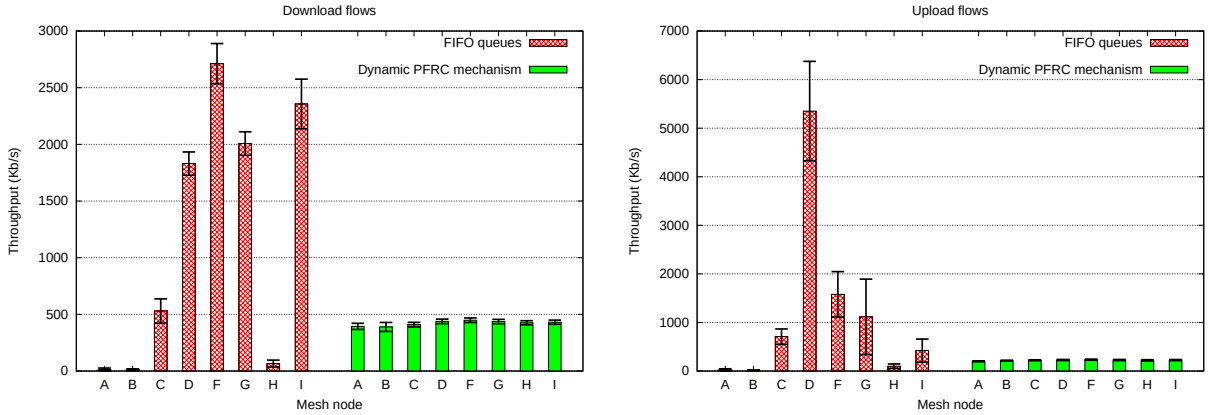

(a) Download flows. JFI: FIFO = 0.55, PFRC = 0.99 (b) Upload flows. JFI: FIFO = 0.33, PFRC = 0.99

Figure 8.8: Comparison of flow rate distribution with FIFO queues and PFRC for download and upload flows.

8.3.1 PFRC with a Single Flow per Node

Our results for download and upload flows are shown in Figures 8.8a and 8.8b, respectively. We also show in parallel the relevant results for FIFO queues that were previously described in Section 6.4. We observe an improvement in JFI of 80% for download flows and approximately a three-fold for upload flows.

PFRC achieves an average throughput of 415 Kb/s for downstream flows and 221 Kb/s for upstream flows. These values correspond closely to the fair share capacity of our testbed as illustrated in Figure 6.9. As with ARC+FQ mechanism, these values are an artifact of changing wireless capacity over time as well as the exponential increase/decrease multiplicative factors used in our experiments.

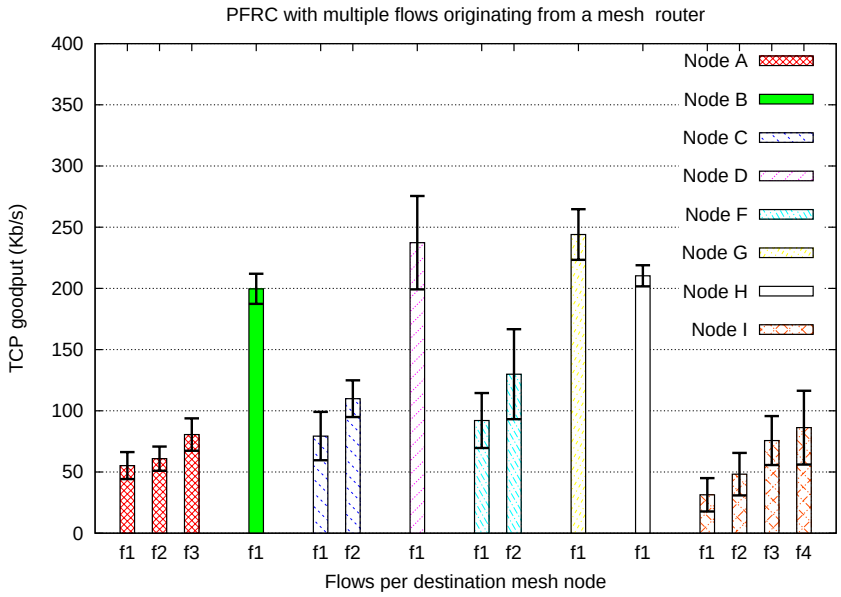

Figure 8.9: PFRC evaluation with multiple uplink flows originating from mesh nodes. Error bars are the 95% confidence intervals.

8.3.2 PFRC with Multiple Flows per Node

Figure 8.9 shows our results with PFRC with multiple upload flows (all equally weighted) originating from a mesh router. We observe a standard deviation of approximately 10 Kb/s for the average throughput distribution between flows of node A, 15 Kb/s between flows of node C, 18 Kb/s between flows of node F, and 22 Kb/s between flows of node I. The sum of the flow rates for each node, however, remains bounded within the fair allocation constraints identified for upload flows in Figure 6.9. Equal allocation of a node's share of network capacity between its subflows needs to be managed in a wireless network insofar as it needs to be enforced in a wired network. We propose studying this aspect in further detail as a part of future work.

8.4 Simulation/Testbed Validation

We validated the performance of our proposed PFRC rate allocation mechanism across both simulation and testbed environment. We reconfigured our testbed per the details in Section 7.8, *i.e.*, uniform static PHY link rates of 6 Mb/s and static routing.

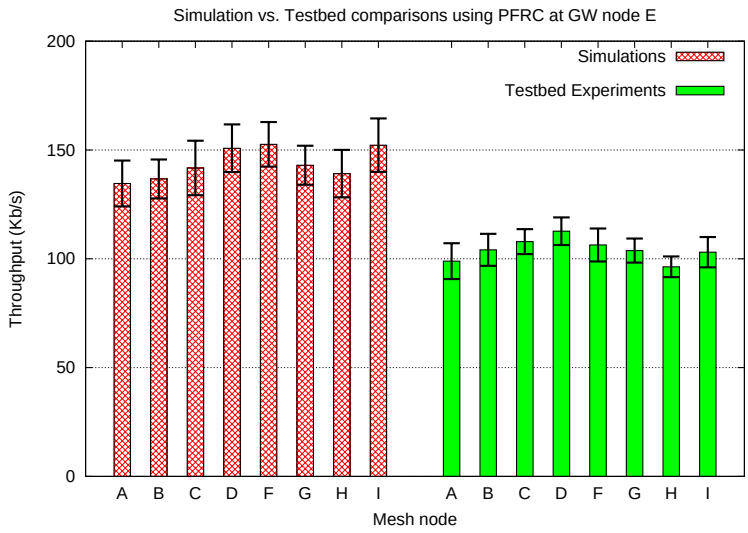

Figure 8.10: Validating PFRC simulation results via testbed experiment on a 9-node testbed with uplink flows originating from the mesh routers.

Our results for PFRC with upload TCP flows from each of the mesh routers to a wired host via the gateway node E are shown in Figure 8.10. Error bars are the 95% confidence intervals. With upload flows, the fair share rate observed in the experiments drops to 115 Kb/s. Our analysis show that this is because of asymmetric wireless links in our testbed. Even though all wireless interfaces operate at 6 Mb/s, the error rate on a wireless link across the two environments still varies because of channel noise. Such asymmetry, however, is not reproducible by the simulation framework. Consequently, the simulator still stabilizes the flows at a throughput of approximately 150 Kb/s, similar to the behavior observed with download flows in Section 7.14.

We excluded the asymmetric wireless links in our testbed to reduce it to a simplified network topology with symmetric links, comprising nodes E, F, G, H, and I. We then repeat our experimental validation of PFRC across the testbed and simulation environments. Our results are shown in Figure 8.11, averaged over 25 runs of the experiments, with error bars reflecting the 95% confidence intervals.

For the simulation framework, we measure an average throughput of 515 Kb/s for the 4 flows. This is within 5% of the average flow throughput of 495 Kb/s measured across the testbed. Removing the 4 nodes (A, B, C, and D) to eliminate the asymmetric links simplifies the topology and improves the degree of similarity between the simulation and testbed environments. Our prior validation results reported in Section 7.8 can perhaps similarly be improved by working with this

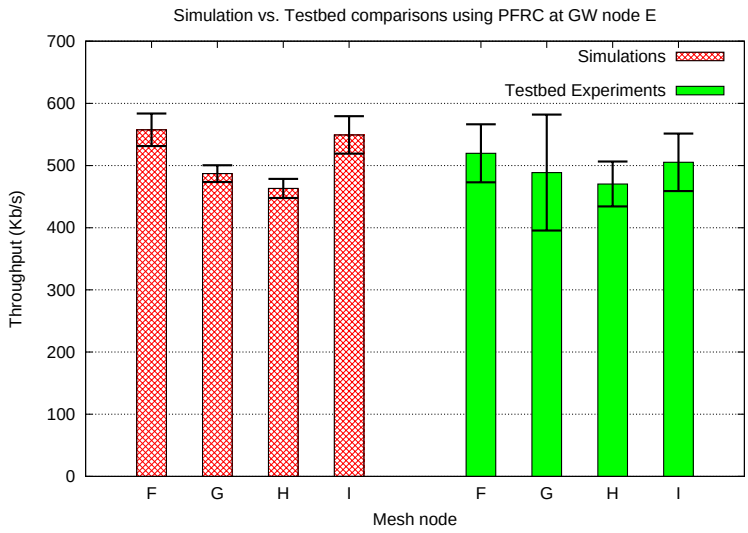

Figure 8.11: Validating PFRC simulation results via testbed experiment on a set of 5 nodes in the testbed with uplink flows originating from the mesh routers.

smaller topology. In hindsight, it would have been useful to confirm this, but time did not permit that investigation.

8.5 Summary

In this chapter we extended the framework of mechanisms previously proposed for ARC to develop PFRC, a centralized, feedback-driven per-flow rate controller for elastic traffic sources. PFRC allows us to exercise fine-grained control over the rate allocation process. In this chapter we showed how PFRC can be used to enforce weighted fairness for adaptive traffic flows in a WMN. Using both simulations and experiments on our WMN testbed, we show that PFRC provides upwards of two-fold improvements in the fairness indices when compared to networks using simple FIFO queues without any rate limiting.

Chapter 9

Conclusions and Future Work

We conclude this dissertation with a summary of our contributions and directions for future work.

9.1 Summary

There is an active interest in both academia and industry in using 802.11-based multihop wireless networks to provide a cost-effective broadband Internet connectivity. In a rural community, for example, we envision that one or more wireless ISPs will provide Internet bridging connectivity via their gateway routers. Residents interested in subscribing to an ISP's service can then simply configure their commodity mesh routers to talk to this gateway, either directly or via multihop communication. Prior results, however, suggest that TCP performs suboptimally in multihop wireless networks, leading to flow unfairness and possible starvation for multihop flows. As a network operator, the ISP therefore needs to exercise some form of traffic management to keep this network functional for majority of its subscribers.

In this dissertation we explore different traffic management solutions that can be used by a wireless ISP. We constrain our solution space based on a practical constraint: the commodity mesh routers in the network are owned by the customer and the ISP has little to no control over them. This constraint is similar to how subscribers today can use any compliant DSL or cable model with their wired ISP. Thus traffic management solutions for a WMN that require MAC or transport-level modifications either to the end-hosts or to the mesh routers are infeasible. This leads us to exploring centralized traffic management and rate allocation solutions

that need only be enforced on gateway mesh routers that are within direct control of the ISP.

Our main contributions in this dissertation are as follows:

1. We showed that a broad category of router-assisted traffic allocation mechanisms that are designed for *fair* allocation of bandwidth across different flows in a wired network are ineffective in the wireless environment. We identified that this is due to key differences in the abstraction of wired and wireless links. First, work-conserving packet scheduling mechanisms are based on the assumption that links can be scheduled independently. This is not possible in a wireless network where transmission on a given link prohibits any concurrent transmissions on all interfering links. Second, packet-loss in a wired networks occurs primarily as queue drops at the congested router. In a WMN, there are limited queue-associated drops even at the gateway mesh router that converges traffic across the entire network. Most packet drops are due to collisions that are distributed across the network. Cross-layer interaction between different layers of the protocol stack means that some of these collisions can lead to long-term unfairness and possible flow starvation.

2. We showed that non-work-conserving, rate-based scheduling techniques can be used to enforce a desired rate allocation using centralized control at the gateway. This can be performed without requiring any modifications to individual mesh routers. We explored the efficacy of this control using a combination of different queueuing strategies with rate limiting enforced at different abstractions of data traffic: *(i)* an aggregate rate limit on the net traffic traversing the gateway, *(ii)* an aggregate rate limit with per-flow queueing that provides isolation between flows, and *(iii)* per-flow rate limiting. Our results show upwards of $2x$ improvement in fairness characteristics compared to TCP without any rate limiting, and are approximately similar to results obtained with source rate limiting techniques proposed in the literature that require software modifications to all mesh routers.

3. Having established the efficacy of centralized rate control, we then proposed heuristics for estimating the *fair* rate allocation for a given set of flows strictly using only the local information available at the gateway. We have proposed *zero-overhead* feedback-driven rate control heuristics that use existing data traffic to probe the network for capacity information, and use the resulting flow response to adjust their behavior. We showed how these heuristics can

be used to achieve approximate max-min fair rate allocation in a multihop network using aggregate rate limiting mechanisms. For tighter control on the desired rate allocation criterion, we extended this heuristic to per-flow rate control. We evaluated the performance of these heuristics under a variety of traffic type and load information, including elastic flows, rate-limited adaptive flows, and HTTP flows.

4. Our performance evaluation methodology uses a combination of simulations and testbed analysis. Using simulations we have experimented with a range of topologies and traffic patterns and types. Further, using a multihop wireless testbed, we have evaluated the performance of our proposed mechanisms under the imperfections of the radio channel that fundamentally makes wireless networking a challenge.

9.2 Open Issues and Future Directions

We hope that the flexibility and convenience of centralized rate control mechanisms as demonstrated in this dissertation will encourage additional research in addressing the challenging problem of rate allocation in multihop wireless networks. Below we identify some extensions to our work as well as avenues for new research in the area.

Centralized rate control with unreliable datagram traffic The centralized rate control mechanisms we evaluated in this dissertation are designed for adaptive transport protocols that respond to congestion notification signaled through packet loss or delay. We showed in Section 6.3 that these mechanisms can limit the end-to-end goodput of non-adaptive UDP streams to their fair value by dropping excess traffic at the gateway; however, upstream UDP flows can still consume excess wireless capacity to reach the gateway. The resulting response is application-dependent; some applications have their own congestion control mechanisms, while others do not.

There are two major avenues for exploring future work in this context:

1. The UDP stream has to be rate-limited to its fair share as close to the source router as possible. If we relax some constraints *vis-à-vis* the enforcement of rates at mesh routers, then a new hybrid rate-based scheme can be developed

where the fair rate is periodically computed by the gateway given its unified via of the network traffic information, and then this rate is communicated to the source nodes for local enforcement.

2. There has been recent work in IETF on DCCP [67], the Datagram Congestion Control Protocol. It provides minimal congestion control mechanisms and is designed to be an alternative to UDP for those applications for which TCP's semantics are inappropriate. Evaluating the performance of centralized control schemes with DCCP is an avenue for interesting future work.

Performance evaluation for large deployments with real workloads Our analysis and evaluation in this dissertation is a combination of simulations as well as validation on a small multihop wireless testbed. This combination allows us to explore the scale of our proposed framework, as well as evaluate it under the real world imperfections associated with the wireless channel. Understanding the challenges associated with extending this work to larger deployments with real world traffic workloads, perhaps on a commercial-grade WMN, is a necessary and a logical next step.

Centralized control with multi-gateway WMNs Our work in this dissertation considers rate allocation mechanisms that operate at a single gateway. Large WMN deployments are expected to have multiple gateway nodes. This creates an opportunity to enhance the efficiency of centralized rate control mechanisms by having the gateways periodically reconcile their views of the network state.

Heuristics for proportional fairness One straightforward extension of our work is to propose heuristics that can approximate proportional fairness between network flows in a WMN. Chiu [22] sketches a centralized algorithm that can be used as a starting reference for such a controller. Starting with max-min allocation, each flow traversing more than one bottleneck reduces its own rate by an amount that yields the maximum increase in utility for the contending set of flows. It is expected that such an algorithm will converge quickly for simple topologies. Scaling this to larger networks needs further evaluation.

Bibliography

[1] iperf. `http://dast.nlanr.net/Projects/Iperf/`.

[2] The network simulator - ns-2. `http://www.isi.edu/nsnam/ns`.

[3] olsr.org OLSR daemon. `http://www.olsr.org`.

[4] The web100 project. `http://www.web100.org/`.

[5] Imad Aad and Claude Casteulluccia. Differentiation Mechanisms for IEEE 802.11. In *Proc. of the IEEE INFOCOM '01*, pages 209–218, April 2001.

[6] Amit Aggarwal, Stefan Savage, and Thomas Anderson. Understanding the Performance of TCP Pacing. In *Proc. of the IEEE INFOCOM '00*, pages 1157–1165, March 2000.

[7] Wi-Fi Alliance and In-Stat Press Release. Wi-Fi ® Chipset Sales Grew 26 percent to 387 Million in 2008, January 8, 2009.

[8] Mark Allman, Vern Paxson, and W. Richard Stevens. TCP Congestion Control. RFC 2581, Internet Engineering Task Force, April 1999.

[9] Paramvir Bahl, Atul Adya, Jitendra Padhye, and Alec Wolman. Reconsidering Wireless Systems with Multiple Radios. *ACM SIGCOMM Computer Communications Review*, 34(5):39–46, October 2004.

[10] Hari Balakrishnan, Venkata N. Padmanabhan, Srinivasasn Seshan, and Randy H. Katz. A Comparison of Mechanisms for Improving TCP Performance over Wireless Links. *IEEE/ACM Transactions on Networking*, 5(6):756–769, December 1997.

[11] Dimitri P. Bertsekas and Robert G. Gallager. *Data Networks*. Prentice-Hall, 1992.

[12] Vaduvur Bharhgavan, A. Demers, S. Shenker, and L. Zhang. MACAW: A Media Access Protocol for Wireless LANs. In *Proc. of ACM SIGCOMM '94*, pages 249–256, September 1994.

[13] John Bicket, Daniel Aguayo, Sanjit Biswas, and Robert Morris. Architecture and Evaluation of an Unplanned 802.11b Mesh Network. In *Proc. of the ACM MobiCom '05*, pages 31–42, August 2005.

[14] Tian Bu, Yong Liu, and Don Towsley. On the TCP-friendliness of VoIP Traffic. In *Proc. of the IEEE INFOCOM '06*, April 2006.

[15] White Paper by Mesh Dynamics. WiMAX and Wi-Fi Mesh – Friends or Foes?, March 2007.

[16] Joseph Camp, Joshua Robinson, Christopher Steger, and Edward Knightly. Measurement Driven Deployment of a Two-Tier Urban Mesh Access Network. In *Proc. of the ACM MobiSys '06*, pages 96–109, June 2006.

[17] Chun-Cheng Chen and Haiyun Luo. The Case for Heterogeneous Wireless MACs. In *Proc. of the ACM HotNets IV*, November 2005.

[18] Kai Chen, Klara Nahrstedt, and Nitin Vaidya. The Utility of Explicit Rate-Based Flow Control in Mobile Ad Hoc Networks. In *Proc. of the IEEE WCNC '04*, pages 1921– 1926, March 2004.

[19] Kai Chen, Yuan Xue, Samarth Shah, and Klara Nahrstedt. Understanding Bandwidth-Delay Product in Mobile Ad hoc Networks. *Elsevier Computer Communications*, 27(10):923–934, June 2004.

[20] Shigang Chen and Zhan Zhang. Localized Algorithm for Aggregate Fairness in Wireless Sensor Networks. In *Proc. of the ACM MobiCom '06*, pages 274–285, September 2006.

[21] Xiang Chen, Hongqiang Zhai, Jianfeng Wang, and Yuguang Fang. A Survey on Improving TCP Performance over Wireless Networks. In *Resource Management in Wireless Networking (Springer Network Theory and Applications Series)*, volume 16, pages 657–695. Kluwer Academic Publishers/Springer, 2005.

[22] Dah Ming Chiu. Some Observations on Fairness of Bandwidth Sharing. In *Proc. of IEEE ISCC*, July 2000.

[23] Dah-Ming Chiu and Raj Jain. Analysis of the Increase and Decrease Algorithms for Congestion Avoidance in Computer Networks. *Computer Networks ISDN Systems*, 17(1):1–14, 1989.

[24] Thomas Clausen and Philippe Jacquet. Optimized Link State Routing Protocol (OLSR). RFC 3626, Internet Engineering Task Force, October 2003.

[25] IEEE LAN/MAN Standards Committee. *IEEE 802.16 - Air Interface for Fixed Broadband Wireless Access Systems*. IEEE, New York, 2004.

[26] IEEE LAN/MAN Standards Committee. *IEEE 802.11 - Wireless LAN Medium Access Control (MAC) and Physical Layer (PHY) Specifications*. IEEE, New York, June 2007.

[27] Douglas De Couto, Daniel Aguayo, John Bicket, and Robert Morris. A High-throughput Path Metric for Multi-hop Wireless Routing. In *Proc. of the ACM MobiCom '03*, pages 134–146, September 2003.

[28] Saumitra M. Das, Himabindu Pucha, and Y. Charlie Hu. Mitigating the Gateway Bottleneck via Transparent Cooperative Caching in Wireless Mesh Networks. *Ad Hoc Networks*, 5(6):680 – 703, August 2007.

[29] Alan J. Demers, Srinivasan Keshav, and Scott Shenker. Analysis and Simulation of a Fair Queueing Algorithm. In *Proc. of the ACM SIGCOMM '89*, pages 1–12, September 1989.

[30] Ken Duffy, Douglas J. Leith, Tianji Li, and David Malone. Improving Fairness in Multi-Hop Mesh Networks Using 802.11e. In *Proc. of the IEEE RAWNET '06*, pages 1–8, April 2006.

[31] Tony Eardley, Jasmine Bruce, and Gerard Goggin. Telecommunications and Community Well-being: A Review of the Literature on Access and Affordability for Low-income and Disadvantaged Groups. SPRC Report 09/09, Social Policy Research Centre and Journalism and Media Research Centre, University of New South Wales, July 2009.

[32] Sherif M. ElRakabawy, Alexander Klemm, and Christoph Lindemann. TCP with Adaptive Pacing for Multihop Wireless Networks. In *Proc. of the ACM MobiHoc '05*, pages 288–299, May 2005.

[33] Sherif M. ElRakabawy, Alexander Klemm, and Christoph Lindemann. TCP with Gateway Adaptive Pacing for Multihop Wireless Networks with Internet Connectivity. *Computer Networks*, 52(1):180–198, January 2008.

[34] Sally Floyd, Tom Henderson, and Andrei Gurtov. The NewReno Modification to TCP's Fast Recovery Algorithm. RFC 3782, Internet Engineering Task Force, April 2004.

[35] Sally Floyd and Van Jacobson. Random Early Detection Gateways for Congestion Avoidance. *IEEE/ACM Transactions on Networking*, 1(4):397–413, August 1993.

[36] Magnus Frodigh, Per Johansson, and Peter Larsson. Wireless Ad hoc Networking: the Art of Networking Without a Network. *Ericsson Review*, (4):248–263, September 2000.

[37] Zhenghua Fu, Haiyun Luo, Petros Zerfos, Songwu Lu, Lixia Zhang, and Mario Gerla. The Impact of Multihop Wireless Channel on TCP Performance. *IEEE Transactions on Mobile Computing*, 4(2):209–221, March/April 2005.

[38] Violeta Gambiroza, Bahareh Sadeghi, and Edward Knightly. End-to-End Performance and Fairness in Multihop Wireless Backhaul Networks. In *Proc. of the ACM MobiCom '04*, pages 287–301, September 2004.

[39] Michele Garetto, Theodoros Salonidis, and Edward Knightly. Modeling Per-flow Throughput and Capturing Starvation in CSMA Multi-hop Wireless Networks. In *Proc. of the IEEE INFOCOM '06*, April 2006.

[40] Matthew S. Gast. *802.11 Wireless Networks: The Definitive Guide*. O'Reilly Media Inc., Sebastopol, California, 2005.

[41] Vasken Genc, Sean Murphy, Yang Yu, and John Murphy. IEEE 802.16j Relay-based Wireless Access Networks: An Overview. *IEEE Wireless Communications*, 15(5):56–63, October 2008.

[42] Panos Gevros, Jon Crowcroft, Peter Kirstein, and Saleem Bhatti. Congestion Control Mechanisms and the Best Effort Service Model. *IEEE Network Magazine*, 15(3):16–26, May/June 2001.

[43] Rajarshi Gupta and Jean Walrand. Approximating Maximal Cliques in Adhoc Networks. In *Proc. of the IEEE Symposium on Personal, Indoor and Mobile Radio Communications (PIMRC) '04*, Barcelona, Spain, September 2004.

[44] Zygmunt J. Haas and Jing Deng. Dual Busy Tone Multiple Access (DBTMA) – A Multiple Access Control Scheme for Ad Hoc Networks. *IEEE Transactions on Communications*, 50(6):975–985, 2002.

[45] Martin Heusse, Franck Rousseau, Gilles Berger-Sabbatel, and Andrzej Duda. Performance Anomaly of 802.11b. In *Proc. of the IEEE INFOCOM '03*, April 2003.

[46] Bert Hubert. Linux Advanced Routing & Traffic Control. In *Proc. of the Ottawa Linux Symposium '02*, June 2002.

[47] Bret Hull, Kyle Jamieson, and Hari Balakrishnan. Mitigating Congestion in Wireless Sensor Networks. In *Proc. of the ACM SenSys '04*, Baltimore, MD, November 2004.

[48] Netgate Inc. and Rubicon Communications. Primer on WiFi Range. Technical report, 2004.

[49] Van Jacobson. Congestion Avoidance and Control. In *Proc. of the ACM SIGCOMM '88*, August 1988.

[50] Kamal Jain, Jitendra Padhye, Venkata N. Padmanabhan, and Lili Qiu. Impact of Interference on Multi-hop Wireless Network Performance. In *Proc. of the ACM MobiCom '03*, pages 66–80, September 2003.

[51] Rajendra K. Jain, Dah-Ming Chiu, and William R. Hawe. A Quantitative Measure of Fairness and Discrimination for Resource Allocation in Shared Computer System. Technical report, DEC Research Report TR-301, September 1984.

[52] Shweta Jain, Samir R Das, and Himanshu Gupta. Distributed Protocol for Maxmin Fair Rate Allocation in Wireless Mesh Networks. In *Proc. of the IEEE WoWMoM '07*, June 2007.

[53] Kamran Jamshaid, Lily Li, and Paul A.S. Ward. Gateway Rate Control of Wireless Mesh Networks. In *Proc. of the WiMeshNets*, August 2006.

[54] Kamran Jamshaid and Paul A.S. Ward. Experiences using Gateway-Enforced Rate-Limiting Techniques in Wireless Mesh Networks. In *Proc. of the IEEE WCNC '07*, pages 3725–3730, March 2007.

[55] Kamran Jamshaid and Paul A.S. Ward. Centralized feedback-driven Rate Allocation Mechanism for CSMA/CA-based Wireless Mesh Networks. In *Proc. of the ACM MSWiM '08*, pages 387–394, October 2008.

[56] Kamran Jamshaid and Paul A.S. Ward. Gateway-assisted Max-Min Rate Allocation for Wireless Mesh Networks. In *Proc. of the ACM MSWiM '09*, pages 38–45, October 2009.

[57] Ying Jian, Shigang Chen, Liang Zhang, and Yuguang Fang. New Adaptive Protocols for Fine-Level End-to-End Rate Control in Wireless Networks. In *Proc. of the IEEE ICNP*, pages 22–32, October 2008.

[58] David B. Johnson, Yih-Chun Hu, and David A. Maltz. The Dynamic Source Routing Protocol (DSR) for Mobile Ad Hoc Networks for IPv4. RFC 4728, Internet Engineering Task Force, February 2007.

[59] Jangeun Jun, Pushkin Peddabachagari, and Mihail L. Sichitiu. Theoretical Maximum Throughput of IEEE 802.11 and its Applications. In *Proc. of IEEE International Symposium on Network Computing and Applications*, pages 249–256, April 2003.

[60] Jangeun Jun and Mihail L. Sichitiu. Fairness and QoS in Multihop Wireless Networks. In *Proc. of the IEEE Vehicular Technology Conference (VTC)*, Orlando, FL, October 2003.

[61] Jangeun Jun and Mihail L. Sichitiu. The Nominal Capacity of Wireless Mesh Networks. *IEEE Wireless Communications*, pages 8–14, October 2003.

[62] Phil Karn. MACA - a New Channel Access Method for Packet Radio. In *AARL/CRRL Amateur Radio 9th Computer Networking Conference*, pages 134–140, April 1990.

[63] Vikas Kawadia and P. R. Kumar. Experimental investigations into tcp performance over wireless multihop networks. In *Proc. of ACM E-WIND Workshop*, 2005.

[64] Frank Kelly. Charging and Rate Control for Elastic Traffic. *European Transactions on Telecommunications*, 8(1):33–37, January/February 1997.

[65] Frank Kelly, Aman Kumar Maulloo, and David Tan. Rate Control in Communication Networks: Shadow Prices, Proportional Fairness and Stability. *Journal of the Operational Research Society*, 49:237–252, 1998.

[66] Srinivasan Keshav. *An Engineering Approach to Computer Networking. ATM Networks, the Internet, and the Telephone Network.* Addison-Wesley, Reading, Massachusetts 01867, 1997.

[67] Eddie Kohler, Mark Handley, and Sally Floyd. Datagram Congestion Control Protocol (DCCP). RFC 4340, Internet Engineering Task Force, March 2006.

[68] Eddie Kohler, Robert Morris, Benjie Chen, John Jannotti, and M. Frans Kaashoek. The Click Modular Router. *ACM Transactions on Computer Systems*, 18(3):263–297, August 2000.

[69] Dimitrios Koutsonikolas, Jagadeesh Dyaberi, Prashant Garimella, Sonia Fahmy, and Y. Charlie Hu. On tcp throughput and window size in a multihop wireless network testbed. In *Proc. of ACM WINTECH Workshop*, September 2007.

[70] Anurag Kumar, D. Manjunath, and Joy Kuri. *Communication Networking: An Analytical Approach*. Morgan Kaufmann Publishers Inc., San Francisco, CA, USA, 2004.

[71] Sunil Kumar, Vineet S. Raghavan, and Jing Deng. Medium Access Control Protocols for Ad Hoc Wireless Networks: A Survey. *Ad Hoc Networks*, 4(3):326–358, May 2006.

[72] Peter Langendorfer. Editorial Comments. *The Journal of Supercomputing*, 23(3):223–224, November 2002.

[73] Jeongkeun Lee, Wonho Kimand, Sung-Ju Lee, Daehyung Jo, Jiho Ryu, Taekyoung Kwon, and Yanghee Choi. An Experimental Study on the Capture Effect in 802.11a Networks. In *Proc. of the ACM WinTECH '07*, pages 19–26, 2007.

[74] Alessandro Leonardi, Sergio Palazzo, Abdul Kader Kabbani, and Edward W. Knightly. Exploiting Physical Layer Detection Techniques to Mitigate Starvation in CSMA/CA Wireless Networks. In *Proc. of the IEEE WONS '07*, pages 14–21, January 2007.

[75] Baochun Li. End-to-End Fair Bandwidth Allocation in Multi-hop Wireless Ad Hoc Networks. In *Proc. of the IEEE ICDCS '05*, pages 471–480, June 2005.

[76] Jinyang Li, Charles Blake, Douglas S. J. De Couto, Hu Imm Lee, and Robert Morris. Capacity of Ad Hoc Wireless Networks. In *Proc. of the ACM MobiCom '01*, pages 61–69, July 2001.

[77] Lily Li. The Efficacy of Source Rate Control in Achieving Fairness in Wireless Mesh Networks. Master's thesis, University of Waterloo, Waterloo, Ontario, 2007.

[78] Lily Li and Paul A.S. Ward. Structural Unfairness in 802.11-based Wireless Mesh Networks. In *Proc. of the IEEE CNSR '07*, pages 213–220, May 2007.

[79] Dong Lin and Robert Morris. Dynamics of Random Early Detection. In *Proc. of the ACM SIGCOMM '97*, October 1997.

[80] Christian Lochert, Bjorn Scheuermann, and Martin Mauve. A Survey on Congestion Control for Mobile Ad Hoc Networks. *Wireless Communications and Mobile Computing*, 7(5):655–676, April 2007.

[81] Haiyun Luo, Jerry Cheng, and Songwu Lu. Self-Coordinating Localized Fair Queueing in Wireless Ad Hoc Networks. *IEEE Transactions on Mobile Computing*, 3(1):86–98, January 2004.

[82] Haiyun Luo and Songwu Lu. A Topology-Independent Fair Queueing Model in Ad Hoc Wireless Networks. In *Proc. of the IEEE ICNP*, pages 325–335, November 2000.

[83] Haiyun Luo, Songwu Lu, and Vaduvur Bharghavan. A New Model for Packet Scheduling in Multihop Wireless Networks. In *Proc. of the ACM MobiCom '00*, pages 76–86, August 2000.

[84] Allison Mankin and K. Ramakrishnan. Gateway Congestion Control Survey. RFC 1254, Internet Engineering Task Force, August 1991.

[85] Matt Mathis, John Heffner, and Raghu Reddy. Web100: Extended TCP Instrumentation for Research, Education and Diagnosis. *SIGCOMM Computer Communications Review*, 33(3):69–79, July 2003.

[86] Matthew Mathis, Jeffrey Semke, Jamshaid Mahdavi, and Teunis Ott. The Macroscopic Behavior of the TCP Congestion Avoidance Algorithm. *SIGCOMM Computer Communications Review*, 27(3):67–82, July 1997.

[87] Kitae Nahm, Ahmed Helmy, and C. C. Jay Kuo. Cross-layer Interaction of TCP and Ad Hoc Routing Protocols in Multihop IEEE 802.11 Networks. *IEEE Transactions on Mobile Computing*, 7(4):458–469, April 2008.

[88] Thyagarajan Nandagopal, Tae-eun Kim, Xia Gao, and Vaduvur Bharghavan. Achieving MAC layer Fairness in Wireless Packet Networks. In *Proc. of the ACM MobiCom '00*, pages 87–98, August 2000.

[89] Richard G. Ogier, Fred L. Templin, and Mark G. Lewis. Topology Dissemination Based on Reverse-Path Forwarding (TBRPF). RFC 3684, Internet Engineering Task Force, February 2004.

[90] Jitendra Padhye, Sharad Agarwal, Venkata N. Padmanabhan, Lili Qiu, Ananth Rao, and Brian Zill. Estimation of Link Interference in Static Multihop Wireless Networks. In *Proc. of the ACM/USENIX IMC '05*, pages 305–310, October 2005.

[91] Alex Pentland, Richard Fletcher, and Amir Hasson. Daknet: Rethinking Connectivity in Developing Nations. *IEEE Computer*, 37(1):78–83, January 2004.

[92] Charles E. Perkins, Elizabeth Belding-Royer, and Samir Das. Ad hoc On-Demand Distance Vector (AODV) Routing. RFC 3561, Internet Engineering Task Force, July 2003.

[93] Larry L. Peterson and Burce S. Davie. *Computer Networks. A Systems Approach*. Morgan Kaufmann, 3rd edition, 2003.

[94] Jon Postel. Transmission Control Protocol. RFC 0793, Internet Engineering Task Force, September 1981.

[95] Anand R. Prasad and Neeli R. Prasad. *802.11 WLANs and IP Networking. Security, QoS, and Mobility*. Artech House, London, UK, 2005.

[96] Bozidar Radunovic and Jean-Yves Le Boudec. Rate Performance Objectives of Multihop Wireless Networks. *IEEE Transactions on Mobile Computing*, 3(4):334–349, December 2004.

[97] Sumit Rangwala, Ramakrishna Gummadi, Ramesh Govindan, and Konstantinos Psounis. Interference-Aware Fair Rate Control in Wireless Sensor Networks. In *Proc. of the ACM SIGCOMM '06*, pages 63–74, September 2006.

[98] Sumit Rangwala, Apoorva Jindal, Ki-Young Jang, Konstantinos Psounis, and Ramesh Govindan. Understanding Congestion Control in Multi-hop Wireless Mesh Networks. In *Proc. of the ACM MobiCom '08*, September 2008.

[99] Ashish Raniwala, Pradipta De, Srikant Sharma, Rupa Krishnan, and T. Chiueh. End-to-End Flow Fairness over IEEE 802.11-based Wireless Mesh Networks. In *Proc. of the IEEE INFOCOM Mini-Conference*, pages 2361–2365, May 2007.

[100] Ananth Rao and Ion Stoica. An Overlay MAC Layer for 802.11 Networks. In *Proc. of the ACM MobiSys '05*, pages 135–148, April 2005.

[101] Theodore S. Rappaport. *Wireless Communications: Principles and Practice*. Prentice Hall, 2nd edition, 2002.

[102] Federal Register. *Broadband Initiatives Program; Broadband Technology Opportunities Program; Notice*. 74(130):33103–33133, July 2009.

[103] Joshua Robinson and Edward Knightly. A Performance Study of Deployment Factors in Wireless Mesh Networks. In *Proc. of the IEEE INFOCOM '07*, May 2007.

[104] Bahareh Sadeghi. Congestion Control in Wireless Mesh Networks. In *Guide to Wireless Mesh Networks (Computer Communications and Networks Series)*, pages 277–298. Springer-Verlag London Limited, 2009.

[105] Jens Schmitt, Martin Karsten, Lars Wolf, and Ralf Steinmetz. Aggregation of Guaranteed Service Flows. In *Proc. of the Seventh International Workshop on Quality of Service (IWQoS '99)*, pages 147–155, June 1999.

[106] Y. Ahmet Sekercioglu, Milosh Ivanovich, and Alper Yegin. A Survey of MAC based QoS Implementations for WiMAX Networks. *Computer Networks*, 53(14):2517–2536, 2009.

[107] Jingpu Shi, Omer Gurewitz, Vincenzo Mancuso, Joseph Camp, and Edward Knightly. Measurement and Modeling of the Origins of Starvation in Congestion Controlled Mesh Networks. In *Proc. of the IEEE INFOCOM '08*, 2008.

[108] Jingpu Shi, Theodoros Salonidis, and Edward Knightly. Starvation Mitigation through Multi-channel Coordination in CSMA Multi-hop Wireless Networks. In *Proc. of the ACM MobiHoc '06*, pages 214–225, May 2006.

[109] W. Richard Stevens. *TCP/IP Illustrated*, volume 1. Addison-Wesley Longman, Inc., 1994.

[110] Karthikeyan Sundaresan, Vaidyanathan Anantharaman, Hung-Yun Hsieh, and Raghupathy Sivakumar. ATP: a Reliable Transport Protocol for Ad-hoc Networks. In *Proc. of the ACM MobiHoc '03*, pages 64–75, New York, NY, USA, 2003. ACM.

[111] Fabrizio Talucci, Mario Gerla, and Luigi Fratta. MACA-BI (MACA By Invitation) - A Wireless MAC Protocol for High Speed ad hoc Networking. In *Proc. of the IEEE PIMRC '97*, volume 2, pages 435–492, September 1997.

[112] Godfrey Tan and John Guttag. Time-based Fairness Improves Performance in Multi-rate Wireless LANs. In *Proc. of the USENIX Annual Technical Conference '04*, June 2004.

[113] Andrew S. Tanenbaum. *Computer Networks*. Pearson Education, 4th edition, 2003.

[114] Leandros Tassiulas and Saswati Sarkar. Maxmin Fair Scheduling in Wireless Networks. In *Proc. of the IEEE INFOCOM '02*, volume 10, pages 320–328, June 2002.

[115] Fouad A. Tobagi and Leonard Kleinrock. Packet Switching in Radio Channels: Part II—The Hidden Terminal Problem in Carrier Sense Multiple-Access and Busy-Tone Solution. *IEEE Transactions on Communication*, 23(12):1417–1433, December 1975.

[116] Bruce Tuch. Development of WaveLAN, an ISM Band Wireless LAN. *AT&T Technical Journal*, 72(4):27–37, July/August 1993.

[117] Arunchandar Vasan, Ramachandran Ramjee, and Thomas Woo. ECHOS - Enhanced Capacity 802.11 Hotspots. In *Proc. of the IEEE INFOCOM '05*, pages 1562–1572, March 2005.

[118] Ping Wang, Hai Jiang, Weihua Zhuang, and H. Vincent Poor. Redefinition of Max-Min Fairness in Multi-Hop Wireless Networks. *IEEE Transactions on Wireless Communications*, 7(12):4786–4791, December 2008.

[119] Yu Wang and J. J. Garcia-Luna-Aceves. Channel Sharing of Competing Flows in Ad Hoc Networks. In *Proc. of the IEEE Symposium on Computers and Communications (ISCC '03)*, pages 87–98, Kemer - Antalya, Turkey, July 2003.

[120] Yu Wang and J. J. Garcia-Luna-Aceves. A Hybrid Collision Avoidance Scheme for Ad hoc Networks. *Wireless Networks*, 10(4):439–446, 2004.

[121] Carey Williamson. Internet Traffic Measurement. *IEEE Internet Computing*, 5(6):70–74, Nov/Dec. 2001.

[122] Cheng-Shong Wu and Victor O. K. Li. Receiver-initiated Busy-Tone Multiple Access in Packet Radio Networks. In *Proc. of the ACM SIGCOMM '87*, pages 336–342, August 1987.

[123] Haitao Wu, Yunxin Liu, Qian Zhang, and Zhi-Li Zhang. SoftMAC: Layer 2.5 Collaborative MAC for Multimedia Support in Multihop Wireless Networks. *IEEE Transactions on Mobile Computing*, 6(1):12–25, January 2007.

[124] Kaixin Xu, Mario Gerla, and Sang Bae. Effectiveness of RTS/CTS Handshake in IEEE 802.11 based Ad Hoc Networks. *Ad Hoc Networks*, 1(1):107 – 123, July 2003.

[125] Kaixin Xu, Mario Gerla, Lantao Qi, and Yantai Shu. Enhancing TCP Fairness in Ad hoc Wireless Networks using Neighborhood RED. In *Proc. of the ACM MobiCom '03*, pages 16–28, September 2003.

[126] Shugong Xu and Tarek Saadawi. Does the IEEE 802.11 MAC Protocol Work Well in Multihop Wireless Ad hoc Networks? *IEEE Communications Magazine*, 39:130–137, June 2001.

[127] Shugong Xu and Tarek Saadawi. Revealing the Problems with 802.11 MAC Protocol in Multi-hop Wireless Ad Hoc Networks. *Computer Networks*, 38(4):531–548, March 2002.

[128] Lily Yang. Issues for Mesh Media Access Coordination Component in 11s. Report 802.11-04/0968R13, IEEE, January 2005.

[129] Luqing Yang, Winston K.G. Seah, and Qinghe Yin. Improving Fairness among TCP Flows Crossing Wireless Ad hoc and Wired Networks. In *Proc. of the ACM MobiHoc '03*, pages 57–63, New York, NY, USA, 2003. ACM Press.

[130] Hongqiang Zhai and Yuguang Fang. Distributed Flow Control and Medium Access in Multihop Ad Hoc Networks. *IEEE Transactions on Mobile Computing*, 5(11):1503–1514, November 2006.

[131] Hongqiang Zhai and Yuguang Fang. Physical Carrier Sensing and Spatial Reuse in Multirate and Multihop Wireless Ad Hoc Networks. In *Proc. of the IEEE INFOCOM '06*, April 2006.

[132] Liang Zhang, Shigang Chen, and Ying Jian. Achieving Global End-to-End Maxmin in Multihop Wireless Networks. In *Proc. of the IEEE ICDCS '08*, pages 225–232, August 2008.

[133] Lixia Zhang, Scott Shenker, and David D. Clark. Observations on the Dynamics of a Congestion Control Algorithm: The Effects of Two-Way Traffic. In *Proc. of the ACM SIGCOMM '91*, pages 133–147, October 1991.